

LAURI AARIK

Atomic layer deposition and  
characterization of thin oxide films  
for application in protective coatings



DISSERTATIONES SCIENTIAE MATERIALIS UNIVERSITATIS TARTUENSIS

**22**

DISSERTATIONES SCIENTIAE MATERIALIS UNIVERSITATIS TARTUENSIS

22

**LAURI AARIK**

Atomic layer deposition and  
characterization of thin oxide films  
for application in protective coatings



UNIVERSITY OF TARTU  
Press

1632

The study was carried out at the Institute of Physics, Department of Material Science, Faculty of Science and Technology, University of Tartu and at Eesti AGA AS, Linde Group.

The Dissertation was admitted on October 11, 2017 in partial fulfilment of the requirements for the degree of Doctor of Philosophy in Material Science and allowed for defense by Scientific Council on Material Science of the Faculty of Science and Technology, University of Tartu.

Supervisor: Prof. Väino Sammelselg, Institute of Physics and Institute of Chemistry  
University of Tartu, Tartu, Estonia

Opponents: Prof. Mato Knez, CIC nanoGUNE/Ikerbasque (Basque Foundation for Science), Donostia-San Sebastián, Spain

Dr. Ilona Oja Acik, Department of Materials and Environmental Technology, Tallinn University of Technology, Tallinn, Estonia

Defense: December 5, 2017, at University of Tartu, Estonia

The thesis was supported by European Social Fund Internationalization Program DoRa (30.1-6/886) and Graduate School of Doctoral Studies in Estonia: "Functional materials and technologies (1.2.0401.09-0079)", by Estonian Ministry of Education and Research (Project IUT2-24), Estonian Science Foundation (Project 8666), by European Regional Development Fund sub-measures Estonian Centre of Excellence in Research (Projects TK117 and TK141) and Project Namur.



ISSN 2228-0928  
ISBN 978-9949-77-602-3 (print)  
ISBN 978-9949-77-603-0 (pdf)

Copyright: Lauri Aarik, 2017

University of Tartu Press  
[www.tyk.ee](http://www.tyk.ee)

## TABLE OF CONTENTS

LIST OF ORGINAL PUBLICATIONS.....	7
AUTHOR'S CONTRIBUTION .....	7
AUTHOR'S OTHER PUBLICATIONS RELATED TO THE TOPIC .....	8
LIST OF ABBREVIATIONS AND SYMBOLS.....	9
1. INTRODUCTION.....	10
2. BACKGROUND.....	11
2.1 Protective and barrier coatings .....	11
2.2 Atomic layer deposition of Al <sub>2</sub> O <sub>3</sub> and TiO <sub>2</sub> .....	11
2.2.1 Principles and specific features of ALD processes.....	11
2.2.2 ALD precursors for Al <sub>2</sub> O <sub>3</sub> and TiO <sub>2</sub> thin films.....	12
2.2.3 Applications of Al <sub>2</sub> O <sub>3</sub> and TiO <sub>2</sub> thin films grown by ALD ....	16
2.2.4 Previous studies on the ALD of Al <sub>2</sub> O <sub>3</sub> and TiO <sub>2</sub> protective and barrier layers .....	17
2.3 Reactors for ALD .....	19
3. RESEARCH OBJECTIVES .....	22
4. EXPERIMENTAL .....	23
4.1 Samples and pretreatment of the sample surfaces .....	23
4.2 Thin film deposition .....	23
4.3 Characterization of the thin films .....	25
5. RESULTS AND DISCUSSION .....	26
5.1 Coating the inner surfaces of hollow bodies.....	26
5.1.1 Reactor for coating the inner walls of hollow bodies .....	26
5.1.2 Growth of TiO <sub>2</sub> films from TiCl <sub>4</sub> and H <sub>2</sub> O on the inner walls of hollow bodies .....	27
5.2 Characterization of O <sub>3</sub> -based growth processes .....	29
5.2.1 TiCl <sub>4</sub> -O <sub>3</sub> process .....	29
5.2.2 AlCl <sub>3</sub> -O <sub>3</sub> process.....	31
5.3 Physical properties of thin films deposited in TiCl <sub>4</sub> -O <sub>3</sub> and AlCl <sub>3</sub> -O <sub>3</sub> processes .....	32
5.4 Chemical stability of Al <sub>2</sub> O <sub>3</sub> and TiO <sub>2</sub> films deposited in TiCl <sub>4</sub> -O <sub>3</sub> and AlCl <sub>3</sub> -O <sub>3</sub> processes on Si substrates .....	36
5.5 Protective properties of TiO <sub>2</sub> and Al <sub>2</sub> O <sub>3</sub> coatings deposited in TiCl <sub>4</sub> -O <sub>3</sub> and AlCl <sub>3</sub> -O <sub>3</sub> processes on AISI 310.....	39
5.5.1 Pretreatment of the AISI 310 substrate surfaces before ALD .....	39
5.5.2 ASTM G48-11 pitting tests of AISI 310 samples coated with Al <sub>2</sub> O <sub>3</sub> and TiO <sub>2</sub> .....	41
5.5.3 Protective properties of TiO <sub>2</sub> coatings on stainless steel in a wet low-pH environment .....	45

SUMMARY AND CONCLUSIONS .....	47
SUMMARY IN ESTONIAN .....	48
ACKNOWLEDGEMENTS .....	50
REFERENCES .....	51
PUBLICATIONS .....	65
CURRICULUM VITAE .....	171
ELULOOKIRJELDUS.....	175

## LIST OF ORGINAL PUBLICATIONS

The thesis is based on the following publications, which will hereafter be referred to using Roman numerals.

- I. L. Aarik, T. Arroval, R. Rammula, H. Mändar, V. Sammelselg, J. Aarik, Atomic layer deposition of TiO<sub>2</sub> from TiCl<sub>4</sub> and O<sub>3</sub>, *Thin Solid Films*, 542 (2013) 100–107.
- II. L. Aarik, T. Arroval, R. Rammula, H. Mändar, V. Sammelselg, B. Hudec, K. Hušeková, K. Fröhlich, J. Aarik, Atomic layer deposition of high-quality Al<sub>2</sub>O<sub>3</sub> and Al-doped TiO<sub>2</sub> thin films from hydrogen-free precursors, *Thin Solid Films*, 565 (2014) 19–24.
- III. L. Aarik, J. Kozlova, H. Mändar, J. Aarik, V. Sammelselg, Chemical resistance of TiO<sub>2</sub> and Al<sub>2</sub>O<sub>3</sub> single-layer and multilayer coatings atomic layer deposited from hydrogen-free precursors on silicon and stainless steel, Submitted to *Mater. Chem. Phys.*.
- IV. V. Sammelselg, J. Kostamo, W. Bayerl, J. Aarik, L. Aarik, S. Lindfors, P. Adam, J. Poutiainen, Protecting an interior of a gas container with an ALD coating, Patent: WO 2015/132443 A1, priority date March 3, 2014.
- V. V. Sammelselg, J. Kostamo, T. Malinen, J. Aarik, L. Aarik, Protecting an interior of a hollow body with an ALD coating, Patent: WO 2015/132444 A1, priority date March 3, 2014.

## AUTHOR'S CONTRIBUTION

**Publication I:** The author carried out the film depositions, quartz crystal microbalance (QCM), X-ray fluorescence (XRF), Raman spectroscopy and spectroscopic ellipsometry measurements, and participated in analysis of grazing incidence X-ray diffraction (GIXRD) and X-ray reflection (XRR) data, took part in the analysis of results and wrote the article.

**Publication II:** The author carried out the sample pretreatment, atomic layer deposition, QCM, XRF and spectroscopic ellipsometry measurements and participated in processing and analysis of GIXRD and XRR data, took part in the analysis of results and wrote the article.

**Publication III:** The author carried out the sample pretreatment, film depositions, XRF, GIXRD, XRR measurements and all chemical stability studies, took part in the analysis of results and wrote the article.

**Publication IV:** The author participated in designing the prototype reactor, which the patent is based on, constructed the reactor and proofed the concept of the invention.

**Publication V:** The author participated in designing the prototype reactor, which the patent is based on, constructed the reactor and proofed the concept of the invention.

## AUTHOR'S OTHER PUBLICATIONS RELATED TO THE TOPIC

- V. Sammelselg, L. Aarik, M. Merisalu. Patent: Method of preparing corrosion resistant coatings. Publication number: WO 2014102758 A1. Priority date: December 31, 2012.
- V. Sammelselg, I. Netšipailo, A. Aidla, A. Tarre, L. Aarik, J. Asari, P. Ritslaid, J. Aarik, Chemical resistance of thin film materials based metal oxides grown by atomic layer deposition, *Thin Solid Films*, 542 (2013) 219–224.
- J. Aarik, T. Arroval, L. Aarik, R. Rammula, A. Kasikov, H. Mändar, B. Hudec, K. Hušeková, K. Fröhlich, Atomic layer deposition of rutile-phase  $TiO_2$  on  $RuO_2$  from  $TiCl_4$  and  $O_3$ : Growth of high-permittivity dielectrics with low leakage current, *J. Cryst. Growth*, 382 (2013) 61–66.
- T. Arroval, L. Aarik, R. Rammula, H. Mändar, J. Aarik, B. Hudec, K. Hušeková, and K. Fröhlich, Influence of growth temperature on the structure and electrical properties of high-permittivity  $TiO_2$  films in  $TiCl_4\text{-H}_2\text{O}$  and  $TiCl_4\text{-O}_3$  atomic-layer-deposition processes, *Phys. Status Solidi, A*, 211 (2014) 425–432.
- J. Mondal, L. Aarik, J. Kozlova, A. Niilisk, H. Mändar, U. Mäeorg, A. Simões, V. Sammelselg, Functionalization of Titanium Alloy Surface by Graphene Nanoplatelets and Metal Oxides: Corrosion Inhibition, *J. Nanosci. Nanotechnol.*, 15 (2015), 6533–6540.
- K. Möldre, L. Aarik, H. Mändar, A. Niilisk, R. Rammula, A. Tarre, J. Aarik, Atomic layer deposition of rutile and  $TiO_2$ -II from  $TiCl_4$  and  $O_3$  on sapphire: Influence of substrate orientation on thin film structure, *J. Cryst. Growth*, 428 (2015) 86–92.
- T. Arroval, L. Aarik, R. Rammula, V. Kruusla, J. Aarik, Effect of substrate-enhanced and inhibited growth on atomic layer deposition and properties of aluminum–titanium oxide films, *Thin Solid Films*, 600 (2016) 119–125.
- J. Mondal, A. Marques, L. Aarik, J. Kozlova, A. Simões, V. Sammelselg, Development of thin ceramic-graphene nanolaminated coating for corrosion protection of stainless steel, *Corrosion Science*, 105 (2016) 161–169.

## LIST OF ABBREVIATIONS AND SYMBOLS

AFM	Atomic force microscopy
AISI	American Iron and Steel Institute
ALD	Atomic layer deposition
ASTM	American Society for Testing and Materials
CET	Capacitance-equivalent thickness
CVD	Chemical vapor deposition
EDX	Energy dispersive X-ray spectroscopy
FWHM	Full width at half maximum
GIXRD	Grazing incidence X-ray diffraction
HR-SEM	High-resolution scanning electron microscopy
MECRALD	Microwave electron cyclotron resonance atomic layer deposition
PEALD	Plasma-enhanced atomic layer deposition
QCM	Quartz crystal microbalance
RMS	Root mean square
SE	Spectroscopic ellipsometry
SEM	Scanning electron microscopy
$T_G$	Growth temperature
TMA	Trimethylaluminum, $\text{Al}(\text{CH}_3)_3$
UV	Ultraviolet
XRD	X-ray diffraction
XRF	X-ray fluorescence
XRR	X-ray reflection

## 1. INTRODUCTION

The need for thin, conformal protective and barrier layers is continuously growing. Therefore, atomic layer deposition (ALD)—in which the gaseous precursors can travel around substrate edges and into deep trenches, and by which the film thickness can be precisely controlled—is a technique of increasing interest. Oxide thin films deposited by the ALD method have already been used in different fields, e.g., in microelectronics [1], optoelectronics [2], biomedicine [3], sensors [4, 5], energetic applications [6–10], and barrier and protective coatings [11–56].

To extend the potential of ALD, deposition chemistries and equipment are being continuously studied and optimized. In particular, reactors and precursor combinations favorable for specific applications are becoming the main targets. Having reactors that are suitable for the desired application is one of the most important requirements, especially as ALD reactors can differ in reaction chamber dimensions, design, and precursor delivery systems. All of these factors can influence the success of ALD in its intended purposes.

In addition, finding the most suitable precursor combinations may be crucial for some applications, because the physical properties and chemical stability of an ALD film may largely depend on the precursors used [14, 15]. The chemical stability is especially important in the case of protective coatings, which are exposed to different reactive environments. In these cases, it is also important to know the chemical stability as a function of the film deposition parameters.

Owing to the excellent barrier properties of aluminum oxide ( $\text{Al}_2\text{O}_3$ ) and high chemical stability of titanium oxide ( $\text{TiO}_2$ ), there are many studies demonstrating the use of  $\text{Al}_2\text{O}_3$  and  $\text{TiO}_2$  films prepared by ALD as protecting materials in different applications [11–56]. In most of these studies,  $\text{Al}_2\text{O}_3$  and  $\text{TiO}_2$  films were deposited using  $\text{Al}(\text{CH}_3)_3\text{-H}_2\text{O}$ ,  $\text{TiCl}_4\text{-H}_2\text{O}$ , and  $\text{Ti}[\text{OCH}(\text{CH}_3)_2]_4\text{-H}_2\text{O}$  ALD processes. However, previous studies have demonstrated that applying  $\text{O}_2$  plasma and  $\text{O}_3$  instead of  $\text{H}_2\text{O}$  has helped to decrease the impurity content [57, 58], increase the chemical resistance of the films [59], lower the film roughness [60], and limit the concentration of defects [61]. To extend the latter research, we have investigated the deposition of  $\text{TiO}_2$  and  $\text{Al}_2\text{O}_3$  thin films using  $\text{TiCl}_4\text{-O}_3$  and  $\text{AlCl}_3\text{-O}_3$  processes to develop ALD methods for depositing thin films from hydrogen-free precursors. Furthermore, an ALD reactor with a novel construction for coating the inner surfaces of hermetic containers was designed and tested, to widen the applications of the ALD technique. This Thesis summarizes the results obtained.

## 2. BACKGROUND

### 2.1 Protective and barrier coatings

The ongoing industrial evolution leads to higher demands on materials used in various applications. Development and application of protective and barrier layers prolonging the lifetime and enhance the properties of well-known materials is a way to support progress in this direction. Protective and barrier layers can shield materials against harmful environments and modify their functional properties to make the coated materials usable also in these cases. For instance, coatings may reduce the influence of the air and humidity. Moreover, coatings may reduce aroma permeability, enhance the resistance to light and temperature, and provide antibacterial properties.

The use of barrier layers on metals to slow corrosion is one of the most established applications of protective layers. This additional protection is of special importance when the metals are used in thermodynamically unfavorable environments that cause changes in the chemical composition. For example, in environments containing enough moisture, Fe can turn to  $\text{Fe(OH)}_3$ ,  $\text{FeO(OH)}$ , or  $\text{Fe}_2\text{O}_3 \cdot \text{H}_2\text{O}$ . The most well-known coating methods for prolonging the lifetime of metals are painting, varnishing, galvanization, and spray deposition. In the cases of more sophisticated and demanding products, physical vapor deposition [62], chemical vapor deposition (CVD) [63, 64], sol-gel deposition [65, 66], magnetron sputtering [67–69], and ALD [11–56], have been used.

The main advantage of ALD compared to the other techniques listed is its ability to coat complex 3D objects with thin, conformal, and pinhole-free coatings with precisely defined thicknesses [1, 12, 70–78]. This is important if very thin barrier layers are needed. For example, Katamreddy et al. [79] demonstrated that a 1.5 nm-thick ALD  $\text{Al}_2\text{O}_3$  layer could serve as an efficient diffusion barrier for oxygen. Moreover, Hirvikorpi et al. [80] compared the barrier properties of  $\text{Al}_2\text{O}_3$  fabricated by different techniques and obtained the most promising results using ALD. The higher chemical stability of ALD  $\text{Al}_2\text{O}_3$  films compared to the films grown by plasma deposition and CVD has been demonstrated in 5% HF solutions [81].

### 2.2 Atomic layer deposition of $\text{Al}_2\text{O}_3$ and $\text{TiO}_2$

#### 2.2.1 Principles and specific features of ALD processes

ALD is a method based on self-terminating gas-solid reactions of two or more precursors with a solid surface [1, 12, 70–78]. The film growth takes place only via surface reactions in a stepwise manner, as the precursors are introduced alternately and the precursor pulses are separated with purge periods. The technology itself has been known for more than fifty years. The principles of this deposition method were published in 1965–1967 [78, 82] and patented in

1974–1975 [78, 83]. The first industrial applications of ALD were related to manufacturing electroluminescent displays [78]. The scaling down of microelectronic devices is considered to be the main driving force for the development and use of the method since 1990s. Concurrently, the interest in the ALD of oxides started to grow. Excellent reviews published by Leskelä and Ritala [70], Puurunen [71], Miikkulainen et al. [75], Devi [76], George et al. [74], Potts and Kessels [57], and Hatanpää et al. [77] have described the ALD of different materials, reaction mechanisms, film properties, and precursor combinations. Ritala and Niinistö [73], Niinistö et al. [1], Marin et al. [12], and Knez et al. [72] have published reviews on the possible applications of ALD. Therefore, in this Chapter, the focus will be on the deposition and key properties of  $\text{TiO}_2$  and  $\text{Al}_2\text{O}_3$  thin films, ALD reactors, and the applications of  $\text{TiO}_2$  and  $\text{Al}_2\text{O}_3$  films as protective and barrier layers. In addition, the main mechanisms and important details required to understand the results of this Thesis will be outlined.

Owing to the ability to deposit conformal coatings on 3D surfaces with atomic-level control over the material thickness and composition, ALD is a promising method for the preparation of coatings for various applications. The disadvantages of the ALD method include the need for suitable precursor combinations and the relatively slow film growth that is typical for most conventional reactors. Moreover, as the film growth takes place via chemical surface reactions, the film properties are influenced by the substrate. This complicates the deposition of homogeneous films with uniform thicknesses on heterogeneous surfaces with unknown and varying compositions.

### 2.2.2 ALD precursors for $\text{Al}_2\text{O}_3$ and $\text{TiO}_2$ thin films

One of the earliest approaches to ALD was the use of metal chlorides for the deposition of metal oxides. For example,  $\text{AlCl}_3$  has been used in the ALD of  $\text{Al}_2\text{O}_3$  [81, 84, 85] together with  $\text{H}_2\text{O}$ , a mixture of 15% He and  $\text{O}_2$ , and several alcohols. The growth temperatures ( $T_G$ ) were varied from 100 to 800°C (Table 1). The as-deposited  $\text{Al}_2\text{O}_3$  films were mainly amorphous. On Si(100) substrates, polycrystalline films grew from  $\text{AlCl}_3$  and  $\text{H}_2\text{O}$  at temperatures exceeding 600°C [86]. In addition, crystalline  $\text{Al}_2\text{O}_3$  films have been obtained from  $\text{AlCl}_3$  and the 15% He/ $\text{O}_2$  mixture at 450°C on single-crystal Nb and at 660°C on sapphire [87]. The solid nature and corrosive by-products complicate handling of  $\text{AlCl}_3$ . For this reason,  $\text{AlCl}_3$  is mostly used in ALD at high substrate temperatures or to avoid carbon and hydrogen contamination in the films [86].

Trimethylaluminum ( $\text{Al}(\text{CH}_3)_3$ ; TMA) combined with various oxygen precursors has been most frequently applied for the ALD of  $\text{Al}_2\text{O}_3$  [12, 71, 75], at substrate temperatures ranging from 25 to 800°C. The formation of crystalline  $\text{Al}_2\text{O}_3$  films in TMA- $\text{H}_2\text{O}_2$  and TMA- $\text{N}_2\text{O}$  processes on Si(100) substrates at 700–800 and 500°C, respectively, has been reported by Kumagai et al. [88]. In contrast, Prokes et al. [89] reported the deposition of crystalline

$\text{Al}_2\text{O}_3$  with TMA- $\text{H}_2\text{O}$  ALD on  $\text{Ga}_2\text{O}_3$ ,  $\text{ZnO}$ , and  $\text{Si}$  nanowires at 200°C. This result is surprising because other authors have reported that ALD  $\text{Al}_2\text{O}_3$  films are amorphous, regardless of the substrate, when deposited at substrate temperatures of up to 600°C [75].

Although many ALD processes have been known for a long time, studies on different precursor combinations—in particular those combining various organic compounds with different oxygen precursors—are still ongoing (Table 1). One reason for such studies is that the high level of residual impurities may cause problems in the applications of the films, especially when low substrate temperatures must be applied during deposition. One way to reduce the concentration of impurities and increase the film quality is to use  $\text{O}_2$  plasma or  $\text{O}_3$  instead of  $\text{H}_2\text{O}$  during ALD [57–61]. Unfortunately, in the case of plasma-based processes, the conformity of the films deposited on complex surfaces may be insufficient [90].

**Table 1.** List of processes used in ALD of  $\text{Al}_2\text{O}_3$ .

Aluminum precursors	Oxygen precursors	$T_G$ , °C	References
Aluminumtrichloride, $\text{AlCl}_3$	Water vapor	100–800	[86, 90]
	Water vapor together with a catalyst	77–327	[91]
	Mixture of helium and oxygen, 15% He in $\text{O}_2$	450–660	[87]
	Methanol, $\text{CH}_3\text{OH}$	500	[92]
	Ethyleneglycol, $\text{CH}_2\text{OHCH}_2\text{OH}$	500	[92]
	Butyl alcohol, t- $\text{C}_4\text{H}_9\text{OH}$	350–500	[92]
	Butyl alcohol, n- $\text{C}_4\text{H}_9\text{OH}$	300–500	[92]
	Aluminum isopropoxide, $\text{Al}(\text{OCH}(\text{CH}_3)_2)$	150–375	[93, 94]
Trimethylaluminum (TMA), $\text{Al}(\text{CH}_3)_3$	Water vapor	33–500	[13, 95]
	Oxygen	300	[96]
	Hydrogen peroxide, $\text{H}_2\text{O}_2$	25–800	[88, 97]
	Mixture of oxygen gas and vapor of water and hydrogen peroxide	150–250	[98]
	Nitrous oxide, $\text{N}_2\text{O}$	100–500	[88]
	Nitrogen dioxide, $\text{NO}_2$	150–310	[99]
	Water vapor and nitrogen dioxide	150–310	[99]
	Ozone	25–450	[58, 100]
	Aluminum isopropoxide, $\text{Al}(\text{OCH}(\text{CH}_3)_2)_3$	300	[93]
	Isopropyl alcohol, $(\text{CH}_3)_2\text{CHOH}$	250	[101]
	Oxygen plasma	25–400	[102]
	Carbon dioxide ( $\text{CO}_2$ ) plasma	25–350	[103, 104]
	Nitrous oxide plasma	140–220	[105]

Aluminum precursors	Oxygen precursors	$T_G, ^\circ\text{C}$	References
Dimethylaluminum-chloride, $\text{Al}(\text{CH}_3)_2\text{Cl}$	Water vapor	125–500	[106]
Dimethylethylamine alane complex, $(\text{CH}_3)_2(\text{C}_2\text{H}_5)\text{N}:\text{AlH}_3$	Hydrogen and oxygen plasma	100–180	[107]
Methylpyrrolidine alane complex, $\text{C}_5\text{H}_{11}\text{N}:\text{AlH}_3$	Oxygen plasma	100	[108]
Dimethylaluminum-isopropoxide, $(\text{CH}_3)_2\text{Al}(\text{OC}_3\text{H}_7)$	Water vapor	100–400	[109]
	Oxygen plasma	25–400	[109]
Aluminummethoxide, $\text{Al}(\text{OC}_2\text{H}_5)_3$	Water vapor	250–500	[92]
	Oxygen	250–500	[92]
Aluminum isopropoxide, $\text{Al}(\text{OC}_3\text{H}_7)_3$	Water vapor	250–500	[92]
	Oxygen	250–500	[92]
Aluminum 1-methoxy-2-methyl-2-propoxide, $\text{Al}(\text{OC}(\text{CH}_3)_2\text{CH}_2\text{OCH}_3)_3$	Water vapor	200–450	[110]
Tris(diethylamino) Aluminum, $\text{Al}(\text{N}(\text{C}_2\text{H}_5)_2)_3$	Water vapor	200–400	[111]
	Ozone	200–275	[112]
Tris(dialkylamino) Aluminum, $\text{Al}(\text{C}_3\text{H}_8\text{N})_3$	Water vapor	250–400	[113]
Heteroleptic amidinate-containing precursor, $[\text{CH}_3\text{C}(\text{C}_3\text{H}_8\text{N})_2]\text{Al}(\text{C}_2\text{H}_5)_2$	Water vapor	125–300	[114]

$\text{TiCl}_4$  has been used as a precursor in the deposition of  $\text{TiO}_2$  starting from 1960s [82]. Since then, different research groups have demonstrated the deposition of  $\text{TiO}_2$  using various oxygen precursors, e.g.,  $\text{H}_2\text{O}$ ,  $\text{H}_2\text{O}_2$ ,  $\text{O}_2$  plasma, and  $\text{CH}_3\text{OH}$  (Table 2). One of the most studied ALD processes, the  $\text{TiCl}_4\text{-H}_2\text{O}$  process, has been thoroughly studied by many groups [82, 115, 116].  $\text{TiCl}_4$  is a liquid precursor with a modest vapor pressure at room temperature. Therefore,  $\text{TiCl}_4$  is convenient to handle and hence is one of the most commonly used precursors for depositing  $\text{TiO}_2$  [118]. However, the corrosive nature of  $\text{TiCl}_4$  and its reaction by-products may cause problems, for example, if it is used for the deposition of multicomponent oxides that may easily form chlorides by reacting with  $\text{TiCl}_4$  [118]. Therefore, alternative precursor systems have been studied (Table 2). Titanium isopropoxide ( $\text{Ti}[\text{OCH}(\text{CH}_3)_2]_4$ ), titanium ethoxide ( $\text{Ti}(\text{OC}_2\text{H}_5)_4$ ), and tetrakis(dimethylamido)titanium ( $\text{Ti}(\text{N}(\text{CH}_3)_2)_4$ ) used together with different oxygen precursors are the most common alternatives to  $\text{TiCl}_4$  (Table 2). Unfortunately, the thermal decomposition of these organic precursors and subsequent carbon contamination of films deposited at lower temperatures limits the application of the precursors in ALD [119].

As polycrystalline  $\text{TiO}_2$  films can be obtained at much lower temperatures than polycrystalline  $\text{Al}_2\text{O}_3$  films, many studies have been performed to understand how the crystallization processes correlate with  $T_G$ , film thickness, and the reactants and substrates used [75].

**Table 2.** List of processes used for ALD of  $\text{TiO}_2$ .

Titanium precursors	Oxygen precursors	$T_G$ , °C	References
Titanium tetrachloride, $\text{TiCl}_4$	Water vapor	25–600	[115, 120–123]
	Hydrogen peroxide, $\text{H}_2\text{O}_2$	100–700	[122, 124, 125]
	Oxygen plasma	25–200	[126]
	Methanol, $\text{CH}_3\text{OH}$	375–420	[127, 128]
	Titanium isopropoxide, $\text{Ti}[\text{OCH}(\text{CH}_3)_2]_4$	125–300	[129]
Titanium tetrafluoride, $\text{TiF}_4$	Water vapor	300–500	[130]
Titanium tetraethoxide (TTEt), $\text{Ti}(\text{OC}_2\text{H}_5)_4$	Water vapor	100–350	[131–133]
Titanium tetraiso- propoxide (TTIP), $\text{Ti}(\text{OC}_3\text{H}_7)_4$	Water vapor	35–350	[132, 134]
	Hydrogen peroxide,	100–300	[135]
	Synthetic air	100–200	[136]
	Ozone	150–380	[137–139]
	Oxygen plasma	25–400	[102]
	Nitrous oxide ( $\text{N}_2\text{O}$ ) plasma	280	[140]
	Oxygen and nitrogen plasma	150–250	[141]
	Water vapor plasma	50–340	[142]
	Oxygen and ammonium, $\text{NH}_3$	140	[143]
	Ammonium	140	[144]
	Carboxylic acid, $\text{HCOOH}$	50–350	[145]
	Water vapor, UV assisted	260	[146]
Titanium tetraiodide, $\text{TiI}_4$	Water and hydrogen peroxide vapor	230–375	[147]
	Oxygen	230–460	[148]
	Water vapor	135–445	[149]
	Hydrogen peroxide	250–490	[150]

Titanium precursors	Oxygen precursors	$T_G$ , °C	References
Tetrakis(dimethylamino)-titanium (TDMAT), $\text{Ti}(\text{N}(\text{CH}_3)_2)_4$	Water vapor	90–210	[151]
	Ozone	60–225	[152–154]
	Oxygen plasma	150–300	[155, 156]
	Water vapor plasma	50–340	[142]
Titanium tetramethoxide, $\text{Ti}(\text{OCH}_3)_4$	Water vapor	200–400	[118]
Titanium methylcyclopentadienyl-tris(isopropoxide), $\text{TiC}_5\text{H}_4(\text{CH}_3)(\text{OCH}(\text{CH}_3)_2)_3$	Oxygen plasma	25–400	[102]
Titanium penta-methylcyclopentadienyl-tri(methoxide), $\text{TiC}_5(\text{CH}_3)_5(\text{OCH}_3)_3$	Oxygen plasma	25–400	[102]
Titanium methyl-cyclopentadienyl-tris(dimethylamido), $\text{TiC}_5\text{H}_4\text{CH}_3(\text{N}(\text{CH}_3)_2)_3$	Oxygen plasma	100–350	[157]
Titanium di(isopropoxide)bis( $\text{N}, \text{N}'$ -dimethyl-aminoethoxide) $\text{Ti}(\text{OCH}(\text{CH}_3)_2(\text{OCH}_2\text{CH}_2\text{N}(\text{CH}_3)_2)_2$	Water vapor	100–300	[158]
Titanium di(isopropoxide)-bis(dipivaloylmethanate) $[\text{Ti}(\text{IP})_2(\text{dpm})_2]$ , $\text{TiOCH}(\text{CH}_3)_2(\text{C}_{11}\text{H}_{19}\text{O}_2)_2$ dissolved in ethyl-cyclohexane, $\text{C}_6\text{H}_{11}\text{C}_2\text{H}_5$	Water vapor	340–470	[159]

### 2.2.3 Applications of $\text{Al}_2\text{O}_3$ and $\text{TiO}_2$ thin films grown by ALD

The deposition of  $\text{Al}_2\text{O}_3$  and  $\text{TiO}_2$  thin films was one of the first successful applications of ALD [1, 82, 84, 85], and the number of studies demonstrating the industrial applications of ALD is still increasing. Since the first applications of ALD oxides in microelectronics, a number of studies has been published to demonstrate that  $\text{Al}_2\text{O}_3$  can be applied as a high-permittivity (high-k) material in gate stacks of metal–oxide–semiconductor devices [1, 160] and in the capacitor structures of dynamic random access memories [1, 161, 162]. Similarly, the use of  $\text{TiO}_2$  as a high-k dielectric material [72, 163–165] has also been investigated. The main advantages of ALD in micro- and nanoelectronic applications are the accurate control over the ultrathin film thickness and the

ability to create conformal coatings of substrates with very complex shapes. Currently, there is an increasing number of works showing that these advantages allow the thin films grown by ALD to be used in other applications too (Fig. 1).

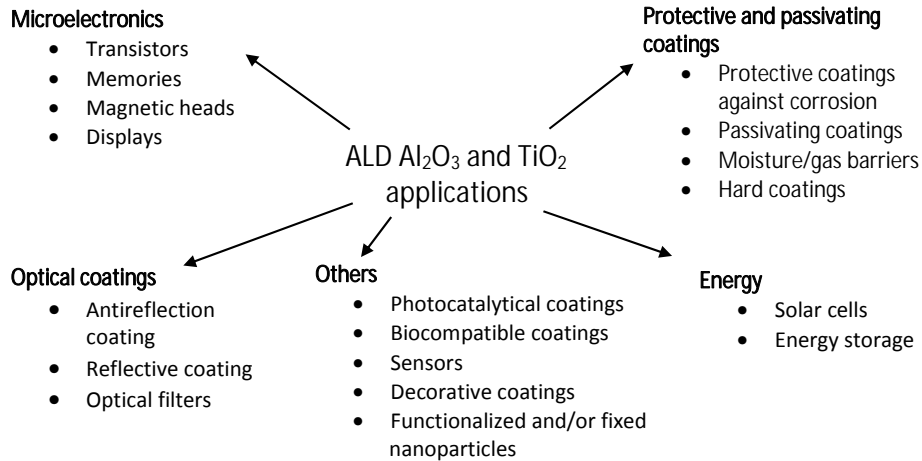


**Figure 1.** Available and potential applications of Al<sub>2</sub>O<sub>3</sub> and TiO<sub>2</sub> films deposited by ALD.

The high optical transparencies and excellent diffusion barrier properties have enabled application of Al<sub>2</sub>O<sub>3</sub> films in optical coatings [2, 72, 121]; medicine [72, 133, 166]; protective, barrier, and hard coatings [28, 167, 168]; and in the functionalization of nanoparticles, e.g., tubes, fibers, and powders [72, 169]. The potential applications of TiO<sub>2</sub> include self-cleaning surfaces [170]; biomedical sensors [5]; implantable sensor membranes and water purification membranes [171]; optical coatings [72, 121, 172]; protective and passivating coatings [11, 19, 32, 52, 54]; and several other fields. Besides their direct usage purposes in different optical, energetic, and microelectronic devices, Al<sub>2</sub>O<sub>3</sub> and TiO<sub>2</sub> can serve as passivating and diffusion barrier coatings in these applications.

#### 2.2.4 Previous studies on the ALD of Al<sub>2</sub>O<sub>3</sub> and TiO<sub>2</sub> protective and barrier layers

Owing to the high chemical stability of TiO<sub>2</sub> and the remarkable diffusion barrier properties of Al<sub>2</sub>O<sub>3</sub> thin films, the number of studies focused on their application as protective coatings is constantly growing [11–56]. The ALD of Al<sub>2</sub>O<sub>3</sub> is one of the most thoroughly studied ALD processes and Al<sub>2</sub>O<sub>3</sub> is one of the most frequently used materials in ALD coatings for protective and barrier purposes. For example, Schmidt et al. [33] applied Al<sub>2</sub>O<sub>3</sub> coatings to a cobalt slanted columnar structure to preserve its optical properties. Hahtela et al. [21]

deposited  $\text{Al}_2\text{O}_3$  on Ni–Cr–Cu–Al–Ge thin film resistors to improve their long-term stability. Görn et al. [22] showed that the high reactivity of the  $\text{Al}_2\text{O}_3$  precursor and formation of the conformal barrier layer could remove the unwanted chemisorbed oxygen from the surface of a thin film transistor, and encapsulate the surface with a moisture-resistant barrier layer. Moreover, there are studies demonstrating the ability of  $\text{Al}_2\text{O}_3$  coatings to protect silver jewelry and collectable coins [30, 41]; encapsulate the polymers used in food packaging and organic and inorganic devices [20, 42, 48]; and protect the surfaces of solar cells, organic light-emitting diodes [9, 38], and aluminum mirrors [23]. Additionally,  $\text{Al}_2\text{O}_3$  coatings have been used to prolong the lifetime of a NiTi alloy [43], stainless steel [28, 49], steel [31], aluminum 2024-T3 alloy [31], a magnesium–lithium alloy [12], magnesium–aluminum alloy [173], and copper [44].

The main drawback of using  $\text{Al}_2\text{O}_3$  in protective layers is the relatively high dissolution rate of amorphous alumina films in acidic and basic solutions [174]. Moreover, there are even reports demonstrating that amorphous ALD  $\text{Al}_2\text{O}_3$  films can dissolve in pure water because of successive hydration and dynamic dissolution processes [174]. On the other hand, Abdulagatov et al. [29] reported that the formation of polycrystalline  $\gamma\text{-}\text{Al}_2\text{O}_3$  during the annealing of  $\text{Al}_2\text{O}_3$  samples at 900°C significantly increased their stability in acidic and basic solutions. Unfortunately, annealing at these very high temperatures is energy and time intensive, and in some cases, is obstructive or even impossible in industrial applications. Therefore, if a coating with a high chemical stability is needed,  $\text{Al}_2\text{O}_3$  should be combined or replaced with other materials, e.g., with  $\text{TiO}_2$ .

Similarly,  $\text{TiO}_2$  deposited by ALD has been used as a protective and barrier layer. For example, Seo et al. [37] demonstrated that  $\text{TiO}_2$  can behave as a moisture barrier. There are also numerous works showing that  $\text{TiO}_2$  can be used as a protective layer on stainless steel [19, 26, 49, 52], a magnesium–aluminum alloy [173], silver nanoparticles [24], carbon nanotubes [175], and different electrode materials including nickel oxide [49],  $\text{CuO}_2$  [55], InP [50], porous ceramic foams [54], and  $\text{ZnO}$  nanorods [176].

The main drawback of using ALD  $\text{TiO}_2$  films in protective and barrier coatings is that, depending on the precursor combination and substrate material, the as-deposited  $\text{TiO}_2$  films tend to be polycrystalline even when grown at temperatures as low as 165°C [120]. Wang et al. [177] showed that the grain boundaries of polycrystalline films might act as preferential routes for corrosion. On the other hand, polycrystalline ALD  $\text{TiO}_2$  films show a higher resistance to acidic environments than amorphous  $\text{TiO}_2$  films [15, 178]. Therefore, in some cases, the relatively low crystallization temperature may be an advantage of ALD  $\text{TiO}_2$  by increasing the durability of protective coatings containing  $\text{TiO}_2$ .

A developing research area is combining ALD films of different compositions with nanoparticles [179, 180]. In most cases, the ALD films functionalize the nanoparticle surfaces or fix them on a substrate. Furthermore, there are

reports that the coatings can improve the resistance of the material to a destructive environment and/or increase the high-temperature durability of the nanoparticles. For instance, this has been displayed in the cases of  $\text{Al}_2\text{O}_3$  and/or  $\text{TiO}_2$  thin films deposited on silver [16], iron [17], copper [45], and cobalt nanoparticles [46]. The ability to increase the high-temperature durability of a material by the ALD of  $\text{Al}_2\text{O}_3$  or  $\text{TiO}_2$  layer on the material surface has been observed also with thin planar materials, e.g., copper plates [34], niobium coupons [18], and silver islands on planar substrates [27].

To enhance the protective properties of the coatings, combinations of different materials deposited as laminates or mixtures have been used. Abdulagatov et al. [29] suggested that including an  $\text{Al}_2\text{O}_3$  layer under the  $\text{TiO}_2$  will improve the adhesion/nucleation and sealing properties of the coating, and the  $\text{TiO}_2$  will in turn confer chemical stability in acidic and basic solutions. For example, some studies have demonstrated that  $\text{TiO}_2$  and  $\text{Al}_2\text{O}_3$  multilayer coatings can be used to protect stainless steel [11, 32, 35], aluminum alloys [12], silver [30, 41], and organic light-emitting diodes [47].

As ALD is a very surface-sensitive and relatively slow deposition method, it is sometimes necessary to combine this method with other film fabrication techniques to achieve the best results. For instance, it has been demonstrated that anodizing the aluminum alloy surface before ALD will increase the protective properties of the coating [36]. Adding a graphene oxide layer between the stainless steel and ALD layer [51, 53], and a magnetron-sputtered Al interlayer between ALD and a Mg–Li–Zn alloy, increased the corrosion resistance of the coating [40]. Furthermore, by combining a CrN matrix, TiAlN/TiN, or TiCN deposited by physical vapor deposition and either  $\text{Al}_2\text{O}_3$ ,  $\text{TiO}_2$ , or  $\text{Al}_2\text{O}_3/\text{TiO}_2$  laminates deposited by ALD, corrosion-resistant hard coatings have been fabricated [25, 56].

### 2.3 Reactors for ALD

The separate supply of precursors is one of the main requirements for ALD. Therefore, ALD reactors can be roughly divided into two groups depending on how the alternate supply of precursors is ensured. For the first type, the sample that needs coating is fixed and the precursor flows – which are directed onto the sample surface – are switched on and off (Fig. 2) so that the precursor pulses are well separated in time [85, 181–183]. In the reactors of the second type, the sample moves from one continuous precursor flow into another [85, 181, 184]. In this case, the precursor flows are separated by an inert atmosphere in which no precursors are present.

Additionally, it is possible to distinguish ALD reactors based on the method of excitation of the gas-solid reactions [57]. In thermal ALD, it is important to obtain a certain temperature (sometimes in the presence of catalysts) to enable a self-limited type of deposition [71]. In the case of energy-enhanced ALD, additional energy is provided to one or all of the gaseous precursors to convert

traditional thermal reactants to species that are more reactive, or to use precursors that are otherwise not suitable for ALD. Examples of energy-enhanced ALD processes are plasma-enhanced ALD (PEALD), photo-induced (including UV-assisted) ALD, microwave electron cyclotron resonance ALD (MECRALD), and hot-wire ALD.

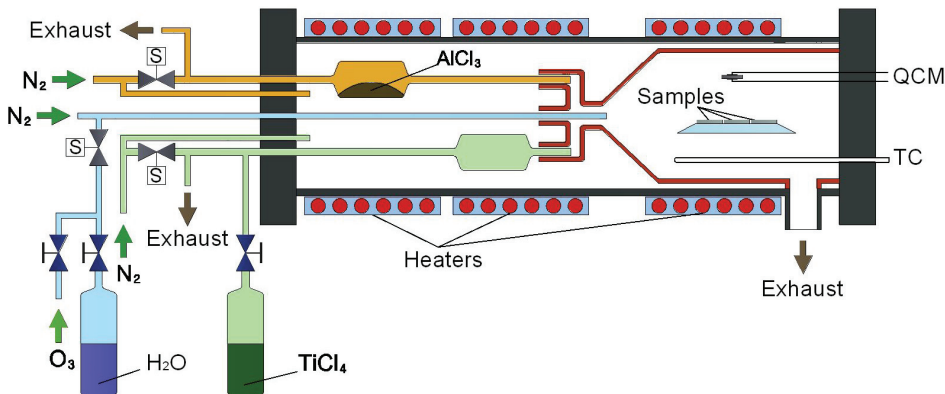


**Figure 2.** Schematic drawing of a flow-type ALD reactor [183]. Reprinted with permissions from Elsevier B. V. (Thin Solid Films).

In PEALD, at least one of the precursors is excited by employing plasma during the deposition process. Depending on the reactor configuration, PEALD can be divided into radical-enhanced, direct plasma, and remote plasma ALD [185]. In the first case, the plasma generation takes place relatively far from the sample surface. Therefore, the most reactive plasma species (electrons and ions) recombine via surface collisions on the way to the surface and hence only radicals are involved in the ALD reactions. In the case of direct plasma ALD, the sample is positioned between the two electrodes that are used for plasma generation. For this reason, the plasma species taking part in ALD are generated very close to and directly impact the sample surface. In the remote plasma ALD configuration, the plasma generation takes place at a significant distance from the substrate surface. In this case, the substrate does not take part in plasma generation but, unlike in radical-enhanced ALD, the electron and ion densities do not decrease to zero at the substrate location. In MECRALD, the gas/vapor is ionized as it flows through the electron cyclotron resonance zone, while in UV-assisted ALD, ultraviolet light is used to irradiate the surface after the purge steps to increase the number of chemisorption sites on the sample surface [146].

ALD reactors can be designed to deposit coatings on one substrate (single-wafer reactors) or on many samples simultaneously (batch reactors). The main differences are that batch reactor chambers are usually larger and have more complex precursor supply systems, to optimize the precursor flows and avoid increasing the times needed to supply and evacuate the precursors. It must be considered that the evacuation of excess precursors might be difficult when the

films are deposited at low temperatures or onto complex-shaped objects. For example, Groner et al. [13] used an additional carrier gas line in the reaction chamber to avoid the diffusion of the precursors inside the hollow poly(ethylene terephthalate) bottle, thereby ensuring relatively short purge periods needed for ALD of coating on the outer side of the bottle.

In addition, depending on the application, reactors with different pressures and carrier gas flow rates, precursor supply methods, and different temperatures of reactor walls compared to that of the substrates, have been described [182]. Most ALD reactors use a carrier gas to transport the precursors to the substrates, and for purging the substrate surfaces between precursor pulses. In some cases, however, no carrier gas is used, and the reactants are removed from the reaction chamber by applying only a throttled pumping. The main disadvantage of this approach is the relatively long purge periods required, which lead to a very slow deposition process. There are also differences in the supply of the precursors into the reaction area in different reactors. One possibility is to supply the precursors using a gas flow that is parallel to the sample surface (Fig. 2). Another possibility is to lead the gas flow into the reaction chamber perpendicularly to the sample surface using the so-called “showerhead” setup.

It is possible to divide ALD reactors into hot- and cold-wall systems. In the most commonly used hot-wall reactors, the reaction chamber walls, interior gas phase, and samples are heated to similar temperatures. In cold-wall reactors, only the sample holder and sample are heated to  $T_G$ , while the walls of the reaction chamber are held at much lower temperatures [186].

To use the full potential of the ALD technique, many different reactors with configurations optimized for special applications have been developed. For instance, to deposit ALD coatings on the surfaces of nanoparticles, fluidized bed reactors have been built [17]. For coating flexible materials and porous or 3D substrates, roll-to-roll reactors [187, 188] and special showerhead systems, respectively, have been designed [189].

### **3. RESEARCH OBJECTIVES**

The first goal of this research was to design a reactor and develop processes for coating the inner walls of containers larger than the reaction chambers of conventional ALD reactors. It was also important that the reactor, which was planned to be constructed, would allow the process developers to control if the ALD-type deposition was achieved inside the container. The aim was to show that ALD could be efficiently applied to coat the inner walls of hermetic containers.

Secondly, the possibility to use hydrogen-free precursor combinations,  $\text{TiCl}_4\text{-O}_3$  and  $\text{AlCl}_3\text{-O}_3$ , in the ALD of  $\text{TiO}_2$  and  $\text{Al}_2\text{O}_3$  films was investigated. The films deposited with these precursor combinations were compared, and the effects of applying  $\text{O}_3$  instead of  $\text{H}_2\text{O}$  on the growth mechanism, structure, and morphology of the films were studied. This research was performed to demonstrate that  $\text{TiO}_2$  and  $\text{Al}_2\text{O}_3$  could be deposited by ALD using  $\text{TiCl}_4\text{-O}_3$  and  $\text{AlCl}_3\text{-O}_3$  precursor combinations, which might have advantages over other ALD processes.

Thirdly, it was of particular interest to characterize the protective and barrier performance of the  $\text{Al}_2\text{O}_3$  and  $\text{TiO}_2$  coatings deposited using the  $\text{AlCl}_3\text{-O}_3$  and  $\text{TiCl}_4\text{-O}_3$  processes, and to reveal the effects of thickness, deposition temperature, and structure on the chemical stability of the films. The aim of the investigation was to create the basis for future studies and possible applications of the films deposited by using these processes, and to demonstrate that the films can be used as barrier layers.

## 4. EXPERIMENTAL

### 4.1 Samples and pretreatment of the sample surfaces

The thin films were deposited onto quartz crystal microbalance (QCM) mass sensors and on Si(100) and AISI 310 stainless steel substrates. In the QCM studies, 6.4 MHz quartz crystal oscillators with silver electrodes were used as the mass sensors. The sizes of the Si(100) samples ranged from  $10 \times 10$  to  $30 \times 30$  mm<sup>2</sup>. Before loading into the reactor, the samples were etched in HF and then rinsed with deionized water. The 0.9 mm-thick annealed AISI 310 stainless steel (Goodfellow Cambridge Ltd.) samples had typical sizes of  $15 \times 15$  mm<sup>2</sup> and contained Ni (20%), Cr (24–26%), Mn (2%), and Si (1%), in addition to Fe [190].

For the pretreatment of the AISI 310 samples, several procedures were tested and compared. Firstly, the samples were pretreated in different organic solvents including acetone (99.5%, Sigma-Aldrich), isopropyl alcohol (99.8%, Sigma-Aldrich), and toluene (99.7%, Sigma-Aldrich). Secondly, surface pretreatments by Ar, N<sub>2</sub>, Ar/O<sub>2</sub>, and H<sub>2</sub> (all Eesti AGA AS) plasmas were tested. Thirdly, the samples were etched in different acids, i.e., HNO<sub>3</sub> (65%, Sigma-Aldrich), HCl (37%, Sigma-Aldrich), H<sub>2</sub>SO<sub>4</sub> (95%, Sigma-Aldrich), and in mixed solutions consisting of (1) 5% HF, 10% HNO<sub>3</sub>, and 85% H<sub>2</sub>O (Solution A); (2) 20% H<sub>2</sub>SO<sub>4</sub>, 4.5% HNO<sub>3</sub>, 14.5% HCl, and 61% H<sub>2</sub>O (Solution B); and (3) 15% H<sub>3</sub>PO<sub>4</sub> (85%, Sigma-Aldrich), 2% HNO<sub>3</sub>, 5% HCl, 5% H<sub>2</sub>SO<sub>4</sub>, and 73% H<sub>2</sub>O (Solution C), the solutions that have been previously used for steel burnishing [191]. The plasma treatments were performed using a Femto RF-UHP-PC low-pressure plasma system (Diener Electronic) at power levels of up to 100 W. Each AISI 310 sample was studied with high-resolution scanning electron microscopy (HR-SEM) using a dual-beam microscope (Helios NanoLab 600, FEI) before and after each pretreatment. The effect of the pretreatment on the film quality was evaluated by conducting etching tests with the films in Solution C at 70°C.

### 4.2 Thin film deposition

The deposition of TiO<sub>2</sub> and Al<sub>2</sub>O<sub>3</sub> films using TiCl<sub>4</sub>-O<sub>3</sub> and Al<sub>2</sub>O<sub>3</sub>-O<sub>3</sub> chemistries was investigated in a low-pressure flow-type hot-wall ALD reactor [183]. The vacuum chamber of the reactor (Fig. 2) has stainless steel outer walls and is surrounded by three independent heaters that allow a uniform temperature distribution over each of the three zones. Two of these zones are meant for volatilization of the solid precursors and one for deposition of the films. A quartz tube with a 50 mm inner diameter separates the stainless-steel reactor walls in the high-temperature region from the gas flowing into the deposition zone. This approach significantly reduces the influence of the stainless steel

walls on the purity of the films deposited at reactor temperatures that can reach as high as 750°C. In addition, the quartz tube can be easily removed and cleaned to ensure that the concentrations of impurities in the films are kept low.

The precursors with a low vapor pressure are volatilized in quartz evaporation cells located in the heated zones of the reactor. Using the carrier gas, the precursors are carried into the 160 mm long quartz reaction chamber, which has an inner diameter of 45 mm. The flow of the carrier gas is controlled with needle valves, and the vapor pressure of each precursor is determined by the temperature of the corresponding heating zone. To turn the injection of the precursors into the reaction zone on and off, the flow direction of the carrier gas in the evaporation cells is changed by opening and closing the solenoid valves, which are operated by a customized control system. The precursors with a high vapor pressure enter the reactor from external containers through needle and solenoid valves that control the flow and form the precursor pulses.

To optimize the deposition process parameters, a QCM system with a mass sensor that can be moved within the reaction chamber can be added for real-time studies. In this study, the QCM data were acquired by using a Q-pod quartz crystal monitor (Inficon). Based on these studies, the ALD cycle times and precursor doses were chosen for the growth of the thin films characterized in the post-growth studies. All the parameters used for the deposition of the TiO<sub>2</sub> and Al<sub>2</sub>O<sub>3</sub> films using TiCl<sub>4</sub>-O<sub>3</sub> and AlCl<sub>3</sub>-O<sub>3</sub> processes are described in detail in the original publications [I–III].

To test the concept of the ALD reactor designed in this work for depositing ALD thin films onto the inner walls of hollow bodies, the well-known TiO<sub>2</sub> thin film deposition process using TiCl<sub>4</sub> (99.9%, Aldrich) and H<sub>2</sub>O precursors was studied by QCM. In these experiments, nitrogen (99.999%, Eesti AGA AS) was used as a carrier and purge gas. The gas pressure in the reaction chamber was maintained below 10 mbar during the deposition. The vapors of TiCl<sub>4</sub> and deionized water were led into the reactor from external reservoirs held at room temperature (20–23°C).

According to the QCM data, the ALD cycle times that allowed self-limited deposition in a container with a diameter of 100 mm and volume of 2 dm<sup>3</sup> were determined to be 5 s–5 s–5 s–10 s for the TiCl<sub>4</sub> pulse–first purge–H<sub>2</sub>O pulse–second purge sequence. These process parameters were used for the deposition of TiO<sub>2</sub> films on the inner walls of the container, as well as on pieces of a Si(100) wafer that were used as test samples and placed into the reactor using a special sample holder. The TiCl<sub>4</sub>-H<sub>2</sub>O ALD process was also used to investigate the efficiency of different surface pretreatments for cleaning the metal substrates.

### 4.3 Characterization of the thin films

The compositions and mass thicknesses of the deposited films were measured with an X-ray fluorescence (XRF) spectrometer-analyzer (ZSX 400, Rigaku). Supplementary information on the film thicknesses and interfacial layers formed between the substrate and film were obtained using a spectroscopic ellipsometer (GES5E, Semilab Sopra). Spectroscopic ellipsometry (SE) was used also for characterization of the refractive indices.

Crystal structures were characterized by grazing incidence X-ray diffraction (GIXRD) using a SmartLab X-ray diffractometer (Rigaku) with Cu K $\alpha$  radiation. The incidence angles chosen for these measurements were 0.27–0.33°. The thickness, density, and surface roughness values of each sample were evaluated by the X-ray reflection (XRR) method using the same X-ray diffractometer. Atomic force microscopy (AFM) was conducted with an Autoprobe CP-II (Veeco Instruments Inc.) equipped with Si cantilevers (typical tip radius of  $\leq 10$  nm) to determine the root mean square (RMS) surface roughness values.

Raman spectra were recorded with an inVia micro-Raman spectrometer (Renishaw). The power of the incident 514-nm laser beam was set to be about 10 mW at the sample, and the spectra were recorded with a resolution of 1.5 cm $^{-1}$ . A Si reference sample was used for the calibration of the Raman shift. The Helios NanoLab 600 microscope was employed for HR-SEM studies to characterize the surface microstructure before and during the etching tests.

The etching rates of the films deposited on Si(100) were determined in an 80% solution of H<sub>2</sub>SO<sub>4</sub> (95%, Sigma-Aldrich) in deionized water. The etching tests were performed in a stepwise manner, with etching steps ranging from 30 s to 5 h depending on the etching rate. Before and after each etching step, the mass thickness and structure of the film was determined with XRF and GIXRD, respectively. Other details of the testing process and measurement conditions are described in the original publication [III].

To test the barrier properties of the coatings, pitting tests of the films deposited on AISI 310 were carried out in a 6 mass% FeCl<sub>3</sub> solution at 22°C according to the ASTM 48G-11 standard test procedure. The other sides of the samples used in these tests were coated with a commercially available protective paint (Rust Stop 4 in 1, MOTIP DUPLI) according to the manufacturer's instructions. During these tests, the sample surfaces were investigated using optical microscopy after 1, 2, 4, 8, 26, 50, and 74 h.

The films deposited on AISI 310 were also etched at 110°C in a solution containing H<sub>3</sub>PO<sub>4</sub>, HNO<sub>3</sub>, HCl, H<sub>2</sub>SO<sub>4</sub>, and H<sub>2</sub>O in a volume ratio of 15:2:5:5:73. Etching steps with durations of 10–70 min were used. After each step, the mass change was determined to characterize the etching rate, as described in the corresponding original publication [III]. The mass changes of the samples were determined with an analytical balance (ABS 220-4, Kern & Sohn) with an accuracy of 1 mg.

## 5. RESULTS AND DISCUSSION

This Chapter describes the development of an ALD reactor suitable for depositing thin films onto the interior surfaces of hollow bodies [IV, V], and summarizes the results of investigation of  $\text{TiCl}_4\text{-O}_3$  and  $\text{AlCl}_3\text{-O}_3$  ALD processes for the deposition of  $\text{TiO}_2$  and  $\text{Al}_2\text{O}_3$  films [I, II]. Additionally, the main properties of the films and, in particular, their chemical stability in wet corrosive environments are described [III].

### 5.1 Coating the inner surfaces of hollow bodies

#### 5.1.1 Reactor for coating the inner walls of hollow bodies

One objective of this research was to develop an ALD apparatus capable of depositing diffusion barrier layers on the inner surfaces of hollow bodies (e.g., containers). In the equipment developed [IV, V], a hollow body connected to the vacuum and precursor supply lines is used as the reaction chamber (Fig. 3) where the thin film deposition takes place. The precursors are transported to the bottom of the interior of the body (Fig. 3) using a separate input line for each precursor to avoid any possible chemical reactions inside the gas lines. The gaseous reaction products and excess precursors are pumped out of the body through the orifice connected to the evacuation system. The evacuation system that consists of the exhaust piping, hot and sorption traps, and vacuum pump ensures the base pressure and a continuous carrier gas flow in the reaction zone. The flow levels of the carrier gas and precursors can be adjusted and controlled using needle and pneumatic valves. The pneumatic valves are operated by a control system, enabling the generation of the cycling sequence needed for the ALD-type growth.

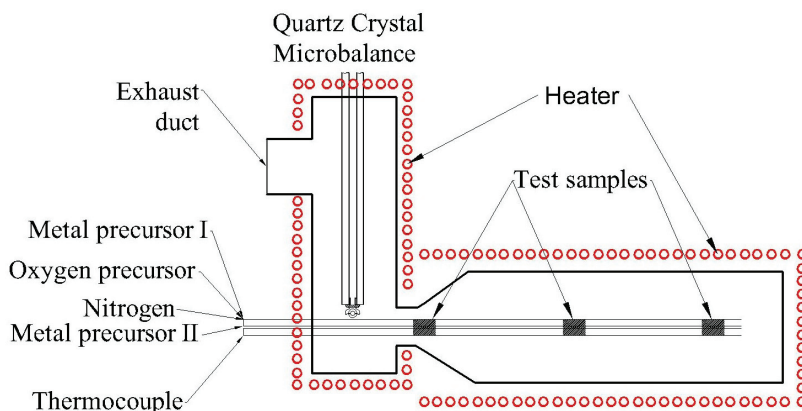


**Figure 3.** Schematic drawing describing the operation principle of the ALD reactor designed for coating the inner walls of hollow bodies.

The reaction chamber (i.e., the hollow body) is surrounded by a heater that ensures a temperature (distribution) suitable for ALD is achieved. The precursor supply and evacuation lines can also be heated to avoid the condensation of precursors and gaseous reaction products in these parts of the equipment. To optimize precursor delivery (precursor doses, precursor pulse durations, and purge periods) and to characterize the ALD processes in real time, a QCM mass sensor can be inserted into the evacuation line close to the reaction chamber outlet (Fig. 3). For additional evaluations of the deposition quality and thin film properties, it is possible to insert up to three test samples with maximum sizes of 15 mm × 15 mm into the interior of the hollow body by using sample holders connected to the precursor supply lines (Fig. 3).

### **5.1.2 Growth of TiO<sub>2</sub> films from TiCl<sub>4</sub> and H<sub>2</sub>O on the inner walls of hollow bodies**

QCM studies carried out in a prototype reactor for coating the inner walls of hollow bodies demonstrated the possibility to obtain ALD-type growth of TiO<sub>2</sub> films using the well-known precursor combination of TiCl<sub>4</sub> and H<sub>2</sub>O (Fig. 4). During the QCM studies the container temperature was kept at 110°C. The relatively low  $T_G$  value was chosen for the test depositions because some components of the vacuum line that required heating to the deposition temperature during the QCM studies contained O-rings with a maximum working temperature of 150°C. Moreover, lower deposition temperatures require usually application of longer purge and pulse times. Therefore, the process parameters that provide the self-limited ALD-type growth at lower temperatures also give a similar growth mode at higher temperatures. Finally, at lower temperatures, the QCM signal is more stable and thus the results obtained are more reliable.

In the QCM studies, the durations of the TiCl<sub>4</sub> and H<sub>2</sub>O pulses and both purge periods were varied systematically while the other time parameters were set at sufficiently high values to ensure self-limited growth. The mass increase per cycle saturated when the durations of the TiCl<sub>4</sub> and H<sub>2</sub>O pulses and post-TiCl<sub>4</sub> purge reached 5 s (Fig. 4); this behavior is similar to that reported earlier for the TiCl<sub>4</sub>-H<sub>2</sub>O [117] and TiCl<sub>4</sub>-O<sub>3</sub> [I] processes. A two times longer (10 s) purge duration was needed after the H<sub>2</sub>O pulse to avoid the overlap of the two successive precursor pulses. The need for a longer purge after the H<sub>2</sub>O pulse is, however, not surprising as water desorbs relatively slowly from solid surfaces, i.e., from the inner walls of the ALD reaction chamber and precursor supply lines [192].

To reduce the purge duration, higher nitrogen flows together with increased pumping speeds have usually been applied to ensure the faster and more efficient removal of precursors from the reaction chamber. Unfortunately, in our experiment, the gas cylinders used as reaction chambers had relatively small inlet diameters compared to the diameter of the cylinder itself. Owing to the bottleneck effect, increasing the carrier gas flow would have increased the

pressure inside of the cylinder. As shown in the case of  $\text{HfCl}_4\text{-H}_2\text{O}$  and  $\text{ZrCl}_4\text{-H}_2\text{O}$  processes [192], such changes in pressure might have had a detrimental influence on the ALD film growth. Therefore, to enable the comparison of these results with those obtained in previous studies, increasing the durations of the ALD cycles was the preferred choice.

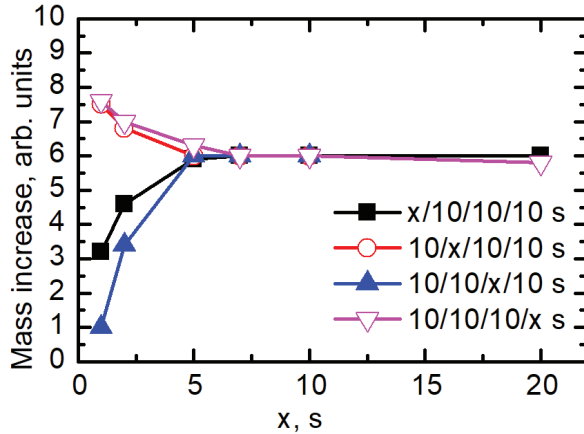


**Figure 4.** Mass increase per cycle determined by QCM as a function of ALD process time parameters.

According to the XRF measurements of the  $\text{TiO}_2$  films deposited on the test samples (Fig. 3) from  $\text{TiCl}_4$  and  $\text{H}_2\text{O}$  at  $110^\circ\text{C}$  by applying 500 ALD cycles, the mass thickness of the  $\text{TiO}_2$  deposited in the main part of the reactor did not differ by more than 5% (Figs. 3 and 5). A significant decrease (~25%) in  $\text{TiO}_2$  mass thickness was detected only for the reference samples positioned at the outlet of the chamber.

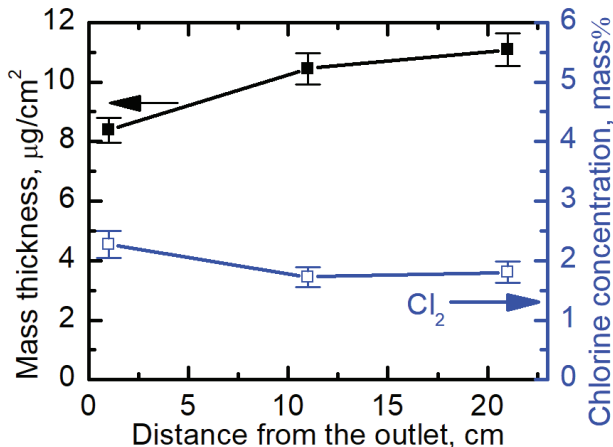


**Figure 5.** The dependence of the mass thickness and chlorine concentration on the position of reference samples inside the ALD reactor.

It should be mentioned that in this configuration the diameter of the reaction chamber was around four times smaller near the outlet than that of the rest of the chamber. Thus, the linear gas flow rate was more than an order of magnitude higher at the outlet. It has been demonstrated in earlier studies of  $\text{HfCl}_4\text{-H}_2\text{O}$  and  $\text{ZrCl}_4\text{-H}_2\text{O}$  processes that an increase in the carrier gas flow rate by 2.0–2.5 times may decrease the growth rate by up to 25–30% [192]. By correlating the growth rate with the chlorine concentration in the films, which increased from  $1.8 \pm 0.1$  mass% in the films grown at the bottom of the container to  $2.3 \pm 0.1$  mass% in those grown at the outlet, it can be concluded that increasing the linear gas flow rate reduces the efficiency of the chlorine replacement of surface species and therefore influences the film growth.

The growth rate of  $\text{TiO}_2$  reached 0.05 nm per cycle at the container outlet and 0.06 nm per cycle at the bottom. For comparison, the growth per cycle of 0.07 nm at 100°C and 0.06 nm at 125°C has previously been reported for this ALD process [193]. Thus, taking into account the influence of the carrier gas flow and  $T_G$  on the growth per cycle, one can conclude that ALD of  $\text{TiO}_2$  in the container was similar to that in a conventional ALD reactor.

## 5.2 Characterization of $\text{O}_3$ -based growth processes

### 5.2.1 $\text{TiCl}_4\text{-O}_3$ process

QCM studies demonstrated the possibility to deposit  $\text{TiO}_2$  from  $\text{TiCl}_4$  and  $\text{O}_3$  at  $\geq 225^\circ\text{C}$  [I]. At lower temperatures, no  $\text{TiO}_2$  film growth was observed, even if pulse times of up to 60 s were used. Similar results were obtained from post-growth studies of films deposited on Si(100) substrates (Fig. 6). Compared to the other processes used for the ALD of  $\text{TiO}_2$  films (Table 2), relatively high substrate temperatures were needed for the  $\text{TiCl}_4\text{-O}_3$  process. Only a few of the processes used, e.g.,  $\text{TiCl}_4\text{-CH}_3\text{OH}$ ,  $\text{TiF}_4\text{-H}_2\text{O}$ , and  $\text{TiOCH}(\text{CH}_3)_2(\text{C}_{11}\text{H}_{19}\text{O}_2)_2\text{-H}_2\text{O}$ , have required similar or higher temperatures to enable the ALD-type growth. The growth rate achieved at 225°C was still low compared to the process involving  $\text{H}_2\text{O}$  [I], but it was comparable with the growth rate obtained in the  $\text{Ti}[\text{OCH}(\text{CH}_3)_2]_4\text{-H}_2\text{O}$  process (Fig. 6). With the increase of  $T_G$  from 225 to 275°C, the growth rate increased up to 0.073 nm per cycle, which is considerably higher than that in the  $\text{Ti}[\text{OCH}(\text{CH}_3)_2]_4\text{-H}_2\text{O}$  process and slightly higher than that in the  $\text{TiCl}_4\text{-H}_2\text{O}$  process. This difference arises from the efficient generation of  $\text{TiCl}_4$  adsorption sites in the  $\text{TiCl}_4\text{-O}_3$  process at  $T_G \geq 275^\circ\text{C}$  (Fig. 6). Moreover, varying the pulse durations revealed that the pulses needed to achieve saturation in the range of 225–275°C were markedly longer with  $\text{TiCl}_4\text{-O}_3$  than with  $\text{TiCl}_4\text{-H}_2\text{O}$  [I]. This occurs since the adsorption reactions in this  $\text{O}_3$ -based process are slower at these temperatures than the corresponding reactions involving  $\text{H}_2\text{O}$  as the oxygen precursor. On increasing the temperature from 275 to 600°C, the growth rate decreased similarly in the  $\text{TiCl}_4\text{-O}_3$  and  $\text{TiCl}_4\text{-H}_2\text{O}$  processes (Fig. 6). However, the growth rate of the  $\text{O}_3$ -based process remained slightly higher, especially at 500–600°C.

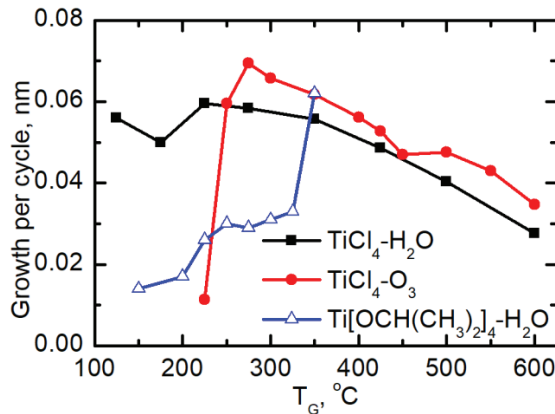


**Figure 6.** Influence of  $T_G$  on  $TiO_2$  film growth per cycle for  $TiCl_4 \cdot H_2O$  [I],  $TiCl_4 \cdot O_3$  [I] and  $Ti[OCH(CH_3)_2]_4 \cdot H_2O$  [194] processes.

Owing to the similar behaviors of the  $TiCl_4 \cdot O_3$  and  $TiCl_4 \cdot H_2O$  processes, the possibility that  $H_2O$  residues present in the carrier gas and/or  $O_2$  could contribute to the deposition of  $TiO_2$  from  $TiCl_4$  and  $O_3$  was checked. In these tests,  $O_2$  was supplied through the  $O_3$  generator that was switched off. In these experiments, however, only a 1 nm-thick  $TiO_2$  film grew on the Si(100) substrate during 1000 ALD cycles [I]. Therefore, the contribution of  $H_2O$  residues is not notable. As the formation of  $TiO_2$  from  $TiCl_4$  and  $O_3$  does not proceed via intermediate hydroxyl groups, the contribution of oxygen bridges – which are expected to participate in surface reactions at higher temperatures [195] – and the effect of excess oxygen had to be considered. Previously, Knapas et al. [196] found that the surface adsorption of excess oxygen during the  $O_3$  pulse could, similarly to hydroxyl groups, enable the formation of intermediate oxychlorides species on the surface and enable ALD in some  $O_3$ -based processes. A similar conclusion was reached based on thermodynamic data [197], which showed that  $TiCl_4$  could not react with  $TiO_2$  at the temperatures used in our experiments.

Different growth rate behaviors were observed for  $TiO_2$  films deposited from  $TiCl_4$  and  $O_3$  on  $RuO_2$  and r-sapphire ( $\alpha\text{-Al}_2\text{O}_3(012)$ ) substrates (Fig. 7). For example, on r-sapphire, the highest growth rate (0.061 nm) was achieved at 300°C while in the range 400–600°C, the growth rate remained at 0.038–0.044 nm per cycle [198]. On  $RuO_2$ , a relatively high growth rate (0.037 nm per cycle for 10 nm-thick films) was achieved also at 225°C [199]. However, with increasing thickness, the difference in growth rates on the Si and  $RuO_2$  substrates decreased. Hence, the higher growth rate on  $RuO_2$  compared to that on Si was clearly caused by the additional oxidation of  $RuO_2$  by  $O_3$  [200] and the contribution of this additional oxygen to the further deposition of  $TiO_2$  [199]. The rapid increase in growth rate obtained on  $RuO_2$  with increasing  $T_G$  values above 400°C was probably related to the decomposition of  $RuO_2$  during the ALD of  $TiO_2$ . This phenomenon has been employed by Jeon et al. [201] to

explain the similar growth rate increase observed when increasing the  $T_G$  above 370°C in the deposition of TiO<sub>2</sub> on RuO<sub>2</sub> from Ti[O(C<sub>3</sub>H<sub>7</sub>)<sub>4</sub>-O<sub>3</sub>. In the latter case, however, also the decomposition of Ti[O(C<sub>3</sub>H<sub>7</sub>)<sub>4</sub> could have contributed to the growth rate increase.

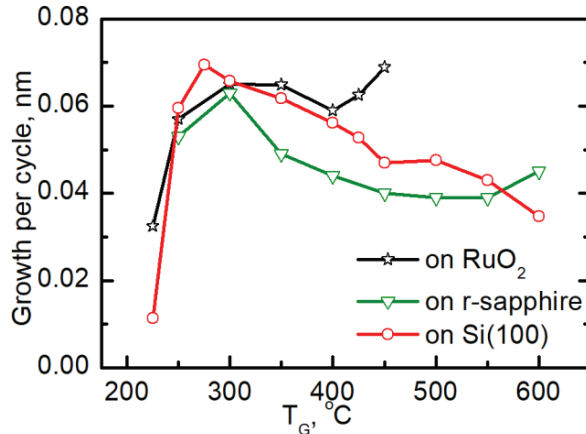


**Figure 7.** Influence of  $T_G$  on growth per cycle of TiO<sub>2</sub> films deposited in TiCl<sub>4</sub>-O<sub>3</sub> process on Si(100) [I], RuO<sub>2</sub> [198] and r-sapphire [199].

### 5.2.2 AlCl<sub>3</sub>-O<sub>3</sub> process

The ALD-type growth of Al<sub>2</sub>O<sub>3</sub> using AlCl<sub>3</sub> and O<sub>3</sub> precursors was obtained at substrate temperatures ranging from 300 to 450°C [II]. The lower growth rate obtained using this precursor combination at 300°C (Fig. 8), and the four times higher chlorine concentration in the films (0.4 at%) compared to the corresponding values measured for films deposited in AlCl<sub>3</sub>-H<sub>2</sub>O process, arise from the insufficient reactivity of O<sub>3</sub>. However, by increasing the temperature from 300 to 350°C, the growth rate increased to 0.069 nm per cycle (Fig. 8) and the chlorine concentration decreased to 0.05 at%. The latter value was even lower than that obtained with the AlCl<sub>3</sub>-H<sub>2</sub>O process. A similar behavior has been previously demonstrated when O<sub>3</sub> was used instead of water vapor together with TMA; a lower concentration of carbon impurities in the films was obtained [202]. In the TMA-based processes, Elliott et al. [203] demonstrated that the surface reactions that occur with both H<sub>2</sub>O and O<sub>3</sub> oxygen sources depend on the formation of surface hydroxyl groups. As a control experiment, deposition at 350°C was performed without switching on the O<sub>3</sub> generator to test whether water or oxygen residues in the carrier gas influence the growth of the films in the AlCl<sub>3</sub>-based process. No film growth was obtained in these experiments. Therefore, it could be concluded that film growth was obtained via reactions involving only AlCl<sub>3</sub> and O<sub>3</sub> as the precursors, and that O<sub>2</sub> was not reactive enough for ALD at these process parameters.

The lower growth rates of the  $\text{Al}_2\text{O}_3$  films obtained with  $\text{AlCl}_3\text{-O}_3$  compared to those observed for  $\text{AlCl}_3\text{-H}_2\text{O}$  process, and the narrower effective  $T_G$  range of the  $\text{AlCl}_3\text{-O}_3$  process compared to those of other metal chloride and  $\text{O}_3$  processes [60, 204, I], arise from the insufficient adsorption of oxygen onto the  $\text{Al}_2\text{O}_3$  film surface. As discussed in Section 5.2.1, excess oxygen might be required for the adsorption of the metal precursor in  $\text{O}_3$ -based processes. The studies on the ALD of layered  $\text{Al}_2\text{O}_3/\text{TiO}_2$  films with chloride– $\text{O}_3$  processes support this assumption. During the first ALD cycle, the growth rate of  $\text{Al}_2\text{O}_3$  on  $\text{TiO}_2$  was about three times higher than that on  $\text{Al}_2\text{O}_3$  [II], while the growth rate of  $\text{TiO}_2$  was around two times higher on  $\text{TiO}_2$  than on  $\text{Al}_2\text{O}_3$ . These results arise from the higher adsorption efficiency of chlorides on  $\text{TiO}_2$ , which is most likely due to the higher concentration of excess oxygen in  $\text{TiO}_2$  than in  $\text{Al}_2\text{O}_3$ .

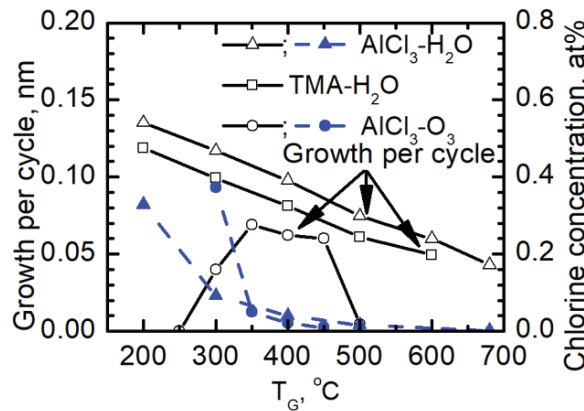


**Figure 8.** Effect of  $T_G$  on growth per cycle (open symbols) of  $\text{Al}_2\text{O}_3$  films deposited in  $\text{AlCl}_3\text{-O}_3$ ,  $\text{AlCl}_3\text{-H}_2\text{O}$ , and  $\text{TMA-H}_2\text{O}$  processes and on chlorine concentration (closed symbols) of films deposited in  $\text{AlCl}_3\text{-O}_3$  and  $\text{AlCl}_3\text{-H}_2\text{O}$  processes [I]. Reprinted with permissions from Elsevier B. V. (Thin Solid Films).

### 5.3 Physical properties of thin films deposited in $\text{TiCl}_4\text{-O}_3$ and $\text{AlCl}_3\text{-O}_3$ processes

The substrate material,  $T_G$ , and film thickness markedly influenced the structure and therefore also other properties, e.g., roughness and density of the  $\text{TiO}_2$  films deposited from  $\text{TiCl}_4$  and  $\text{O}_3$  [198, 199, I]. The deposition of amorphous films with densities of 3.7–3.8 g/cm<sup>3</sup> (Fig. 9) was attained on Si(100) surfaces at 225–400°C, provided that the film thickness did not exceed 7 nm [I]. In the thicker films, the formation of anatase-phase  $\text{TiO}_2$  on Si(100) was detected at  $\geq 250^\circ\text{C}$ ; correspondingly, the density increased to 3.9 g/cm<sup>3</sup>. The presence of the rutile phase on Si(100) was confirmed only in the films deposited at 600°C [I]. However, the concentration of the rutile phase was lower than in films deposited using  $\text{TiCl}_4\text{-H}_2\text{O}$  at the same temperature [I].

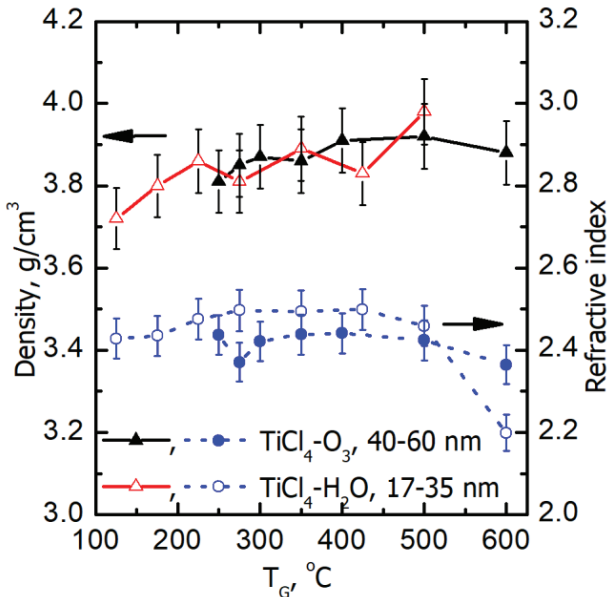


**Figure 9.** Effect of  $T_G$  on density and refractive index of  $\text{TiO}_2$  films deposited in  $\text{TiCl}_4\text{-O}_3$  and  $\text{TiCl}_4\text{-H}_2\text{O}$  ALD processes by applying 1000 and 600 ALD cycles, respectively [I]. The densities were measured by XRR and refractive indices were determined by SE at a wavelength of 633 nm.

On  $\text{RuO}_2$  [199] and r-sapphire [198], however, the growth of the rutile phase was obtained with the  $\text{TiCl}_4\text{-O}_3$  process at temperatures as low as 225 and 300°C, respectively. In addition, on c-sapphire ( $\alpha\text{-Al}_2\text{O}_3$  (001)), a mixture of (100)-oriented rutile and  $\text{TiO}_2$ -II grew from  $\text{TiCl}_4\text{-O}_3$  at 400–600°C [198].

The ability to deposit rutile-phase  $\text{TiO}_2$  films on  $\text{RuO}_2$  at low temperatures enabled us to obtain dielectrics with relative permittivity values as high as 106–122, and prepare  $\text{Pt}/\text{TiO}_2/\text{RuO}_2$  structures with leakage current densities below  $10^{-7} \text{ A/cm}^2$  at capacitance equivalent thickness (CET) values of 0.41–0.45 nm [199]. The latter result is of particular importance in the development of capacitor structures for memory devices and several other components at nanoelectronics. The investigation of electrical characteristics demonstrated that replacing  $\text{H}_2\text{O}$  with an  $\text{O}_3$  oxygen precursor had a positive effect, and allowed the preparation of capacitor structures with a leakage current density as low as  $6.6 \times 10^{-8} \text{ A/cm}^2$  at 0.8 V and CET of 0.41 nm [205].

In addition to the changes in phase composition of the films deposited on  $\text{Si}(100)$  substrates, the crystal orientations in polycrystalline anatase films changed with increasing  $T_G$ . The increase of the  $T_G$  from 350 to 450°C reduced the intensity of the 101 anatase reflection that was the strongest one according to the powder diffraction pattern database (ICSD, FIZ Karlsruhe, collection code 202242) and dominated in the GIXRD patterns of the films deposited at 250–350°C (Fig. 10a). At the same time the intensity of the 004 anatase reflection increased significantly. For comparison, no significant changes in the

intensity of the main anatase Raman band ( $142\text{--}143\text{ cm}^{-1}$ ) was detected (Fig. 10b). Consequently, the decrease in the intensity of the GIXRD 101 reflection was due to changes in the crystallite orientations rather than in the phase composition, as Raman spectroscopy – which is less sensitive to crystallite orientation than X-ray diffraction (XRD) – showed no considerable decrease in the amounts of anatase in the films.

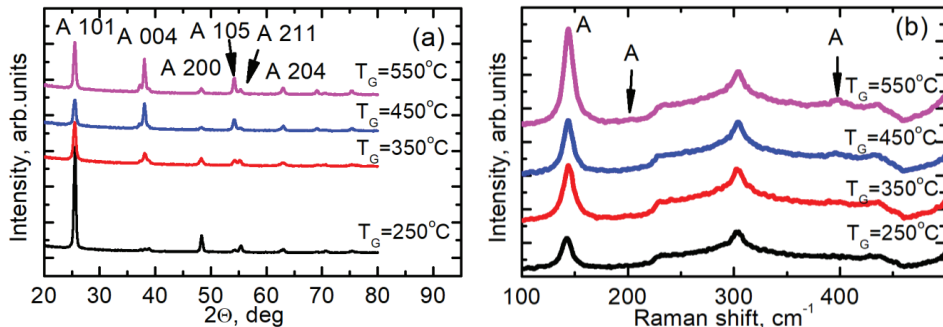


**Figure 10.** (a) GIXRD patterns and (b) RAMAN spectra of 26–44 nm-thick  $\text{TiO}_2$  films deposited by  $\text{TiCl}_4\text{-O}_3$  at different  $T_G$  values.

The HR-SEM studies of  $\text{TiO}_2$  films deposited at different temperatures demonstrated the marked dependence of grain size on  $T_G$  [III]. The lateral sizes of the grains formed in a 26 nm-thick film deposited at  $250^\circ\text{C}$  were about 10 times larger than the film thickness (Fig. 11a). Puurunen et al. [206] observed a similar phenomenon, and explained this in terms of the laterally spreading crystallization that occurs in amorphous films after the formation of crystalline nuclei that are located sufficiently far from each other.

With the increase of  $T_G$  from 250 to  $450^\circ\text{C}$ , the lateral grain sizes decreased by around six times, i.e., to 30–40 nm for the 35 nm-thick films (Figs. 11b, 11c). The further increase in  $T_G$  from 450 to  $550^\circ\text{C}$  increased the grain size to 50–80 nm for the 45 nm-thick  $\text{TiO}_2$  films (Fig. 11d).

An interesting result is that the large differences in grain sizes had only a minor influence on the surface roughness, determined to be 2.3, 2.5, and 2.8 nm for the 26, 36, and 35 nm-thick  $\text{TiO}_2$  films deposited at 250, 350, and  $450^\circ\text{C}$ , respectively (Fig. 12). A slightly different behavior was observed when the 56 and 57 nm-thick films (deposited at  $250^\circ\text{C}$  and  $400^\circ\text{C}$ , respectively) were investigated. The surface roughness decreased from 3.6 to 1.9 nm with the increase of  $T_G$  from 250 to  $400^\circ\text{C}$  [I]. However, in both cases, the further increase of  $T_G$  to  $550\text{--}600^\circ\text{C}$  increased the surface roughness to 5–6 nm.

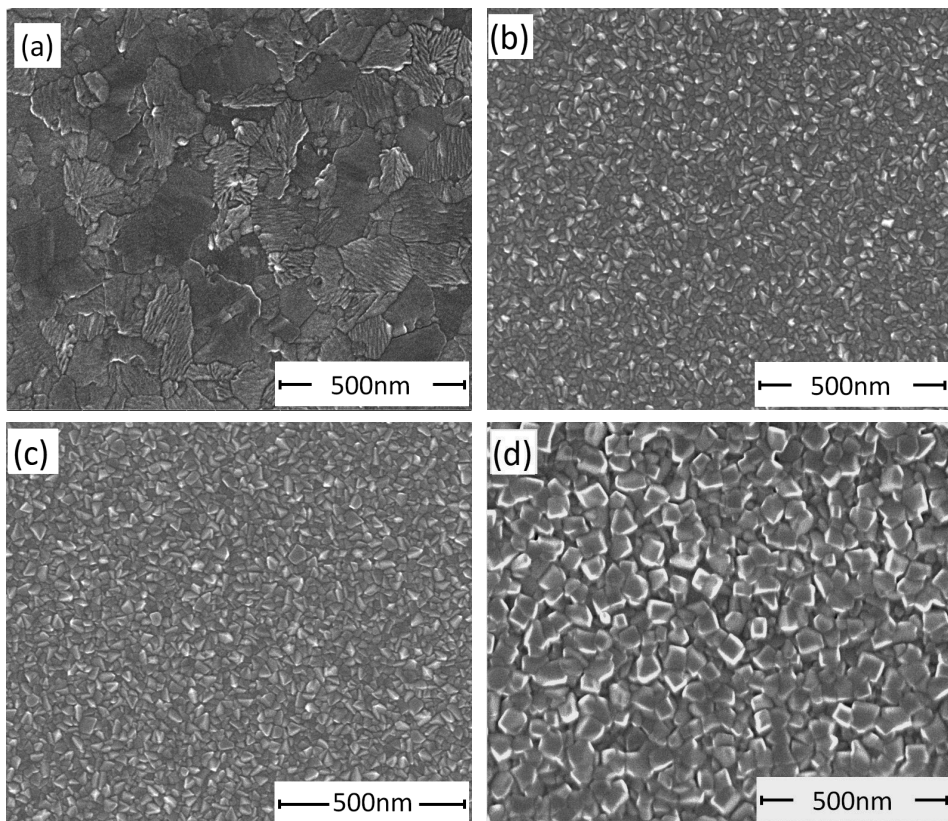


**Figure 11.** HR-SEM images of  $\text{TiO}_2$  films deposited at (a) 250, (b) 350, (c) 450, and (d) 550°C. The mass thicknesses of the films were (a) 26, (b) 36, (c) 35, and (d) 45 nm, respectively. Printed with permissions from Elsevier B.V, (Mater. Chem. Phys) [III].

The refractive indices determined at a wavelength of 633 nm for  $\text{TiO}_2$  films deposited from  $\text{TiCl}_4$  and  $\text{O}_3$  [I] were comparable to the corresponding values obtained for the films deposited using  $\text{TiCl}_4$  and  $\text{H}_2\text{O}$ , with values lying between 2.37 and 2.45 (Fig. 9). The lowest refractive indices obtained for the films deposited at 275 and 600°C were probably related to optical inhomogeneities caused by the transition from an amorphous to a randomly oriented polycrystalline structure at 275°C, and the high surface roughness of the films grown at 600°C [I].

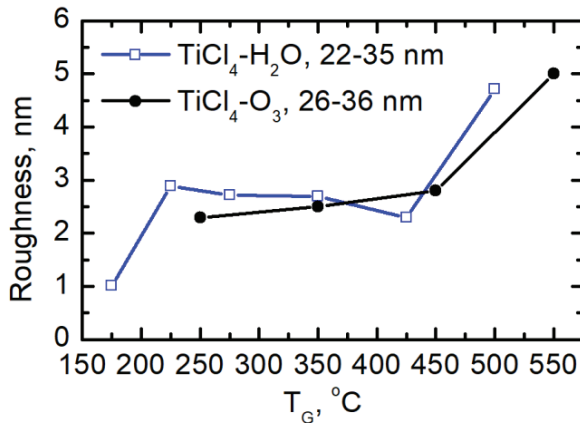


**Figure 12.** Effect of  $T_G$  on surface roughness of  $\text{TiO}_2$  films deposited in  $\text{TiCl}_4\text{-O}_3$  and  $\text{TiCl}_4\text{-H}_2\text{O}$  [I] ALD processes. The surface roughness was measured by XRR.

The  $\text{Al}_2\text{O}_3$  films deposited on  $\text{Si}(100)$  using  $\text{AlCl}_3$  and  $\text{O}_3$  were amorphous, and had roughness values of 0.5–1.1 nm, similar to the films deposited by other  $\text{Al}_2\text{O}_3$  ALD processes at these temperatures [II]. The film densities varied from 3.0 to  $3.2 \text{ g/cm}^3$ . Markedly higher  $\text{Al}_2\text{O}_3$  densities (up to  $3.7 \text{ g/cm}^3$ ) have been obtained in ALD processes only for crystalline films deposited at temperatures exceeding  $600^\circ\text{C}$  [86].

The refractive indices of the films deposited from  $\text{AlCl}_3$  and  $\text{O}_3$  were comparable to the corresponding values of  $\text{Al}_2\text{O}_3$  deposited from  $\text{AlCl}_3\text{-H}_2\text{O}$  and  $\text{TMA-H}_2\text{O}$  at  $300\text{--}600^\circ\text{C}$ , and were 1.67–1.69 at a wavelength of 633 nm [III].

#### 5.4 Chemical stability of $\text{Al}_2\text{O}_3$ and $\text{TiO}_2$ films deposited in $\text{TiCl}_4\text{-O}_3$ and $\text{AlCl}_3\text{-O}_3$ processes on Si substrates

Before applying materials in protective and barrier coatings, it is important to know their performance in aggressive environments, even if the primary role of the coatings is not protection against corrosion. For this reason, chemical tests were conducted on  $\text{Al}_2\text{O}_3$  and  $\text{TiO}_2$  films deposited on  $\text{Si}(100)$  at different temperatures.

The chemical stability tests performed in hot  $\text{H}_2\text{SO}_4$  for  $\text{Al}_2\text{O}_3$  deposited on  $\text{Si}(100)$  from  $\text{AlCl}_3$  and  $\text{O}_3$  demonstrated the significant dependence of the etching rate on  $T_G$ . With the increase of  $T_G$  from  $300$  to  $450^\circ\text{C}$ , the etching rate determined for the first 30 s of etching decreased from  $\geq 0.9 \text{ nm/s}$  to  $0.085\text{--}0.095 \text{ nm/s}$  (Fig. 13). This decrease correlated with the changes in concentration of the chlorine impurities from ( $0.4 \text{ at\%}$  at  $T_G = 300^\circ\text{C}$  to  $< 0.02 \text{ at\%}$  at  $T_G = 450^\circ\text{C}$ ) [III]. A similar dependence of the etching rate on  $T_G$  and the concentration of impurities (Fig. 13) has been previously reported for films deposited using  $\text{AlCl}_3$  and  $\text{H}_2\text{O}$  and tested in the same solution [15], and for

films deposited with TMA-H<sub>2</sub>O and TiCl<sub>4</sub>-H<sub>2</sub>O processes and tested in various etchants [178]. The etching rates of the Al<sub>2</sub>O<sub>3</sub> films deposited from AlCl<sub>3</sub> and O<sub>3</sub> increased to 0.16–0.21 nm/s when etched for 120 s (Fig. 13). A possible reason for this increase in etching rate could be the increased surface roughness. For instance, Gorrea et al. [207] demonstrated that the surface roughness of Al<sub>2</sub>O<sub>3</sub> deposited from TMA and H<sub>2</sub>O increased by two orders of magnitude during chemical stability tests in 1 M KCl. Surface roughness correlates with specific surface area and therefore should influence the contact area between Al<sub>2</sub>O<sub>3</sub> and the etchant. Consequently, this should have a direct effect on the etching process.

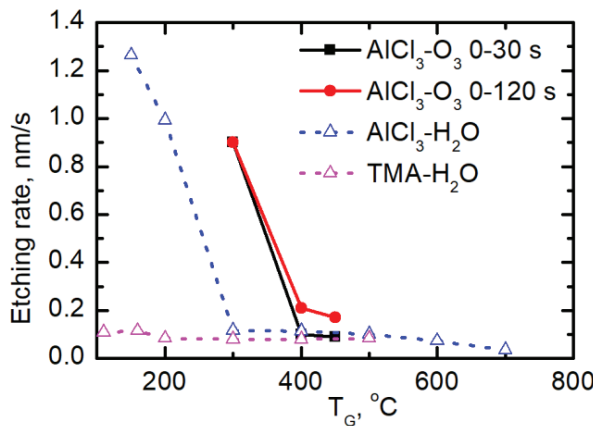


**Figure 13.** Dependence of the etching rate on  $T_G$  of Al<sub>2</sub>O<sub>3</sub> films deposited in AlCl<sub>3</sub>-O<sub>3</sub> [III], AlCl<sub>3</sub>-H<sub>2</sub>O [15] and TMA-H<sub>2</sub>O [15] processes.

In our etching experiments, however, the surface roughness remained between 0.6 and 1.2 nm for the 6–34 nm-thick Al<sub>2</sub>O<sub>3</sub> films deposited from AlCl<sub>3</sub> and O<sub>3</sub>. During the 120 s etching of a 34 nm-thick film deposited at 450°C, the surface roughness increased only from  $1.2 \pm 0.1$  to  $1.4 \pm 0.1$  nm, while the etching rate increased by a factor of two. Therefore, the changes in surface roughness were small and could not be the main reason for the increased etching rate in this case.

The etching rate of the TiO<sub>2</sub> films deposited on Si(100) from TiCl<sub>4</sub> and O<sub>3</sub> decreased with increasing  $T_G$  from 0.53–0.62 pm/s at 250°C to 0.22–0.49 pm/s at 450°C (Fig. 14). These etching rates were up to 1000 times lower than those measured for Al<sub>2</sub>O<sub>3</sub> and comparable to or slightly lower than those of the TiO<sub>2</sub> films deposited in the TiCl<sub>4</sub>-H<sub>2</sub>O process [15].

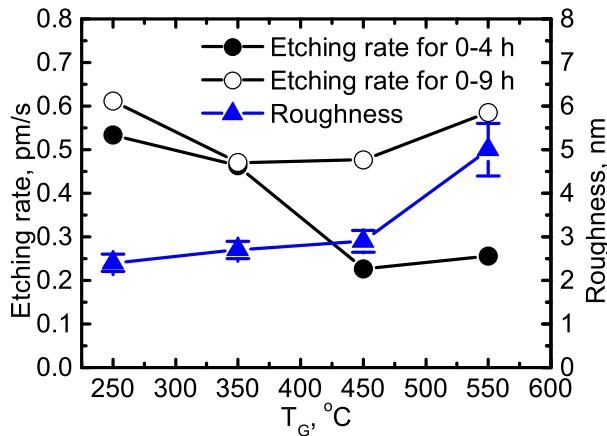


**Figure 14.** Etching rates and initial surface roughness values of 26–37 nm-thick TiO<sub>2</sub> films deposited at different temperatures [III]. Printed with permissions from Elsevier B. V. (Mater. Chem. Phys.).

The decrease in the etching rate of TiO<sub>2</sub> film correlated, similarly to that of the Al<sub>2</sub>O<sub>3</sub> films, with the concentration of chlorine impurities in the films. However, the chlorine concentration was as low as 0.12 at% in the films deposited from TiCl<sub>4</sub> and O<sub>3</sub> at 250°C, and ≤ 0.06 at% in the films deposited at 300°C and higher temperatures. It is hence unlikely that such a low chlorine concentration was the main factor influencing the etching rate of these films. Therefore, the correlation between the etching rate and film thickness, roughness, density, and structure was studied [III]. The etching rate was found to correlate significantly with the surface roughness only for films deposited at 450–550°C (Fig. 14). In this temperature range, the film density decreased from  $3.9 \pm 0.1$  to  $3.7 \pm 0.1$  g/cm<sup>3</sup> with the increase of  $T_g$  from 450 to 550°C. The lowered density can be related to the less perfect packing of crystallites in the films deposited at 550°C, and therefore is one potential reason for the increased etching rate.

It is worth mentioning that Puurunen et al. [178] reported the reduced chemical resistance for TiO<sub>2</sub> films containing crystallites with a “peculiar nature,” like those obtained in the TiO<sub>2</sub> films deposited from TiCl<sub>4</sub> and O<sub>3</sub> at 550°C (Fig. 11d). This result indicates that the etching rate might depend on the sizes as well as orientations of the crystallites in a film. As the TiO<sub>2</sub> films studied in our wet-chemistry tests were polycrystalline (Fig. 10), the different crystallite (grain) sizes and orientations obtained at different temperatures were considered as possible reasons for the different etching rates. The grain sizes were evaluated from HR-SEM images (Fig. 11) while the crystallite sizes were estimated from the full width at half maximum (FWHM) values of the GIXRD reflections. The HR-SEM images enabled the characterization of the lateral grain sizes, though the possibility that each grain could contain several crystallites had to be accounted for. In contrast, GIXRD allowed the determination of crystallite sizes only in the out-of-plane directions. No obvious

relationship between the etching rates and grain sizes of the as-deposited films could be detected [III], although some films with smaller lateral grain sizes and larger out-of-plane crystallite sizes showed lower etching rates.

Comparing the GIXRD patterns and etching data demonstrated that the decrease of etching rate with increasing  $T_G$  correlated with changes in the preferred orientation of the crystallites. In films with randomly orientated crystallites, the intensity ratio of the 004 and 101 anatase reflections was expected to be 0.22 (ICSD, FIZ Karlsruhe, collection code 202242). However, for the 26–37 nm-thick films, this ratio increased from 0.06 to 0.82 with the increase of  $T_G$  from 250 to 450°C. In addition, with the increase of the film thickness from 9 to 67 nm, the ratio determined for the films deposited at 450°C increased from 0.3 to 1.1. In both cases, the chemical resistance of the film increased, allowing us to conclude that crystallite orientation had an influence on this property.

## 5.5 Protective properties of $\text{TiO}_2$ and $\text{Al}_2\text{O}_3$ coatings deposited in $\text{TiCl}_4\text{-O}_3$ and $\text{AlCl}_3\text{-O}_3$ processes on AISI 310

Prolonging the lifetime of the AISI 310 alloy could be one possible application of the  $\text{TiO}_2$  and  $\text{Al}_2\text{O}_3$  thin coatings deposited using the  $\text{TiO}_2\text{-O}_3$  and  $\text{AlCl}_3\text{-O}_3$  processes. As such, the barrier properties of these coatings deposited at different temperatures and with various thicknesses will be described in this Chapter. It should be noted that the coating thicknesses reported in this Section were measured for the films grown on Si(100) substrates that were in the reactor simultaneously with the AISI 310 samples. Therefore, the coatings should have similar thicknesses on Si(100) and AISI310, but, according to cross-sectional HR-SEM studies, the thicknesses of ALD  $\text{Al}_2\text{O}_3$  coatings, can differ by up to 10% owing to the somewhat different nucleation conditions on the different substrates.

### 5.5.1 Pretreatment of the AISI 310 substrate surfaces before ALD

ALD is a result of successive chemical reactions on a solid surface; therefore, the film growth and resulting properties of coatings are affected by the substrate [208, 209]. Hence, different methods for pretreating the AISI 310 samples were tested, and the best method was selected for the following studies.

In these experiments, a well-known  $\text{TiCl}_4\text{-H}_2\text{O}$  ALD process was used to deposit  $\text{TiO}_2$  coatings by applying 1000 ALD cycles on samples with different surface pretreatments. Then, the chemical stability of each coating in Solution C (see Section 4.1) at 70°C was investigated. When the pretreatment involved an organic solution such as acetone, isopropyl alcohol, and toluene with or without a following Ar, N<sub>2</sub>, Ar/O<sub>2</sub>, or H<sub>2</sub> plasma clean, the  $\text{TiO}_2$  coatings caused no considerable increase of the acid resistance. Scanning electron microscopy (SEM)

showed that some surface areas staid still contaminated after the treatment (Fig. 15, darker area). According to the energy-dispersive X-ray (EDX) studies, these areas contained different carbon compounds. The surface contamination obviously caused the non-uniform nucleation and growth of the films, and so reduced the adhesion of the coating to the substrate. However, that the plasma treatment did not increase the quality of the TiO<sub>2</sub> coatings is surprising, as there are reports about employing plasma for cleaning stainless steel surfaces before deposition of coatings [210–212]. For instance, Härkönen et al. [212] concluded that the plasma pretreatment increased the corrosion protection properties of the ALD Al<sub>2</sub>O<sub>3</sub> coatings deposited on the top of a AISI 52100 low alloy steel sample. Nevertheless, similar problems with carbon contamination were encountered in their work [212]. Moreover, they demonstrated that the plasma cleaning results may vary significantly.

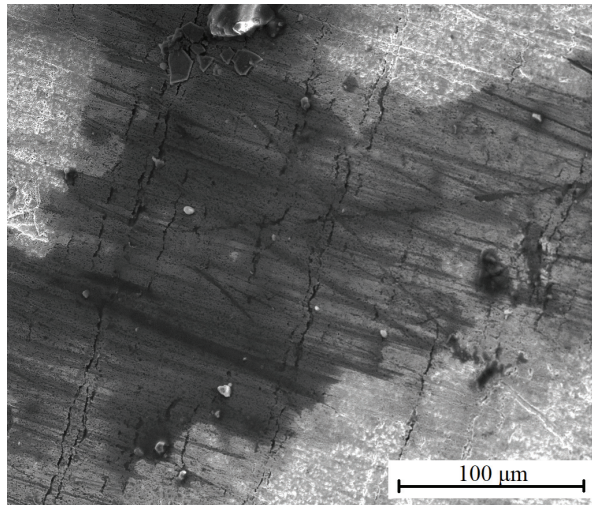


**Figure 15.** SEM image of the AISI 310 surface after pretreatment in toluene, acetone and isopropyl alcohol followed by treatment in Ar/O<sub>2</sub> plasma for 10 minutes.

In our experiments, the quality and barrier properties of the TiO<sub>2</sub> coatings deposited on AISI 310 samples increased when different acids, i.e., HNO<sub>3</sub>, HCl, H<sub>2</sub>SO<sub>4</sub>, and Solutions A, B, and C (see Section 4.1) were used for the pretreatment. The chemical resistance increased most significantly, when Solution C (15% H<sub>3</sub>PO<sub>4</sub>, 2% HNO<sub>3</sub>, 5% HCl, 5% H<sub>2</sub>SO<sub>4</sub>, and 73% water) was used for the surface pretreatment at 70°C. This treatment more than doubled the lifetime of the AISI 310 samples. SEM images (Fig. 16) showed that the porous top layer of AISI 310 was removed only during the pretreatment with Solution C. This appeared to be crucially important for releasing the carbon residues from the surface, reducing the surface porosity, and removing the contamination that may be present in the pores.

As demonstrated in Sections 5.3 and 5.4, the growth process and physical properties of the ALD coatings can depend on the material, composition, and

even crystal orientation of the substrate. Therefore, the results obtained for films deposited on other materials and even on other stainless steel alloys could differ. For this reason, treatment in Solution C at 70°C may not be the best choice for other materials. In the present work, however, this pretreatment preceded ALD on AISI 310 in all the experiments performed to test the barrier properties described in the following Sections.

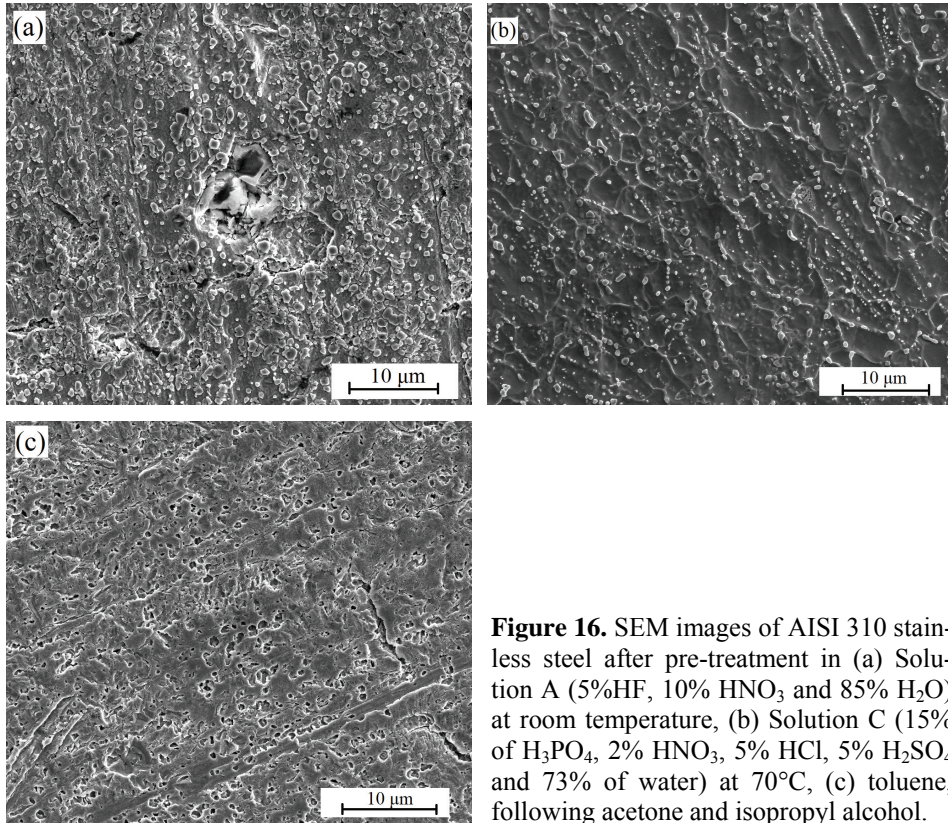


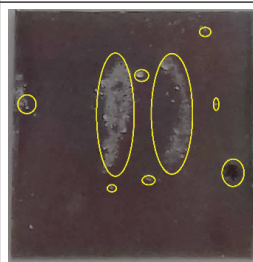
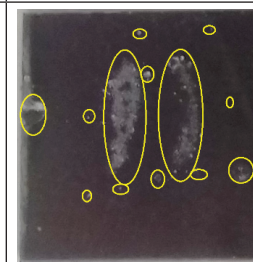
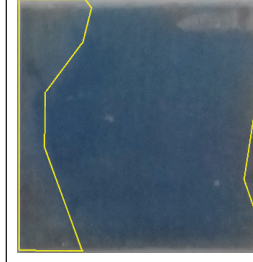
**Figure 16.** SEM images of AISI 310 stainless steel after pre-treatment in (a) Solution A (5%HF, 10% HNO<sub>3</sub> and 85% H<sub>2</sub>O) at room temperature, (b) Solution C (15% of H<sub>3</sub>PO<sub>4</sub>, 2% HNO<sub>3</sub>, 5% HCl, 5% H<sub>2</sub>SO<sub>4</sub> and 73% of water) at 70°C, (c) toluene, following acetone and isopropyl alcohol.

### 5.5.2 ASTM G48-11 pitting tests of AISI 310 samples coated with Al<sub>2</sub>O<sub>3</sub> and TiO<sub>2</sub>

The pitting corrosion resistance of the materials was evaluated by ASTM G48-11 tests [213]. This test imitates the material performance in seawater and strongly oxidizing chlorine-containing environments with a low pH [213]. In this work, the ASTM G48-11 tests (performance of coatings in 6 mass% FeCl<sub>3</sub> solution) were performed to investigate the influence of  $T_G$  and thickness on the protective properties of the coatings deposited on AISI 310 using the TiCl<sub>4</sub>-O<sub>3</sub> and AlCl<sub>3</sub>-O<sub>3</sub> processes.

Tests lasting 74 h were performed on 27–44 nm-thick TiO<sub>2</sub> coatings deposited at different temperatures. No signs of pitting corrosion appeared when the AISI 310 surface was coated with the 37 nm and 36 nm-thick films deposited at 350°C and 450°C, respectively (Table 4).

**Table 4.** Results of pitting tests for 26, 36 and 35 nm-thick TiO<sub>2</sub> coatings deposited at 250, 350 and 450°C, respectively, on AISI 310 from TiCl<sub>4</sub> and O<sub>3</sub>.

Time $T_G$ , °C	Before	After 26 h	After 74 h
250			
350			
450			

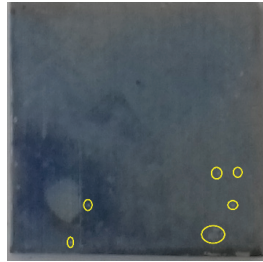
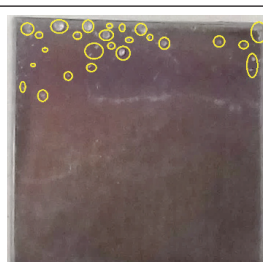
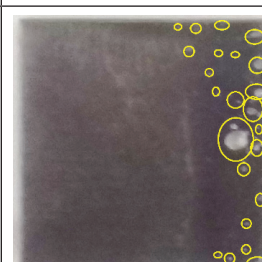
Although the coating deposited at 350°C started to delaminate from one side of the sample after 74 h of testing, this was due to sample handling rather than the lower quality of the coating. The lowest resistance to the 6 mass% FeCl<sub>3</sub> solution was detected for the 44 nm-thick TiO<sub>2</sub> coating deposited at 550°C. In this film, pinhole-type defects appeared during the first hour of testing. After the following 4 h of testing, no TiO<sub>2</sub> coating remained on the surface (image not presented in this work). As for the 27 nm-thick TiO<sub>2</sub> coatings deposited at 250°C, signs of pitting appeared after 26 h (Table 4). These results agree with those of the chemical resistance tests on Si(100) in 80% H<sub>2</sub>SO<sub>4</sub> (Section 5.4). In the latter tests, the highest etching rates during the first 4 h were obtained also

for  $\text{TiO}_2$  coatings deposited at 250 and 550°C (Fig. 14). A possible explanation for the lower barrier properties obtained for  $\text{TiO}_2$  coatings deposited at 250°C on both AISI 310 and Si(100) could be the higher concentration of impurities and unfavorable crystal structure of the coatings compared to those deposited at 350 or 450°C. The higher structural inhomogeneity of the  $\text{TiO}_2$  coatings deposited at 550°C (Sections 5.2 and 5.3) could enhance the possibility that the grain boundaries of polycrystalline coatings act as preferential routes for corrosive media and cause the formation of pinholes. It is worth noting that penetration of the etchant into the coating might increase the etching rate, as described in Section 5.4 for the coatings deposited at 550°C on Si(100) (Fig. 14). Similarly, once the 6 mass%  $\text{FeCl}_3$  solution has sufficient access to the AISI 310 substrate through the already generated pinholes, the lift-off of the remaining protective layer can occur, as can be seen in Table 4 (after 74 h testing of  $\text{TiO}_2$  coatings deposited at 350°C).

To evaluate the effect of coating thickness on the barrier properties of the  $\text{TiO}_2$  coatings, the ASTM G48-11 test was conducted on the 9, 19, 36, and 67 nm-thick films deposited on AISI 310 at 450°C (Table 5). The samples coated with 36 and 67 nm-thick  $\text{TiO}_2$  layers showed no signs of defect formation during the 74 h tests. However, in the coatings with thicknesses of 9 and 19 nm, pitting corrosion occurred after 26 h (Table 5). In the  $\text{H}_2\text{SO}_4$  etching tests of the coatings deposited on Si(100) (Section 5.4), the etching rate significantly decreased (from 3.5 to 0.8  $\text{pg}/\text{mm}^2/\text{s}$ ) with the increase of the coating thickness from 9 to 19 nm, and only slightly increased (from 0.8 to 0.6  $\text{pg}/\text{mm}^2/\text{s}$ ) with the following increase of the thickness to 67 nm [III]. The somewhat different barrier behavior on AISI 310 is probably due to differences in the thicknesses and structures of the coatings deposited on different substrates.

For the AISI 310 samples with the 31 and 23 nm-thick  $\text{Al}_2\text{O}_3$  coatings deposited from  $\text{AlCl}_3$  and  $\text{O}_3$  at 300 and 450°C, respectively, the first traces of corrosion were detected after 4 h of testing. (Table 6). However, the pinhole density was markedly higher in the coatings deposited at 450°C than 300°C. The highest resistance of  $\text{Al}_2\text{O}_3$  observed in the ASTM G48-11 tests was obtained for a 41 nm-thick coating deposited on the AISI 310 surface at 400°C (Table 6). Nevertheless, the durability of the coating (< 26 h) was more than three times shorter than that of the  $\text{TiO}_2$  coatings deposited at  $T_G$  values of 300–450°C from  $\text{TiCl}_4$  and  $\text{O}_3$ . The higher resistance of  $\text{TiO}_2$  was not surprising, considering the etching rates in  $\text{H}_2\text{SO}_4$  solution (Section 5.4) and the results reported by Puurunen et al. [178] for performance of  $\text{Al}_2\text{O}_3$  and  $\text{TiO}_2$  in various corrosive environments.

**Table 5.** Results of ASTM G48-11 pitting tests for TiO<sub>2</sub> coatings deposited on AISI 310 at 450°C from TiCl<sub>4</sub> and O<sub>3</sub> to different thicknesses.

Thickness \ Time	Before testing	After 26 h testing	After 74 h testing
67 nm			
36 nm			
19 nm			
9 nm			

**Table 6.** Results of ASTM G48-11 pitting tests for 31, 41 and 23 nm-thick  $\text{Al}_2\text{O}_3$  coatings deposited on AISI 310 from  $\text{AlCl}_3$  and  $\text{O}_3$  at 300, 400 and 450°C, respectively.

Time $T_G$ , °C \	Before testing	After 4 h testing	After 26 h testing
300			
400			
450			

### 5.5.3 Protective properties of $\text{TiO}_2$ coatings on stainless steel in a wet low-pH environment

To evaluate how the  $\text{TiO}_2$  coatings influence the lifetime of the AISI 310 stainless steel samples in a corrosive environment, the mass losses of coated and uncoated samples were measured. The tests were carried out at 110°C in Solution C, which was also chosen for the sample pretreatment, as described in Sections 4.1 and 5.5.1.

During 20 min, the uncoated samples lost about 34% of their mass. For comparison, the mass loss was only 8% for a sample with a 36 nm-thick  $\text{TiO}_2$  coating deposited at 450°C; 10% for a sample with a 37 nm-thick  $\text{TiO}_2$  coating deposited at 350°C; and 11% for a sample with a 27 nm-thick  $\text{TiO}_2$  coating deposited at 250°C [III]. Furthermore, even if the coatings started to fail at weak points during the early stages of etching (Fig. 17), the coatings continued to

protect the samples even after the etchant could access the metal through the defects. Therefore, these films markedly prolonged the possible functional lifetime of the material [III].

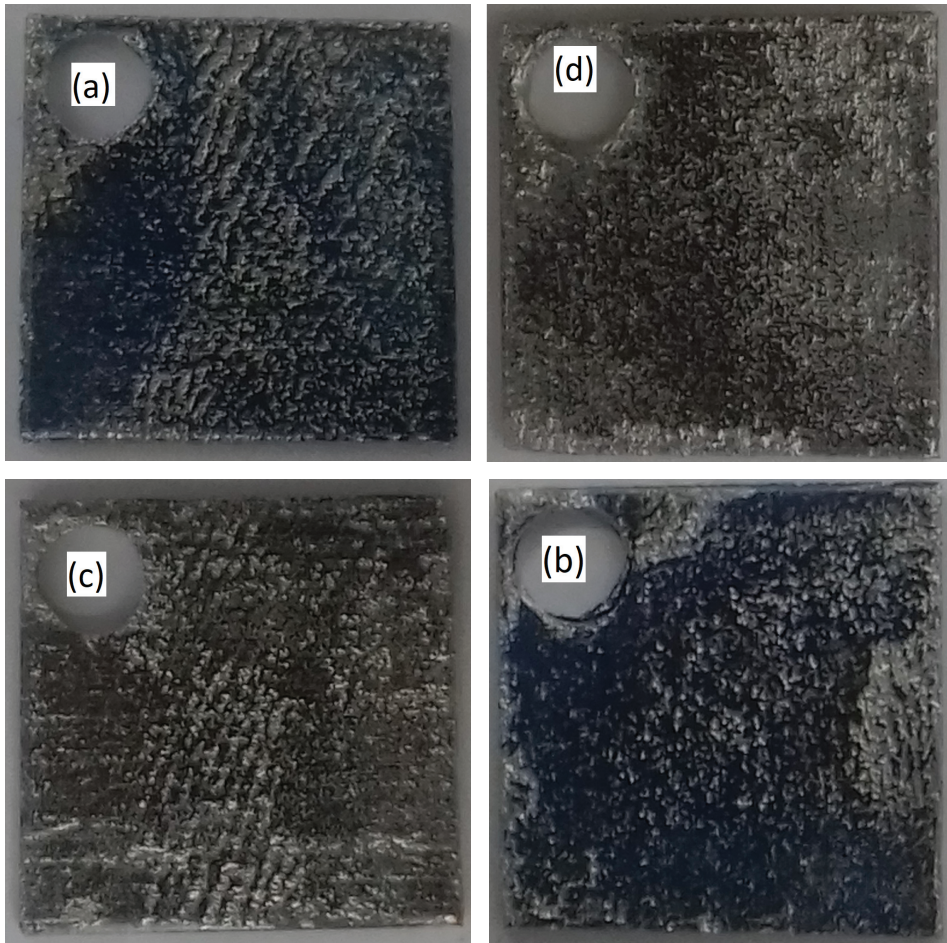


**Figure 17.** Photographs (a and b) of 36 nm-thick  $\text{TiO}_2$  coating deposited at 450°C and (c and d) 37 nm-thick  $\text{TiO}_2$  coating deposited at 350°C simultaneously on the both sides of the AISI 310 samples. Images of front sides (a and c) and back sides (b and d) of the coated samples were recorded after 20 min etching in solution C at 110°C.

Similar to the chemical resistance tests of the coatings deposited on Si(100) and ASTM G48-11 pitting tests of the coatings on AISI 310, these tests demonstrated that the highest acid resistance and best barrier properties were achieved with  $\text{TiO}_2$  coatings deposited from  $\text{TiCl}_4$  and  $\text{O}_3$  at 450°C [III]. Furthermore, our studies confirmed that ALD allows the conformal deposition of protective coatings on 3D samples, as no marked differences in performance of coatings on different sides of samples were observed (Fig. 17). The studies also confirmed that the lifetime of coatings deposited on AISI 310 depended on the concentration of weak points. The latter depends on the surface cleanliness, composition, and morphology, as discussed in previous publications [44, 214].

## SUMMARY AND CONCLUSIONS

To extend applications of ALD a special reactor for the deposition of thin films on the inner surfaces of hermetic containers was designed and constructed. The reactor was equipped with a QCM for the real-time characterization of the deposition. Also, it contained substrate holders that allowed test samples to be placed at different positions inside the container to study the film properties according to the sample location. Based on the QCM data recorded, it was demonstrated that by using the constructed reactor, the self-limited growth of  $\text{TiO}_2$  from  $\text{TiCl}_4$  and  $\text{H}_2\text{O}$  was achieved inside the containers. The growth rates of the  $\text{TiO}_2$  films deposited at 110°C on Si(100) test samples placed at three positions in the reactor remained between 0.05 and 0.06 nm per cycle, while the growth rate variations were mainly due to differences in the linear speed of the gas flow in the container.

The deposition of  $\text{TiO}_2$  films using  $\text{TiCl}_4$  and  $\text{O}_3$  was demonstrated at substrate temperatures of 225–600°C. Growth rates of up to 0.07 nm per cycle at 275°C were obtained on Si(100) substrates. This growth rate was higher than the corresponding value of 0.06 nm per cycle obtained for the  $\text{H}_2\text{O}$ -based process at the same temperature in the same reactor. The structure of the  $\text{TiO}_2$  films depended on the deposition temperature and substrates. Films containing amorphous, anatase, rutile, and/or  $\text{TiO}_2$ -II phases were obtained in the  $\text{TiCl}_4$ - $\text{O}_3$  ALD process. The ALD of  $\text{Al}_2\text{O}_3$  films from  $\text{AlCl}_3$  and  $\text{O}_3$  was also demonstrated at temperatures ranging from 300 to 450°C. All the  $\text{Al}_2\text{O}_3$  films deposited were amorphous, with lower growth rates than those obtained in the  $\text{AlCl}_3$ - $\text{H}_2\text{O}$  process at the same temperatures. The highest growth rate of 0.07 nm per cycle was observed for the  $\text{AlCl}_3$ - $\text{O}_3$  process at a substrate temperature of 350°C.

The chemical stabilities of the  $\text{TiO}_2$  and  $\text{Al}_2\text{O}_3$  films deposited on Si(100) using  $\text{TiCl}_4$ - $\text{O}_3$  and  $\text{AlCl}_3$ - $\text{O}_3$  precursor combinations were tested in hot  $\text{H}_2\text{SO}_4$ . According to these tests, the chemical stability depended on the deposition temperature, composition, and structure of the film. The lowest etching rate of 0.2 pm/s (6.3  $\mu\text{m}$ /per year) was obtained for  $\text{TiO}_2$  films containing the anatase phase deposited at 450°C. The etching rate of the  $\text{Al}_2\text{O}_3$  films depended mainly on the amount of chlorine residues in the film, with the lowest values ranging from 0.09 to 0.10 nm/s (2.8–3.2 mm/per year) for films deposited at 450°C.

The protective properties of the  $\text{TiO}_2$  and  $\text{Al}_2\text{O}_3$  films deposited in the  $\text{TiCl}_4$ - $\text{O}_3$  and  $\text{AlCl}_3$ - $\text{O}_3$  ALD processes on AISI 310 stainless steel were evaluated using the ASTM G48-11 pitting test. In addition, the  $\text{TiO}_2$  films were tested by etching in a solution containing 15%  $\text{H}_3\text{PO}_4$ , 2%  $\text{HNO}_3$ , 5%  $\text{HCl}$ , 5%  $\text{H}_2\text{SO}_4$ , and 73%  $\text{H}_2\text{O}$ . According to both tests, most of the films deposited on the AISI 310 surface prolonged the lifetime of the material. The best protection was achieved with  $\text{TiO}_2$  films with thicknesses of  $\geq 36$  nm deposited at 450°C. The results allowed us to conclude that the  $\text{TiO}_2$  and  $\text{Al}_2\text{O}_3$  films deposited using the  $\text{TiCl}_4$ - $\text{O}_3$  and  $\text{AlCl}_3$ - $\text{O}_3$  ALD processes have marked potential to be applied as protective coatings in the future.

## SUMMARY IN ESTONIAN

### Õhukeste kilede aatomkihtsadestamine, karakteriseerimine ja rakendamine kaitsekatetena

Eesmärgiga avardada aatomkihtsadestamise rakendusvõimalusi konstrueeriti uurimistöö käigus spetsiaalne reaktor, mis võimaldab sadestada kaitsekatteid hermeetiliste anumate sisepindadele. Loodud reaktor varustati sadestamisprotsessi reaalajalist jälgimist võimaldava kvartsresonantskaalumise süsteemiga. Selleks, et koguda infot sadestatud kilede omaduste kohta, varustati reaktor objektihoidjatega, mis võimaldasid paigutada testobjekte erinevatesse kohtadesse anuma sisemusse. Kvartsresonantskaaluga  $110^{\circ}\text{C}$  juures läbi viidud mõõtmiste tulemustest oli võimalik järeltõsta, et valminud reaktoris saab sadestada kilesid iseküllastuvas, aatomkihtsadestamisele omases režiimis. Proovisadesstused, milles lähteainetena olid kasutusel  $\text{TiCl}_4$  ja  $\text{H}_2\text{O}$ , näitasid, et  $\text{TiO}_2$  kasvukiirus  $\text{Si}(100)$  katseobjektide pinnal jääb selles seadmes vahemikku  $0,05\text{--}0,06\text{ nm tsüklis}$  ja tulenevalt erinevast gaasivoo kiirusest anuma sees sõltus objekti asukohast.

Uurimistöös demonstreeriti võimalust  $\text{TiO}_2$  aatomkihtsadestamiseks temperatuuridel  $225\text{--}600^{\circ}\text{C}$  protsessis, milles lähteaineteks olid  $\text{TiCl}_4$  ja  $\text{O}_3$ . Suurim kasvukiirus räni pinnal,  $0,07\text{ nm tsüklis}$ , saavutati  $275^{\circ}\text{C}$  juures. See kasvukiirus oli suurem, kui samal temperatuuril  $\text{TiCl}_4$  ja  $\text{H}_2\text{O}$  protsessis saadud kasvukiirus,  $0,06\text{ nm tsüklis}$ .  $\text{TiCl}_4\text{-O}_3$  protsessis sadestatud  $\text{TiO}_2$  struktuur sõltus sadestamise temperatuurist ja alusmaterjalist. Erinevatel alustel oli võimalik saada kas amorfseid või kristallilisi anataasi, rutiili ja/või  $\text{TiO}_2$  II faasi sisaldavaid kilesid.

Lisaks näidati uurimistöös, et kasvutemperatuuride vahemikus  $300\text{--}450^{\circ}\text{C}$  on võimalik sadestada  $\text{Al}_2\text{O}_3$  kilesid aatomkihtsadestamise protsessis, milles lähteaineteks olid  $\text{AlCl}_3$  ja  $\text{O}_3$ . Kõik sadestatud  $\text{Al}_2\text{O}_3$  kiledad olid amorfsed ja nende sadestamise kiirused olid veidi väiksemad kui  $\text{AlCl}_3\text{-H}_2\text{O}$  protsessile tüüpilised kasvukiirused samadel aluse temperatuuridel. Suurim  $\text{Al}_2\text{O}_3$  kasvukiirus,  $0,07\text{ nm tsüklis}$ , mõõdeti  $\text{AlCl}_3\text{-O}_3$  protsessis aluse temperatuuril  $350^{\circ}\text{C}$ .

Uurimistöös testiti  $\text{TiCl}_4\text{-O}_3$  ja  $\text{AlCl}_3\text{-O}_3$  protsessides  $\text{Si}(100)$  pinnale sadestatud  $\text{TiO}_2$  ja  $\text{Al}_2\text{O}_3$  kilede keemilist vastupidavust kuumas  $80\%$  väavelhappe lahuses. Saadud tulemuste järgi sõltus keemiline vastupidavus kile sadestamise temperatuurist, koostisest ja struktuurist. Madalaim söövituskiirus,  $0,2\text{ pm/s}$  ( $6,3\text{ }\mu\text{m}$  aastas), mõõdeti  $\text{TiO}_2$  kiledel, mis sisaldasid anataasi faasi ja olid sadestatud  $450^{\circ}\text{C}$  juures.  $\text{Al}_2\text{O}_3$  kilede söövituskiirus sõltus peamiselt klori jäädvusest ja oli madalaim, s.o  $0,09\text{--}0,10\text{ nm/s}$  ( $2,8\text{--}3,2\text{ mm aastas}$ ),  $450^{\circ}\text{C}$  juures sadestatud kiledel.

$\text{TiCl}_4\text{-O}_3$  ja  $\text{AlCl}_3\text{-O}_3$  protsessides AISI 310 roostevabale terasele sadestatud  $\text{TiO}_2$  ja  $\text{Al}_2\text{O}_3$  katete kaitsvaid omadusi hinnati ASTM G48-11 punktkorrosiooni testides. Lisaks sellele testiti ka  $\text{TiO}_2$  katete vastupidavust lahuses, mis sisaldas  $15\% \text{H}_3\text{PO}_4$ ,  $2\% \text{HNO}_3$ ,  $5\% \text{HCl}$ ,  $\text{H}_2\text{SO}_4$  ja  $73\% \text{H}_2\text{O}$ . Mõlema eelmainitud testi tulemuste järgi enamus AISI 310-le sadestatud katetest pikendas roostevaba

terase eluiga. Parim kaitse saadi siis, kui kasutati  $\geq 36$  nm paksuseid  $\text{TiO}_2$  katteid, mis sadestati 450°C juures. Töös kogutud tulemuste järgi on võimalik järeldada, et  $\text{TiCl}_4\text{-O}_3$  ja  $\text{AlCl}_3\text{-O}_3$  aatomkihtsadestamise protsesside abil valmistatud  $\text{TiO}_2$  and  $\text{Al}_2\text{O}_3$  õhukesed katted omavad suurt rakenduspotentsiaali kaitsekatetes.

## ACKNOWLEDGEMENTS

I would like to thank my supervisor Prof. Väino Sammelselg for the support and guidance during the years necessary to complete this thesis. I would like to express my gratitude to Tarvo Staal and Andrus Laur from Eesti AGA AS and Peter Adam from Linde AG for their support.

All the co-authors are thanked for their contribution in the publications. I am also thankful to all the personnel from the Laboratory of Thin-Film Technology for help and friendly working atmosphere. I wish to thank my family and all my friends for their support and patient during my PhD studies.

The thesis was supported by European Social Fund Internationalisation Program DoRa (30.1-6/886) and Graduate School of Doctoral Studies in Estonia: “Functional materials and technologies (1.2.0401.09-0079)”, by Estonian Ministry of Education and Research (Project IUT2-24), Estonian Science Foundation (Project 8666), by European Regional Development Fund sub-measures Estonian Centre of Excellence in Research (Projects TK117 and TK141) and Project Namur.



## REFERENCES

1. J. Niinistö, K. Kukli, M. Heikkilä, M. Ritala and M. Leskelä, Atomic Layer Deposition of High-k Oxides of the Group 4 Metals for Memory Applications, *Adv. Eng. Mater.*, 11 (2009) 223–234.
2. J. Maula, Atomic layer deposition for industrial optical coatings, *Chen. Opt. Lett.*, 8 (2010) 53–58.
3. W. Zhou, X. Dai, T.-M. Fu, C. Xie, J. Liu, C. M. Lieber, Long Term Stability of Nanowire Nanoelectronics in Physiological Environments. *Nano Lett.*, 14 (2014) 1614–1619.
4. A. Rosenthal, A. Tarre, A. Gerst, J. Sundqvist, A. Härsta, A. Aidla, J. Aarik, V. Sammelselg, T. Uustare, Gas sensing properties of epitaxial SnO<sub>2</sub> thin films prepared by atomic layer deposition, *Sens. Actuators, B* 93 (2003) 552–555.
5. A. Purniawana, P.J. French, G. Pandraud, P.M. Sarro, TiO<sub>2</sub> ALD Nanolayer as Evanescent Waveguide for Biomedical Sensor Applications, *Procedia Engineering*, 5 (2010) 1131–1135.
6. M. Cassir, A. Ringueude and L. Niinistö, Input of atomic layer deposition for solid oxide fuel cell applications, *J. Mater. Chem.*, 41 (2010) 8987–8993.
7. X. Meng, X. Q. Yang and X. L. Sun, Emerging Applications of Atomic Layer Deposition for Lithium-Ion Battery Studies, *Adv. Mater.*, 24 (2012) 3589–3615.
8. C. Marichy, M. Bechelany and N. Pinna, *Adv. Mater.*, 24 (2012) 1017–1032.
9. J. A. van Delft, D. Garcia-Alonso and W. M. M. Kessels, Atomic layer deposition for photovoltaics: applications and prospects for solar cell manufacturing, *Semicond. Sci. Technol.*, 27 (2012) 074002.
10. T. Wang, Z. B. Luo, C. C. Li and J. L. Gong, Controllable fabrication of nanostructured materials for photoelectrochemical water splitting via atomic layer deposition, *Chem. Soc. Rev.*, 43 (2014) 7469–7484.
11. R. Matero, M. Ritala, M. Leskelä, T. Salo, J. Aromaa, O. Forsen, Atomic layer deposited thin films for corrosion protection, *J. Phys. IV France*, 9 (1999) 493.
12. E. Marin, A. Lanzutti, F. Andreatta, M. Lekka, L. Guzman and L. Fedrizzi, Atomic layer deposition: state-of-the-art and research/industrial perspectives, *Corros. Rev.*, 29 (2011) 191–208.
13. M. D. Groner F. H. Fabreguette J. W. Elam, S. M. George, Low-Temperature Al<sub>2</sub>O<sub>3</sub> Atomic Layer Deposition, *Chem. Mater.*, 16 (2004) 639–645.
14. M. Ritala, M. Leskelä, *Handbook of Thin Film Materials*, Vol. 1, Nalwa, H.S. (Ed.), Academic Press, San Diego, (2001).
15. V. Sammelselg, I. Netšipailo, A. Aidla, A. Tarre, L. Aarik, J. Asari, P. Ritslaid, J. Aarik, Chemical resistance of thin film materials based on metal oxides grown by atomic layer deposition, *Thin Solid Films*, 542 (2013) 219–224.
16. X. Zhang, J. Zhao, A. V. Whitney, J. W. Elam, R. P. Van Duyne, Ultrastable Substrates for Surface-Enhanced Raman Spectroscopy: Al<sub>2</sub>O<sub>3</sub> Overlayers Fabricated by Atomic Layer Deposition Yield Improved Anthrax Biomarker Detection, *J. Am. Chem. Soc.*, 128 (2006) 10304–10309.
17. D. M. King, J. A. Spencer, X. Liang, L. F. Hakim and A. W. Weimer, Atomic layer deposition on particles using a fluidized bed reactor with in situ mass spectrometry, *Surf. Coat. Technol.*, 201 (2007) 9163–9171.
18. M. J. Pellin, J. W. Elam, J. F. Moore, ALD Capping Layers for Superconducting Radio Frequency Accelerator Cavities, *ECS Transactions*, 11 (2007) 23–28.

19. C.X. Shan, X. Hou, K.L. Choy, Corrosion resistance of TiO<sub>2</sub> films grown on stainless steel by atomic layer deposition, *Surf. Coat. Technol.*, 202 (2008) 2399–2402.
20. A. A. Dameron, S. D. Davidson, B. B. Burton, P. F. Garcia, R. S. McLean, S. M. George, Gas Diffusion Barriers on Polymers Using Multilayers Fabricated by Al<sub>2</sub>O<sub>3</sub> and Rapid SiO<sub>2</sub> Atomic Layer Deposition, *J. Phys. Chem., C*, 112 (2008) 4573–4580.
21. O. M. Hahtela, A. F. Satrapinski, P. H. Sievilä N. Chekurov, Atomic-Layer-Deposited Alumina (Al<sub>2</sub>O<sub>3</sub>) Coating on Thin-Film Cryoresistors, *IEEE Trans. Instrum. Meas.*, 58 (2009) 1183–1187.
22. P. Görnn, T. Riedl, W. Kowalsky, Encapsulation of Zinc Tin Oxide Based Thin Film Transistors, *J. Phys. Chem., C*, 113 (2009) 11126–11130.
23. X. H. Du, K. Zhang, K. Holland, T. Tombler, M. Moskovits, Chemical corrosion protection of optical components using atomic layer deposition, *Appl. Optics*, 48 (2009) 6470–6474.
24. S. D. Standridge, G. C. Schatz, J. T. Hupp, Distance Dependence of Plasmon-Enhanced Photocurrent in Dye-Sensitized Solar Cells, *Langmuir*, 25 (2009) 2596–2600.
25. E. Marin, L. Guzman, A. Lanzutti, L. Fedrizzi, M. Saikkonen, Chemical and electrochemical characterization of hybrid PVD + ALD hard coatings on tool steel, *Electrochim. Commun.*, 11 (2009) 2060–2063.
26. N. Padhy, S. Kamal, R. Chandra, U. K. Mudali, B. Raj, Corrosion performance of TiO<sub>2</sub> coated type 304L stainless steel in nitric acid medium, *Surf. Coat. Technol.*, 204 (2010) 2782–2788.
27. J. F. John, S. Mahurin, S. Daib, M. J. Sepaniak, Use of atomic layer deposition to improve the stability of silver substrates for in situ, high-temperature SERS measurements, *J. Raman Spectrosc.*, 41 (2010) 4–11.
28. B. Díaz, E. Häkkinen, J. Świątowska, V. Maurice, A. Seyeux, P. Marcus, M. Ritala, Low-temperature atomic layer deposition of Al<sub>2</sub>O<sub>3</sub> thin coatings for corrosion protection of steel: Surface and electrochemical analysis, *Corros. Sci.*, 53 (2011) 283–288.
29. A. I. Abdulagatov, Y. Yan, J. R. Cooper, Y. Zhang, Z. M. Gibbs, A. S. Cavanagh, R. G. Yang, Y. C. Lee, S. M. George, Al<sub>2</sub>O<sub>3</sub> and TiO<sub>2</sub> Atomic Layer Deposition on Copper for Water Corrosion Resistance, *ACS Appl. Mater. Interfaces*, 3 (2011) 4593–4601.
30. L. Paussa, L. Guzman, E. Marin, N. Isomaki, L. Fedrizzi, Protection of silver surfaces against tarnishing by means of alumina/titania-nanolayers, *Surf. Coat. Technol.*, 206 (2011) 976–980.
31. S. E. Potts, L. Schmalz, M. Fenker, B. Diaz, J. Świątowska, V. Maurice, A. Seyeux, P. Marcus, G. Radnoci, L. Toth, W. M. M. Kessels, Ultra-Thin Aluminium Oxide Films Deposited by Plasma-Enhanced Atomic Layer Deposition for Corrosion Protection, *J. Electrochem. Soc.*, 158 (2011) C132–C138.
32. E. Marin, L. Guzman, A. Lanzutti, W. Ensinger, L. Fedrizzi, Multilayer Al<sub>2</sub>O<sub>3</sub>/TiO<sub>2</sub> Atomic Layer Deposition coatings for the corrosion protection of stainless steel, *Thin Solid Films*, 522 (2012) 283–288.
33. D. Schmidt, E. Schubert, M. Schubert, Optical properties of cobalt slanted columnar thin films passivated by atomic layer deposition, *Appl. Phys. Lett.*, 100 (2012) 011912.

34. M.L. Chang, T.C. Cheng, M.C. Lin, H.C. Lin, M.J. Chen, Improvement of oxidation resistance of copper by atomic layer deposition, *Appl. Surf. Sci.*, 258 (2012) 10128–10134.
35. E. Marin, A. Lanzutti, M. Lekka, L. Guzman, W. Ensinger, L. Fedrizzi, Chemical and mechanical characterization of TiO<sub>2</sub>/Al<sub>2</sub>O<sub>3</sub> atomic layer depositions on AISI 316 L stainless steel, *Surf. Coat. Technol.*, 211 (2012) 84–88.
36. V. Sammelselg, L. Aarik, M. Merisalu, Patent: Method of preparing corrosion resistant coatings, publication number: WO 2014102758 A1, priority date: Dec 31,2012.
37. S. W. Seo, E. Jung, C. Lim, H. Chae, S. M. Cho, Moisture Permeation through Ultrathin TiO<sub>2</sub> Films Grown by Atomic Layer Deposition, *Appl. Phys. Express*, 5 (2012) 035701.
38. Y.-Q. Yang, Y. Duan, P. Chen, F.-B. Sun, Y.-H. Duan, X. Wang, D. Yang, Realization of Thin Film Encapsulation by Atomic Layer Deposition of Al<sub>2</sub>O<sub>3</sub> at Low Temperature, *J. Phys. Chem.*, C, 117 (2013) 20308–20312.
39. A. Meléndez-Ceballos, S. M. Fernández-Valverde, C. Barrera-Díaz, V. Albin, V. Lair, A. Ringuedé, M. Cassir, TiO<sub>2</sub> protective coating processed by Atomic Layer Deposition for the improvement of MCFC cathode, *Int. J. Hydrot. Energy*, 38 (2013) 13443–13452.
40. P. C. Wang, T. C. Cheng, H. C. Lina, M. J. Chen, K. M. Lin, M. T. Yeh, Effects of pre-sputtered Al interlayer on the atomic layer deposition of Al<sub>2</sub>O<sub>3</sub> films on Mg-10Li-0.5Zn alloy, *Appl. Surf. Science*, 270 (2013) 452–456.
41. M. Mäkelä, P. Soininen, S. Sneck, Patent: Protective coating of silver, publication number US8883258 B2, priority date: Feb. 02, 2006.
42. G. B. Lee, S. H. Song, S. W. Moon, J. W. Kim, J. H. Shim, B.-H. Choi, Improvement in mechanical and barrier properties of polyethylene blown films using atomic layer deposition, *J. Vac. Sci. Technol.*, A, 32 (2014) 01A126-1.
43. C. Kei, Y. S. Yu, J. Racek, D. Vokoun, P. Sittner, Atomic Layer-Deposited Al<sub>2</sub>O<sub>3</sub> Coatings on NiTi Alloy, *J. Mater. Eng. Perform.*, 23 (2014) 2641–2649.
44. Z. Chai, Y. Liu, J. Li, X. Lu, D. He, Ultra-thin Al<sub>2</sub>O<sub>3</sub> films grown by atomic layer deposition for corrosion protection of copper, *RCS Adv.*, 4 (2014) 50503–50509.
45. A. C. Alba-Rubio, B. J. O'Neill, F. Shi, C. Akatay, C. Canlas, T. Li, R. Winans, J. W. Elam, E. A. Stach, P. M. Voyles, J. A. Dumesic, Pore Structure and Bi-functional Catalyst Activity of Overlays Applied by Atomic Layer Deposition on Copper Nanoparticles, *ACS Catal.*, 4 (2014) 1554–1557.
46. J. C. Lee, D. H. K. Jackson, T. Li, R. E. Winans, J. A. Dumesic, T. F. Kuech, G. W. Huber, Enhanced stability of cobalt catalysts by atomic layer deposition for aqueous-phase reactions, *Energ. Environ. Sci.*, 7 (2014) 1657–1660.
47. A. Singh, F. Nehm, L. Muller-Meskamp, C. Hossbach, M. Albert, U. Schroeder, K. Leo, T. Mikolajick, OLED compatible water-based nanolaminate encapsulation systems using ozone based starting layer, *Org. Electron.*, 15 (2014) 2587–2592.
48. S. Lange, T. Arroval, R. Saar, I. Kink, J. Aarik, A. Krumme, Oxygen Barrier Properties of Al<sub>2</sub>O<sub>3</sub>- and TiO<sub>2</sub>-coated LDPE Films, *Polymer-Plastics Technology and Engineering*, 54 (2015) 301–304.
49. E. Marin, A. Lanzutti, L. Paussa, L. Guzman, L. Fedrizzi, Long term performance of atomic layer deposition coatings for corrosion protection of stainless steel, *Mater. Corros.*, 66 (2015) 907–914.

50. Y. Lin, R. Kapadia, J. Yang, M. Zheng, K. Chen, M. Hettick, X. Yin, C. Battaglia, I. D. Sharp, J. W. Ager, A. Javey, Role of TiO<sub>2</sub> Surface Passivation on Improving the Performance of p-InP Photocathodes, *J. Phys. Chem. C*, 119 (2015) 2308–2313.
51. J. Mondal, L. Aarik, J. Kozlova, A. Niilisk, H. Mändar, U. Mäeorg, A. Simões, V. Sammelselg, Functionalization of Titanium Alloy Surface by Graphene Nano-platelets and Metal Oxides: Corrosion Inhibition, *J. Nanosci. Nanotechnol.*, 15 (2015), 6533–6540.
52. M. Basiaga, M. Staszuk, W. Walke, T. Tański, W. Kajzer, Potentiostatic, potentiodynamic and impedance study of TiO<sub>2</sub> layers deposited of 316 LVM steel used for coronary stants, *Arch. Metall. Mater.*, 61 (2016) 821–824.
53. J. Mondal, A. Marques, L. Aarik, J. Kozlova, A. Simões, V. Sammelselg, Development of thin ceramic-graphene nanolaminated coating for corrosion protection of stainless steel, *Corrosion Science*, 105 (2016) 161–169.
54. B. Müller, H. Haugen, O. Nilsen, H. Tiainen, Atomic layer deposited TiO<sub>2</sub> protects porous ceramic foams from grain boundary corrosion, *Corrosion Science*, 106 (2016) 35–42.
55. J. Choi, J. T. Song, H. S. Jang, M.-J. Choi, D. M. Sim, S. Yim, H. Lim, Y. S. Jung, J. Oh, Interfacial Band-Edge Engineered TiO<sub>2</sub> Protection Layer on Cu<sub>2</sub>O Photocathodes for Efficient Water Reduction Reaction, *Electron. Mater. Lett.*, 13 (2017) 57–65.
56. Z. Wan, T. F. Zhang, J. C. Ding, C.-M. Kim, S.-W. Park, Y. Yang, K.-H. Kim, S.-H. Kwon, Enhanced Corrosion Resistance of PVD-CrN Coatings by ALD Sealing Layers, *Nanoscale Res. Lett.*, (2017) 12:248.
57. S. E. Potts, W. M. M. Kessels, Energy-enhanced atomic layer deposition for more process and precursor versatility, *Coordin. Chem. Rev.*, 257 (2013) 3254–3270.
58. S. Jakschik, U. Schroeder, T. Hecht, D. Krueger, G. Dollinger, A. Bergmaier, C. Luhmann, J. W. Bartha, Physical characterization of thin ALD-Al<sub>2</sub>O<sub>3</sub> films, *Appl. Surf. Sci.*, 211 (2003) 352–359.
59. J. B. Kim, D. R. Kwon, K. Chakrabarti, C. Lee, K. Y. Oh, J. H. Lee, Improvement in Al<sub>2</sub>O<sub>3</sub> dielectric behavior by using ozone as an oxidant for the atomic layer deposition technique, *J. Appl. Phys.*, 92 (2002) 6739–6742.
60. H. B. Park, M. Cho, J. Park, S. W. Lee, C. S. Hwang, J.-P. Kim, J.-H. Lee, N.-I. Lee, H.-K. Kang, J.-C. Lee, S.-J. Oh, Comparison of HfO<sub>2</sub> films grown by atomic layer deposition using HfCl<sub>4</sub> and H<sub>2</sub>O or O<sub>3</sub> as the oxidant, *J. Appl. Phys.*, 94 (2003) 3641–3647.
61. M. Putkonen, L. Niinistö, Zirconia thin films by atomic layer epitaxy. A comparative study on the use of novel precursors with ozone, *J. Mater. Chem.*, 12 (2001) 3141–3147.
62. H.-P. Feng, C.-H. Hsu, J.-K. Lu, Y.-H. Shy, Effects of PVD sputtered coatings on the corrosion resistance of AISI 304 stainless steel, *Mater. Sci. Eng., A*, 347 (2003) 123–129.
63. F. Guidi, G. Moretti, G. Carta, M. Natali, G. Rossetto, Z. Pierino, G. Salmaso, V. Rigato, Electrochemical anticorrosion performance evaluation of Al<sub>2</sub>O<sub>3</sub> coatings deposited by MOCVD on an industrial brass substrate, *Electrochim. Acta*, 50 (2005) 4609–4614.
64. Y. Balcaen, N. Radutoiu, J. Alexis, J.-D. Beguin, L. Lacroix, D. Samélor, C. Vahlas, Mechanical and barrier properties of MOCVD processed alumina coatings on Ti<sub>6</sub>Al<sub>4</sub>V titanium alloy, *Surf. Coat. Technol.*, 206 (2011) 1684–1690.

65. C. García, S. Ceré, A. Durán, Bioactive coatings prepared by sol–gel on stainless steel 316L, *J. Non-Cryst. Solids*, 348 (2004) 218–224.
66. S. K. Poznyak, M. L. Zheludkevich, D. Raps, F. Gammel, K. A. Yasakau, M. G. S. Ferreira, Preparation and corrosion protective properties of nanostructured titania-containing hybrid sol–gel coatings on AA2024, *Prog. Org. Coat.*, 62 (2008) 226–235.
67. Z. E. Sánchez-Hernández, M. A. Domínguez-Crespo, A. M. Torres-Huerta, E. Onofre-Bustamante, J. Andraca Adame, H. Dorantes-Rosales, Improvement of adhesion and barrier properties of biomedical stainless steel by deposition of YSZ coatings using RF magnetron sputtering, *Mater. Charact.*, 91 (2014) 50–57.
68. L. Gladczuk, A. Patel, C. S. Paur, M. Sosinowski, Tantalum films for protective coatings of steel, *Thin Solid Films*, 467 (2004) 150–157.
69. D. Krishna, Y. Sun, Z. Chen, Magnetron sputtered TiO<sub>2</sub> films on a stainless steel substrate: Selective rutile phase formation and its tribological and anti-corrosion performance, *Thin Solid Films*, 519 (2011) 4860–4864.
70. M. Leskelä, M. Ritala, Atomic layer deposition (ALD): from precursors to thin film structures, *Thin Solid Films*, 409 (2002) 138–146.
71. R. L. Puurunen, Surface chemistry of atomic layer deposition: A case study for the trimethylaluminum/water process, *J. Appl. Phys.*, 97, (2005) 121301.
72. M. Knez, K. Nielsch, L. Niinistö, Synthesis and Surface Engineering of Complex Nanostructures by Atomic Layer deposition, *Adv. Mater.*, 19 (2007) 3425–3438.
73. M. Ritala, J. Niinistö, Atomic Layer Deposition, in *Chemical Vapour Deposition: Precursors, Processes and Applications*, A. C. J. Jones and M. L. Hitchman, Eds.; Royal Society of Chemistry: Cambridge, U.K. (2009) 158–206.
74. S. M. George, B. Yoon, A. A. Dameron, Surface Chemistry for Molecular Layer Deposition of Organic and Hybrid Organic-Inorganic Polymers, *Accounts Chem. Res.*, 42 (2009) 498–508.
75. V. Miikkulainen, M. Leskelä, M. Ritala, R. L. Puurunen, Crystallinity of inorganic films grown by atomic layer deposition: overview and general trends, *J. Appl. Phys.*, 113(2013) 021301.
76. A. Devi, “Old Chemistries” for new applications: Perspectives for development of precursors for MOCVD and ALD applications, *Coordination Chemistry Reviews* 257 (2013) 3332–3384.
77. T. Hatanpää M. Ritala, M. Leskelä, Precursors as enablers of ALD technology: Contributions from University of Helsinki, *Coordination Chemistry Reviews*, 257 (2013) 3297–3322.
78. E. Ahvenniemi, A. R. Akbashev, S. Ali, M.I Bechelany, M. Berdova, S. Boyadjieva, D. C. Cameron, R. Chen, M. Chubarov, V. Cremers, A. Devi, V. Drozd, L. Elnikova, G. Gottardi, K. Grigoras, D. M. Hausmann, C. S. Hwang, S.-H. Jen, T. Kallio, J. Kanervo, I. Khmelnitskiy, D. H. Kim, L. Klibanov, Y. Koshtyal, A. Outi, I. Krause, J. Kuhs, I. Kärkkänen, M.-L. Kääriäinen, T. Kääriäinen, L. Lamagna, A. A. Łapicki, M. Leskelä, H. Lipsanen, J. Lyttinen, A. Malkov, A. Malygin, A. Mennad, C. Militzer, J. Molarius, M. Norek, Ç. Özgit-Akgün, M. Panov, H. Pedersen, F. Piallat, G. Popov, R. L. Puurunen, G. Rampelberg, R. H. A. Ras, E. Rauwel, F. Roozeboom, T. Sajavaara, H. Salami, H. Savin, N. Schneider, T. E. Seidel, J. Sundqvist, D. B. Suyatin, T. Törndahl, J. R. van Ommen, C. Wiemer, O. M. E. Ylivaara, O. Yurkevich, Review Article: Recommended reading list of early publications on atomic layer deposition – Outcome of the “Virtual Project on

- the History of ALD, *J. Vac. Sci. Technol., A: Vacuum, Surfaces, and Films*, 35 (2017) 010801.
79. R. Katamreddy, R. Inman, G. Jursich, A. Soulet, C. Taoudis, Controlling interfacial reactions between  $\text{HfO}_2$  and Si using ultrathin  $\text{Al}_2\text{O}_3$  diffusion barrier layer, *Appl. Phys. Lett.*, 89 (2006), 262906.
  80. T. Hirvikorpi, M. Vähä-Nissi, A. Harlin, M. Karppinen, Comparison of some coating techniques to fabricate barrier layers on packaging materials, *Thin Solid Films*, 518 (2010) 5463–5466.
  81. J. Aarik, A. Aidla, A. Jaek, A. A. Kiisler, A. A. Tammik, Properties of amorphous  $\text{Al}_2\text{O}_3$  films grown by ALE, *Acta Polytechn. Scand., Chem. Techn. Ser.*, 195 (1990) 201–208.
  82. A. M. Shevjakov, G. N. Kuznetsova, and V. B. Aleskovskii, Interaction of titanium and germanium tetrachlorides with hydroxylated silicon dioxide, in *Chemistry of High Temperature Materials*. Proceedings of the 2nd USSR Conference on High Temperature Chemistry of Oxides, Leningrad, USSR, 26–29 November 1965 (Nauka, Leningrad, 1967), 149–155 (in Russian).
  83. T. Suntola, J. Antson, patent FIN 52359, Priority date 29 November 1974, corresponds to U.S. Patent No. US 4058430 A, Method for producing compound thin films, priority date: 25 November 1975.
  84. T. S. Suntola, A. J. Pakkala, S. G. Lindfors, Method for performing growth of compound thin films, U.S. Patent No.US 4413022 A, Priority date: Feb 28, 1979.
  85. T. S. Suntola, A. J. Pakkala, S. G. Lindfors, Apparatus for Performing Growth of Compound Thin Films, U.S. Patent No. US 4389973A, Priority date: Mar 18, 1980.
  86. S. Dueñas, H. Castán, H. García, A. de Castro, L. Bailón, K. Kukli, A. Aidla, J. Aarik, H. Mändar, T. Uustare, J. Lu, A. Härsta, Influence of single and double deposition temperatures on the interface quality of atomic layer deposited  $\text{Al}_2\text{O}_3$  dielectric thin films on silicon, *J. Applied Phys.*, 99 (2006) 054902.
  87. G. Oya, M. Yoshida, Y. Sawada, Growth of  $\alpha\text{-Al}_2\text{O}_3$  films by molecular layer epitaxy, *Appl. Phys. Lett.*, 51 (1987) 1143–1145.
  88. H. Kumagai, K. Toyoda, M. Matsumoto, M. Obara, Comparative Study of  $\text{Al}_2\text{O}_3$  Optical Crystalline Thin Films Grown by Vapor Combinations of  $\text{Al}(\text{CH}_3)_3/\text{N}_2\text{O}$  and  $\text{Al}(\text{CH}_3)_3/\text{H}_2\text{O}_2$ , *Jpn. J. Appl. Phys.*, 32, (1993) 6137–6140.
  89. S. M. Prokes, M. B. Katz, M. E. Twigg, Growth of crystalline  $\text{Al}_2\text{O}_3$  via thermal atomic layer deposition: Nanomaterial phase stabilization, *Apl. Materials*, 2 (2014) 032105.
  90. H. C. M. Knoops, E. Langereis, M. C. M. van de Sanden, W. M. M. Kessels, Conformality of Plasma-Assisted ALD: Physical Processes and Modeling, *J. Electrochem. Soc.*, 157 (2010) G241–G249.
  91. Y. K. Ezhovskii, V. Y. Kholkin, Growth and Properties of  $\text{Al}_2\text{O}_3$  and  $\text{SiO}_2$  Nanolayers on III–V Semiconductors, *Inorg. Mater.*, 46 (2010) 38–42.
  92. L. Hiltunen, H. Kattelus, M. Leskelä, M. Mäkelä, L. Niinistö, E. Nykänen, P. Soiniainen, M. Tiitta, Growth and characterization of aluminum oxide thin films deposited from various source materials by atomic layer epitaxy and chemical vapor deposition processes, *Mater. Chem. Phys.*, 28 (1991) 379–388.
  93. M. Ritala, K. Kukli, A. Rahtu, P. I. Räisänen, M. Leskelä, T. Sajavaara, J. Keinonen, Atomic Layer Deposition of Oxide Thin Films with Metal Alkoxides as Oxygen Sources, *Sci. Rep.*, 288 (2000) 319–321

94. P. I. Räisänen, M. Ritala, and M. Leskelä, Atomic layer deposition of  $\text{Al}_2\text{O}_3$  films using  $\text{AlCl}_3$  and  $\text{Al}(\text{O}i\text{Pr})_3$  as precursors, *J. Mater. Chem.*, 12 (2002) 1415–1418.
95. R. Matero, A. Rahtu, M. Ritala, M. Leskelä, T. Sajavaara, Effect of water dose on the atomic layer deposition rate of oxide thin films, *Thin Solid Films*, 368 (2000) 1–7.
96. X. Song, C. G. Takoudis, Cyclic Chemical-Vapor-Deposited  $\text{TiO}_2/\text{Al}_2\text{O}_3$  Film Using Trimethyl Aluminum, Tetrakis(diethylamino)titanium, and  $\text{O}_2$ , *J. Electrochem. Soc.*, 154, (2007) G177–G182.
97. J. F. Fan, K. Toyoda, Growth-Temperature Dependence of the Quality of  $\text{Al}_2\text{O}_3$  Prepared by Sequential Chemical Reaction of Trimethylaluminum and  $\text{H}_2\text{O}_2$ , *Jpn. J. Phys.*, 32 (1993) 1349–1351.
98. D. H. Levy, D. Freeman, S. F. Nelson, P. J. Cowdery-Corvan, Stable  $\text{ZnO}$  thin film transistors by fast open air atomic layer deposition, *Appl. Phys. Lett.*, 92 (2008) 192101.
99. V. E. Drozd, A. P. Baraban, I. O. Nikiforova, Electrical properties of  $\text{Si} - \text{Al}_2\text{O}_3$  structures grown by ML-ALE, *Appl. Surf. Sci.*, 82/83 (1994) 583–586.
100. Y. Shen, Y. Li, J. Zhang, X. Zhu, Z. Hu, J. Chu, Excellent insulating behavior  $\text{Al}_2\text{O}_3$  thin films grown by atomic layer deposition efficiently at room temperature, *Optoelectron. Adv. Mat.–RAPID COMMUNICATIONS*, 6 (2012) 618–622.
101. W.-S. Jeon, S. Yang, C.-s. Lee, S.-W. Kang, Atomic Layer Deposition of  $\text{Al}_2\text{O}_3$  Thin Films Using Trimethylaluminum and Isopropyl Alcohol, *J. Electrochem. Soc.*, 149 (2002) C306–C310.
102. E. Potts, W. Keuning, E. Langereis, G. Dingemans, M. C. M. van de Sanden, W. M. M. Kessels, Low Temperature Plasma-Enhanced Atomic Layer Deposition of Metal Oxide Thin Films, *J. Electrochem. Soc.*, 157 (2010) P66–P74.
103. Y. Catherine, A. Talebian, Plasma Deposition of Aluminum Oxide Films, *J. Electron. Mater.*, 12 (1988) 127–134.
104. A. Ali, H. S. Madan, A. P. Kirk, D. A. Zhao, D. A. Mourey, M. K. Hudait, R. M. Wallace, T. N. Jackson, B. R. Bennett, J. B. Boos, S. Datta, Fermi level unpinning of  $\text{GaSb}$  (100) using plasma enhanced atomic layer deposition of  $\text{Al}_2\text{O}_3$ , *Appl. Phys. Lett.*, 97 (2010) 143502.
105. S. Lee, H. Jeon, Characteristics of an  $\text{Al}_2\text{O}_3$  Thin Film Deposited by a Plasma Enhanced Atomic Layer Deposition Method Using  $\text{N}_2\text{O}$  Plasma, *Electron. Mater. Lett.*, 3 (2007) 17–21.
106. K. Kukli, M. Ritala, M. Leskelä, J. Jokinen, Atomic layer epitaxy growth of aluminum oxide thin films from a novel  $\text{Al}(\text{CH}_3)_2\text{ClAl}(\text{CH}_3)_2\text{Cl}$  precursor and  $\text{H}_2\text{O}$ , *J. Vac. Sci. Technol.*, A, 15 (1997) 2214.
107. C.-W. Jeong, B.-il Lee, S.-K. Joo, Growth and characterization of aluminum oxide films by plasma-assisted atomic layer deposition, *Mater. Sci. Eng.*, C, 16 (2001) 59–64.
108. B. H. Kim, W. S. Jeon, S. H. Jung, B. T. Ahn, Interstitial Oxygen Incorporation into Silicon Substrate during Plasma Enhanced Atomic Layer Deposition of  $\text{Al}_2\text{O}_3$ , *Electrochem. Solid-State Lett.*, 8 (2005) G294–G296.
109. S. E. Potts, G. Dingemans, C. Lachaud, W. M. M. Kessels, Plasma-enhanced and thermal atomic layer deposition of  $\text{Al}_2\text{O}_3$  using dimethylaluminum isopropoxide,  $[\text{Al}(\text{CH}_3)_2(\text{l-O}i\text{Pr})_2]_2$ , as an alternative aluminum precursor, *J. Vac. Sci. Technol.*, A, 30(2) (2012) 021505.

110. Y.-S. Min, Y. J. Cho, C. S. Hwang, Atomic Layer Deposition of  $\text{Al}_2\text{O}_3$  Thin Films from a 1-Methoxy-2-methyl-2-propoxide Complex of Aluminum and Water, *Chem. Mater.*, 17 (2005) 626–631.
111. R. Katamreddy, R. Inman, G. Jursich, A. Soulet, C. Takoudis, ALD and Characterization of Aluminum Oxide Deposited on Si(100) using Tris(diethylamino) Aluminum and Water Vapor, *J. Electrochem. Soc.*, 153 (2006) C701–C706.
112. R. Katamreddy, R. Inman, G. Jursich, A. Soulet, C. Takoudis, Atomic layer deposition of  $\text{HfO}_2$ ,  $\text{Al}_2\text{O}_3$ , and  $\text{HfAlO}_x$  using  $\text{O}_3$  and metal(diethylamino) precursors, *J. Mater. Res.*, 22 (2007) 3455–3464.
113. C. R. Wade, C. Silvernail, C. Banerjee, A. Soulet, J. McAndrew, J.A. Belot, Tris(dialkylamino)aluminums: Syntheses, characterization, volatility comparison and atomic layer deposition of alumina thin films, *Mater. Lett.*, 61 (2007) 5079–5082.
114. A. L. Brazeau, S. T. Barry, Atomic Layer Deposition of Aluminum Oxide Thin Films from a Heteroleptic, Amidinate-Containing Precursor, *Chem. Mater.*, 20 (2008) 7287–7291.
115. E. L. Lakomaa, S. Haukka, T. Suntola, Atomic layer growth of  $\text{TiO}_2$  on silica, *Appl. Surf. Sci.*, 60/61 (1992) 742–748.
116. S. Haukka, E. L. Lakomaa, T. Suntola, Surface coverage of ALE precursors on oxides, *Appl. Surf. Sci.*, 82/83 (1994) 155–162.
117. J. Aarik, A. Aidla, H. Mändar, T. Uustare, Atomic layer deposited of titanium dioxide from  $\text{TiCl}_4$  and  $\text{H}_2\text{O}$ : investigation of growth mechanism, *Appl. Surf. Sci.*, 172 (2001) 148–158.
118. V. Pore, A. Rahtu, M. Leskelä, M. Ritala, T. Sajavaara, J. Keinonen, Atomic Layer Deposition of Photocatalytic  $\text{TiO}_2$  Thin Films from Titanium Tetramethoxide and Water, *Chem. Vap. Deposition*, 10 (2004) 143–148.
119. A. Rahtu, K. Kukli, M. Ritala, In Situ Mass Spectrometry Study on Atomic Layer Deposition from Metal (Ti, Ta, and Nb) Ethoxides and Water, *Chem. Mater.*, 13 (2001) 817–823.
120. J. Aarik, A. Aidla, T. Uustare, V. Sammelselg, Morphology and structure of  $\text{TiO}_2$  thin films grown by atomic layer deposition, *J. Crystal Growth*, 148 (1995) 268–275.
121. S. Zaitsu, S. Motokoshi, T. Jitsuno, M. Nakatsuka, T. Yamanaka, Large-Area Optical Coatings with Uniform Thickness Grown by Surface Chemical Reactions for High-Power Laser Applications, *Jpn. J. Appl. Phys.*, 41 (2002) 160–165.
122. X. Liang, A. D. Lynn, D. M. King, S. J. Bryant, A. W. Weimer, Biocompatible Interface Films Deposited within Porous Polymers by Atomic Layer Deposition (ALD), *ACS Appl. Mater. Interfaces*, 1 (2009) 1988–1995.
123. G. Triani, J. A. Campbell, P. J. Evans, J. Davis, B. A. Latella, R. P. Burford, Low temperature atomic layer deposition of titania thin films, *Thin Solid Films*, 518 (2010) 3182–3189.
124. H. Kumagai, M. Matsumoto, Y. Kawamura, Fabrication of Multilayers with Growth Controlled by Sequential Surface Chemical Reactions, *Jpn. J. Appl. Phys.*, 33, (1994) 7086–7089.
125. H. Kumagai, M. Matsumoto, K. Toyoda, M. Obara, M. Suzuki, Fabrication of titanium oxide thin films by controlled growth with sequential surface chemical reactions, *Thin Solid Films*, 263 (1995) 47–53.
126. N. G. Kubala and C. A. Wolden, Self-limiting growth of anatase  $\text{TiO}_2$ : A comparison of two deposition techniques, *Thin Solid Films*, 518, (2010) 6733–6737.

127. R. Pärna, A. Tarre, A. Gerst, H. Mändar, A. Niilisk, T. Uustare, A. Rosental, V. Sammelselg, Influence of annealing on atomic layer deposited Cr<sub>2</sub>O<sub>3</sub>-TiO<sub>2</sub> thin films, *Proc. SPIE*, 6596 (2007) 659618.
128. V. Sammelselg, A. Tarre, J. Lu, J. Aarik, A. Niilisk, T. Uustare, I. Netšipailo, R. Rammula, R. Pärna, A. Rosental, Structural characterization of TiO<sub>2</sub>-Cr<sub>2</sub>O<sub>3</sub> nanolaminates grown by atomic layer deposition, *Surf. Coat. Technol.* 204 (2010) 2015–2018.
129. V. R. Anderson, A. S. Cavanagh, A. I. Abdulagatov, Z. M. Gibbs, S. M. George, Waterless TiO<sub>2</sub> atomic layer deposition using titanium tetrachloride and titanium Tetraisopropoxide, *J. Vac. Sci. Technol., A: Vacuum, Surfaces, and Films*, 32 (2014) 01A114.
130. V. Pore, T. Kivelä, M. Ritala, and M. Leskelä, Atomic layer deposition of photocatalytic TiO<sub>2</sub> thin films from TiF<sub>4</sub> and H<sub>2</sub>O, *Dalton Trans.*, (2008) 6467–6474.
131. M. Ritala, M. Leskelä, E. Rauhala, Atomic Layer Epitaxy Growth of Titanium Dioxide Thin Films from Titanium Ethoxide, *Chem. Mater.*, 6 (1994) 556–561.
132. J. Aarik, A. Aidla, V. Sammelselg, T. Uustare, M. Ritalac, M. Leskelä, Characterization of titanium dioxide atomic layer growth from titanium ethoxide and water, *Thin Solid Films*, 370 (2000) 163–172.
133. M. Knez, A. Kadri, C. Wege, U. Géosele, H. Jeske, K. Nielsch, Atomic Layer Deposition on Biological Macromolecules: Metal Oxide Coating of Tobacco Mosaic Virus and Ferritin, *Nano. Lett.*, 6 (2006) 1172–1177.
134. M. Ritala, M. Leskäla, E. Nykänen, P. Soinine, L. Niinistö, Titanium Isopropoxide as a Precursor in Atomic Layer Epitaxy of Titanium Dioxide Thin Films, *Thin Solid Films*, 225 (1993) 288–295.
135. J. Aarik, A. Aidla, T. Uustare, M. Ritala, M. Leskelä, Titanium isopropoxide as a precursor for atomic layer deposition: characterization of titanium dioxide growth process, *Appl. Surf. Sci.* 161 (2000) 385–395.
136. M. Linndbad, S. Haukka, A. Kytkivi, E.-L. Lakomaa, A. R. Autiainen, T. Suntola, Processing of catalysts by atomic layer epitaxy: modification of supports, *Appl. Surf. Sci.* 121/122 (1997) 286–291.
137. C. H. Ko, W. J. Lee, Formation of Al<sub>2</sub>O<sub>3</sub>–TiO<sub>2</sub> bilayer using atomic layer deposition and its application to dynamic random access memory, *J. Solid State Electrochem.*, 11, (2007) 1391–1397.
138. S. K. Kim, W. D. Kim, K. M. Kim, C. S. Hwang, J. Jeong, High dielectric constant TiO<sub>2</sub> thin films on a Ru electrode grown at 250 °C by atomic-layer deposition, *Appl. Phys. Lett.*, 85 (2004) 4112–4114.
139. V. R. Rai, S. Agarwal, Surface Reaction Mechanisms during Ozone-Based Atomic Layer Deposition of Titanium Dioxide, *J. Phys. Chem., C*, 112, (2008) 9552–9554.
140. S. J. Won, S. Suh, S. W. Lee, G. J. Choi, C. S. Hwang, H. J. Kim, Substrate Dependent Growth Rate of Plasma-Enhanced Atomic Layer Deposition of Titanium Oxide Using N<sub>2</sub>O Gas, *Electrochem. Solid-State Lett.*, 13 (2010) G13 –G16.
141. W. S. Yang, S. W. Kang, Comparative study on chemical stability of dielectric oxide films under HF wet and vapor etching for radiofrequency microelectromechanical system application, *Thin Solid Films*, 500 (2006) 231–236.
142. Q. Xie, J. Musschoot, D. Deduytsche, R. L. Van Meirhaeghe, C. Detavernier, S. Van den Berghe, Y. L. Jiang, G. P. Ru, B. Z. Li, X. P. Qu, Growth Kinetics and Crystallization Behavior of TiO<sub>2</sub> Films Prepared by Plasma Enhanced Atomic Layer Deposition, *J. Electrochem. Soc.*, 155, (2008) H688–H692.

143. S.-W. Kim, T. H. Han, J. Kim, H. Gwon, H.-S. Moon, S.-W. Kang, S. O. Kim, K. Kang, Fabrication and Electrochemical Characterization of TiO<sub>2</sub> Three-Dimensional Nanonetwork Based on Peptide Assembly, *ACS Nano*, 3, (2009) 1085–1090.
144. T. H. Han, J. K. Oh, J. S. Park, S.-H. Kwon, S.-W. Kim, S. O. Kim, Highly entangled hollow TiO<sub>2</sub> nanoribbons templating diphenylalanine assembly, *J. Mater. Chem.*, 19 (2009) 3512–3516.
145. E. Rauwel, M. G. Willinger, F. Ducroquet, P. Rauwel, I. Matko, D. Kiselev, N. Pinna, Carboxylic Acids as Oxygen Sources for the Atomic Layer Deposition of High-K Metal Oxides, *J. Phys. Chem., C*, 112 (2008) 12754–12759.
146. S. K. Kim, S. Hoffmann-Eifert, R. Waser, High Growth Rate in Atomic Layer Deposition of TiO<sub>2</sub> thin films by UV Irradiation, *Electrochem. Solid-State Lett.*, 14 (2011) H146–H148.
147. K. Kukli, A. Aidla, J. Aarik, M. Schuisky, A. Härsta, M. Ritala, M. Leskelä, Real-Time Monitoring in Atomic Layer Deposition of TiO<sub>2</sub> from TiI<sub>4</sub> and H<sub>2</sub>O–H<sub>2</sub>O<sub>2</sub>, *Langmuir*, 16 (2000) 8122–8128.
148. M. Schuisky, J. Aarik, K. Kukli, A. Aidla, A. Härsta, Atomic Layer Deposition of Thin Films Using O<sub>2</sub> as Oxygen Source, *Langmuir*, 17 (2001) 5508–5512.
149. J. Aarik, A. Aidla, T. Uustare, K. Kukli, V. Sammelselg, M. Ritala, M. Leskelä, Atomic layer deposition of TiO<sub>2</sub> thin films from TiI<sub>4</sub> and H<sub>2</sub>O, *Appl. Surf. Sci.*, 193 (2002) 277–286
150. K. Kukli, M. Ritala, M. Schuisky, M. Leskelä, T. Sajavaara, J. Keinonen, T. Uustare, A. Härsta, Atomic Layer Deposition of Titanium Oxide from TiI<sub>4</sub> and H<sub>2</sub>O<sub>2</sub>, *Chem. Vap. Deposition*, 6 (2000) 303–310.
151. G. T. Lim, D.-H. Kim, Characteristics of TiO<sub>x</sub> films prepared by chemical vapor deposition using tetrakis-dimethyl-amido-titanium and water, *Thin Solid Films*, 498 (2006) 254–258.
152. Y.-W. Kim, D.-H. Kim, Atomic layer deposition of TiO<sub>2</sub> from tetrakis-dimethylamido-titanium and ozone, *Korean J. Chem. Eng.*, 29(7) (2012) 969–973.
153. T. O. Kääriäinen, D. C. Cameron, M. Tanttari, Adhesion of Ti and TiC Coatings on PMMA Subject to Plasma Treatment: Effect of Intermediate Layers of Al<sub>2</sub>O<sub>3</sub> and TiO<sub>2</sub> Deposited by Atomic Layer Deposition Plasma Process, *Polym.*, 6 (2009) 631–641.
154. R. Katamreddy, V. Omarjee, B. Feist, C. Dussarrat, Ti Source Precursors for Atomic Layer Deposition of TiO<sub>2</sub>, STO and BST, *ECS Trans.*, 16 (2008) 113–122.
155. C. S. Lee, J. Kim, J. Y. Son, W. Choi, H. Kim, Photocatalytic functional coatings of TiO<sub>2</sub> thin films on polymer substrate by plasma enhanced atomic layer deposition, *Appl. Catal., B*, 91 (2009) 628–623.
156. C. S. Lee, J. Kim, G. H. Gu, D. H. Jo, C. G. Park, W. Choi, H. Kim, Photocatalytic activities of TiO<sub>2</sub> thin films prepared on Galvanized Iron substrate by plasma-enhanced atomic layer deposition, *Thin Solid Films*, 518 (2010) 4757–4761.
157. A. Sarkar, S. E. Potts, S. A. Rushworth, F. Roozeboom, M. C. M. van de Sanden, W. M. M. Kessels, Plasma-Enhanced ALD of TiO<sub>2</sub> Using a Novel Cyclopentadienyl Alkylamido Precursor [Ti(CpMe)(NMe<sub>2</sub>)<sub>3</sub>] and O<sub>2</sub> Plasma, *ECS Trans.*, 33 (2010) 385–393.

158. J. P. Lee, M. H. Park, T.-M. Chung, Y. Kim, M. M. Sung, Atomic Layer Deposition of TiO<sub>2</sub> Thin Films from Ti(OiPr)<sub>2</sub>(dmae)<sub>2</sub> and H<sub>2</sub>O, *Bull. Korean Chem. Soc.*, 25 (2004) 475–479.
159. S. K. Kim, S. Hoffmann-Eifert, S. Mi, R. Waser, Liquid Injection Atomic Layer Deposition of Crystalline TiO<sub>2</sub> Thin Films with a Smooth Morphology from Ti(O-i-Pr)<sub>2</sub>(DPM)<sub>2</sub>, *J. Electrochem. Soc.*, 156 (2009) D296–D300.
160. L. Manchanda, M. D. Morris, M. L. Green, R. B. van Dover, F. Klemens, T. W. Sorsch, P. J. Silverman, G. Wilk, B. Busch, S. Aravamudhan, Multi-component high-K gate dielectrics for the silicon industry, *Microelectronic Engineering*, 59 (2001) 351–359.
161. M. Juppo, A. Rahtu, M. Ritala, M. Leskela, In Situ Mass Spectrometry Study on Surface Reactions in Atomic Layer Deposition of Al<sub>2</sub>O<sub>3</sub> Thin Films from Trimethylaluminum and Water, *Langmuir*, 16 (2000) 4034–4039.
162. S. K. Kim, C. S. Hwang, Atomic-layer-deposited Al<sub>2</sub>O<sub>3</sub> thin films with thin SiO<sub>2</sub> layers grown by in situ O<sub>3</sub> oxidation, *J. Appl. Phys.*, 96, (2004) 2323–2329.
163. S. A. Campbell, D. C. Gilmer, X. Wang, M. Hsieh, H.-S. Kim, W. L. Gladfelter, J. Yan, MOSFET transistors fabricated with high permittivity TiO<sub>x</sub>/sub2/dielectrics, *IEEE Trans. Electron Devices*, 44 (1997) 104–109.
164. K. Fröhlich, M. Čapajna, A. Rosová, E. Dobročka, K. Hušeková, J. Aarik, A. Aidla, Growth of High-Dielectric-Constant TiO<sub>2</sub> Films in Capacitors with RuO<sub>2</sub> Electrodes, *Electrochem. Solid-State Lett.*, 11 (2008) G19–G21.
165. J. Aarik, B. Hudec, K. Hušekova, R. Rammula, A. Kasikov, T. Arroval, T. Uustare, K. Fröhlich, Atomic layer deposition of high-permittivity TiO<sub>2</sub> dielectrics with low leakage current on RuO<sub>2</sub> in TiCl<sub>4</sub>-based processes, *Semicond. Sci. Technol.*, 27 (2012) 074007.
166. F. Wang, Y. Zhang, X. Chen, B. Leng, X. Guo, T. Zhang, ALD mediated heparin grafting on nitinol for self-expanded carotid stents, *Colloids Surf. B: Biointerfaces*, 143 (2016) 390–398.
167. T. Jõgiaas, L. Kollo, J. Kozlova, A. Tamm, I. Hussainova, K. Kukli, Effect of atomic layer deposited aluminium oxide on mechanical properties of porous silicon carbide, *Ceram. Int.*, 41 (2015) 7519–7528.
168. K. Kukli, E. Salmi, T. Jõgiaas, R. Zabels, M. Schuisky, J. Westlinder, K. Mizohata, M. Ritala, M. Leskelä, Atomic layer deposition of aluminum oxide on modified steel substrates, *Surf. Coat. Technol.*, 304 (2016) 1–8.
169. J. A. McCormick, K. P. Rice, D. F. Paul, A. W. Weimer, S. M. George, Analysis of Al<sub>2</sub>O<sub>3</sub> Atomic Layer Deposition on ZrO<sub>2</sub> Nanoparticles in a Rotary Reactor, 13 (2007) 491–498.
170. C. J. W. Ng, H. Gao, T. T. Y. Tan, Atomic layer deposition of TiO<sub>2</sub> nanostructures for self-cleaning applications, *Nanotechnology*, 19 (2008) 445604.
171. R. J. Narayan, S. P. Adiga, M. J. Pellin, L. A. Curtiss, A. J. Hryni, S. Stafslien, B. Chisholm, C.-C. Shih, C.-M. Shih, S.-J. Lin, Y.-Y. Su, C. Jin, J. Zhang, N. A. Monteiro-Riviere, J. W. Elam, Atomic layer deposition-based functionalization of materials for medical and environmental health applications, *Philos. Trans. A Math. Phys. Eng. Sci.*, 368 (2010) 2033–2064.
172. T. Honda, K. Yanashima, J. Yoshino, H. Kukimoto, F. Koyama, K. Ito, Fabrication of a ZnSe-Based Vertical Fabry-Perot Cavity Using SiO<sub>2</sub>/TiO<sub>2</sub> Multilayer Reflectors and Resonant Emission Characteristics, *Jpn. J. Appl. Phys.*, 33 (1994) 3960–3961.

173. E. Marin A. Lanzutti, L. Guzman, L. Federizzi, Chemical and electrochemical characterization of TiO<sub>2</sub>/Al<sub>2</sub>O<sub>3</sub> atomic layer depositions on AZ-31 magnesium alloy, *J. Coat. Technol. Res.*, 9 (3) (2012) 347–355.
174. G. C. Correa, B. Bao, N. C. Strandwitz, Chemical Stability of Titania and Alumina Thin Films Formed by Atomic Layer Deposition, *ACS Appl. Mater. Interfaces*, 7 (2015) 14816–14821.
175. K. Jukk, N. Kongi, A. Tarre, A. Rosental, A.B. Treshchalov, J. Kozlova, P. Ritslaid, L. Matisen, V. Sammelselg, K. Tammeveski, Electrochemical oxygen reduction behaviour of platinum nanoparticles supported on carbon nanotube/titanium dioxide composites, *J. Electroanal. Chem.*, 735 (2014) 68–76.
176. I. Oja Acik, A. Katerskia, A. Mere, J. Aarik, A. Aidla, T. Dedova, M. Krunks, Nanostructured solar cell by spray pyrolysis: Effect of titania barrier layer on the cell performance, *Thin Solid Films*, 517 (2009) 2443–2447.
177. H.-B. Wang, D.-Y. Ma, F. Ma and K.-W. Xu, Impact of ultrathin Al<sub>2</sub>O<sub>3</sub> interlayer on thermal stability and leakage current properties of TiO<sub>2</sub>/Al<sub>2</sub>O<sub>3</sub> stacking dielectrics, *J. Vac. Sci. Technol.*, B, 30 (2012) 040601.
178. R. L. Puurunen, J. Saarilahti, H. Kattelus, Implementing ALD Layers in MEMS processing, *ECS Transactions*, 11 (2007) 3–14.
179. A. Tamm, A.-L. Peikolainen, J. Kozlova, H. Mändar, A. Aidla, R. Rammula, L. Aarik, K. Roosalu, J. Lu, L. Hultman, M. Koel, K. Kukli, J. Aarik, Atomic layer deposition of high-k dielectrics on carbon nanoparticles, *Thin Solids Films*, 538 (2013) 16–20.
180. A. Tamm, A.-L. Peikolainen, J. Kozlova, L. Aarik, K. Roosalu, I. Kärkkänen, H. Mändar, J. Aarik, K. Kukli, Atomic Layer Deposition of Zirconium Oxide on Carbon Nanoparticles, *IOP Conf. Series: Materials Science and Engineering*, 49 (2013) 012019.
181. J. Aarik, A. Aidla, A.-A. Kiisler, T. Uustare, V. Sammelselg, Influence of substrate temperature on atomic layer growth and properties of HfO<sub>2</sub> thin films, *Thin Solid Films*, 340 (1999) 110–116.
182. S. M. George, Atomic Layer Deposition: An Overview, *Chem. Rev.*, 110 (2010) 111–131.
183. T. Arroval, L. Aarik, R. Rammula, V. Kruusla, J. Aarik, Effect of substrate-enhanced and inhibited growth on atomic layer deposition and properties of aluminum-titanium oxide films, *Thin Solid Films*, 600 (2016) 119–125.
184. P. S. Maydannik, T. O. Kääriäinen, D. C. Cameron, An atomic layer deposition process for moving flexible substrates, *Chem. Eng. J.*, 171 (2011) 345–349.
185. H. B. Profijt, S. E. Potts, M. C. M. van de Sanden, W. M. M. Kessels, Plasma-Assisted Atomic Layer Deposition: Basics, Opportunities, and Challenges, *J. Vac. Sci. Technol.*, A, 29(5) (2011) 050801.
186. M. Yang, A. A. I. Aarnink, A. Y. Kovalgin, D. J. Gravesteijn, R. A. M. Wolters, J. Schmitz, Comparison of tungsten films grown by CVD and hot-wire assisted atomic layer deposition in a cold-wall reactor, *J. Vac. Sci. Technol.*, A, 34 (2015) 01A129-1.
187. P. Poodt, D. C. Cameron, E. Dickey, S. M. George, V. Kuznetsov, G. N. Parsons, F. Roozeboom, G. Sundaram, A. Vermeer, Spatial Atomic Layer Deposition: A Route Towards Further Industrialization of ALD, *J. Vac. Sci. Technol.*, A 30 (2012) 010802.
188. P. S. Maydannik, T. O. Kääriäinen, K. Lahtinen, D. C. Cameron, M. Söderlund, P. Soininen, P. Johansson, J. Kuusipalo, L. Moro, X. Zeng, Roll-to-roll atomic

- layer deposition process for flexible electronics encapsulation applications, *J. Vac. Sci. Technol.*, A 32 (2014) 051603.
189. A. U. Mane, J. Libera, J. W. Elam, Patent: ALD reactor for coating porous substrates U. S. patent No US20140220244 A1, priority date Feb 7, 2013.
  190. Data available in Goodfellow Cambridge Limited Home Page, Catalogue, [http://www.goodfellow.com/catalogue/GFCat4I.php?ewd\\_token=HF3LbO88GJ2oGm9BNHWB4bdxaJ8Dm4&n=8fbEMBKupIqHiTFA8eEHqsWkofwfDM&ewd\\_urlNo=GFCat4B11&Catite=FE250220&CatSearNum=1](http://www.goodfellow.com/catalogue/GFCat4I.php?ewd_token=HF3LbO88GJ2oGm9BNHWB4bdxaJ8Dm4&n=8fbEMBKupIqHiTFA8eEHqsWkofwfDM&ewd_urlNo=GFCat4B11&Catite=FE250220&CatSearNum=1) (visited 28.08.2017).
  191. O. N. Grigorov, M. E. Pozin, B. A. Porai-Koshits, V. A. Rabinovich, F. J. Patsintschi, P. G. Pomankov, D. A. Fpidrihsberg, *Spravotchnik himika V*, Leningrad (196) 940–941.
  192. J. Aarik, A. Aidla, A. Kasikov, H. Mändar, R. Rammula, V. Sammelselg, Influence of carrier gas pressure and flow rate on atomic layer deposition of  $\text{HfO}_2$  and  $\text{ZrO}_2$  thin films, *Appl. Surf. Sci.*, 252 (2006) 5723–5734.
  193. J. Aarik, A. Aidla, H. Mändar, V. Sammelselg, Anomalous effect of temperature on atomic layer deposition of titanium dioxide, *J. Cryst. Growth*, 220 (2000) 531–537.
  194. M. Ritala, M. Leskelä, L. Niinistö, Titanium Isopropoxide as a Precursor in Atomic Layer Epitaxy of Titanium Dioxide Thin Films, *Chem. Mater.*, 5 (1993) 1174–1181.
  195. R. L. Puurunen, Formation of Metal Oxide Particles in Atomic Layer Deposition During the Chemisorption of Metal Chlorides: A Review, *Chem. Vap. Dep.*, 11 (2005) 79–90.
  196. K. Knapas, M. Ritala, In Situ Studies on Reaction Mechanisms in Atomic Layer Deposition, *Crit. Rev. Solid State Mater. Sci.*, 38 (2013) 167–202.
  197. M. Kh. Karapet'yants, M. L. Karapet'yans: *Thermodynamic constants of inorganic and organic compounds*, Ann Arbor, Humprey Science Publishers, London (1970) 461.
  198. K. Möldre, L. Aarik, H. Mändar, A. Niilisk, R. Rammula, A. Tarre, J. Aarik, Atomic layer deposition of rutile and  $\text{TiO}_2$ -II from  $\text{TiCl}_4$  and  $\text{O}_3$  on sapphire: Influence of substrate orientation on thin film structure, *J. Cryst. Growth*, 428, (2015) 86–92.
  199. J. Aarik, T. Arroval, L. Aarik, R. Rammula, A. Kasikov, H. Mändar, B. Hudec, K. Hušeková, K. Fröhlich, Atomic layer deposition of rutile-phase  $\text{TiO}_2$  on  $\text{RuO}_2$  from  $\text{TiCl}_4$  and  $\text{O}_3$ : Growth of high-permittivity dielectrics with low leakage current, *J. Cryst. Growth*, 382 (2013) 61–66.
  200. M. Nakahara, S. Tsunekawa, K. Watanabe, T. Arai, T. Yunogami, K. Kuroki, Etching technique for ruthenium with a high etch rate and high selectivity using ozone gas, *J. Vac. Sci. Technol.*, B, 19 (2001), 2133–2136.
  201. W. Jeon, W. Lee, Y. W. Yoo, C. H. An, J. H. Han, S. K. Kim, C. S. Hwang, Chemistry of active oxygen in  $\text{RuO}_x$  and its influence on the atomic layer deposition of  $\text{TiO}_2$  films, *J. Mater. Chem.*, C, 2 (2014) 9993–1001.
  202. D. N. Goldstein, J. A. McCormick, S. M. George,  $\text{Al}_2\text{O}_3$  Atomic Layer Deposition with Trimethylaluminum and Ozone Studied by in Situ Transmission FTIR Spectroscopy and Quadrupole Mass Spectrometry, *J. Phys. Chem., C*, 112 (2008) 19530–19539.
  203. S. D. Elliott, G. Scarel, C. Wiemer, M. Fanciulli, G. Pavia, Ozone-Based Atomic Layer Deposition of Alumina from TMA: Growth, Morphology, and Reaction Mechanism, *Chem. Mater.*, 18 (2006) 3764–3773.

204. K. Kukli, M. Kemell, J. Köykkä, K. Mizohata, M. Vehkämäki, M. Ritala, M. Leskelä, Atomic layer deposition of zirconium dioxide from zirconium tetrachloride and ozone, *Thin Solid Films*, 589 (2015) 597–604.
205. T. Arroval, L. Aarik, R. Rammula, H. Mändar, J. Aarik, B. Hudec, K. Hušeková, K. Fröhlich, Influence of growth temperature on the structure and electrical properties of high-permittivity  $\text{TiO}_2$  films in  $\text{TiCl}_4\text{-H}_2\text{O}$  and  $\text{TiCl}_4\text{-O}_3$  atomic-layer-deposition processes, *Phys. Status Solidi A*, 211 (2014) 425–432.
206. R. L. Puurunen, T. Sajavaara, E. Santala, V. Miikkulainen, T. Saukkonen, M. Laitinen, M. Leskelä, Controlling the Crystallinity and Roughness of Atomic Layer Deposited Titanium Dioxide Films, *J. Nanosci. Nanotechnol.*, 11 (2011) 8101–8107.
207. G. C. Gorrea, B. Bao, N. C. Strandwitz, Chmeical Stability of Titania and Alumina Thin Films Formed by Atromic Layer Deposition, *ACS Appl. Mater. Interfaces*, 7 (2015) 14816–14821.
208. R. Rammula, J. Aarik, H. Mändar, P. Ritslaid, V. Sammelselg, Atomic layer deposition of  $\text{HfO}_2$ : Effect of structure development on growth rate, morphology and optical properties of thin films, *Appl. Surf. Sci.*, 257 (2010) 1043–1052.
209. Y. D. Zhang, D. Seghete, A. Abdulagatov, Z. Gibbs, A. Cavanagh, R. G. Yang, S. George, Y. C. Lee, Investigation of the defect density in ultra-thin  $\text{Al}_2\text{O}_3$  films grown using atomic layer deposition, *Surf. Coat. Technol.*, 205 (2011) 3334–3339.
210. M. Mozetic, Discharge cleaning with hydrogen plasma, *Vacuum*, 61 (2001) 367–371.
211. R. Subasri, A. Jyothirmayi, D.S. Reddy, Effect of plasma surface treatment and heat treatment ambience on mechanical and corrosion protection properties of hybrid sol-gel coatings on aluminum, *Surf. Coat. Technol.*, 205 (2010) 806–813.
212. E. Hätkönen, S. Potts, W. W. M. Kessels, B. Díaz, A. Seyeux, J. Wiatowska, V. Maurice, P. Marcus, G. Radnóczti, L. Tóth, M. Kariniemi, J. Niinistö, M. Ritala, Hydrogen-argon plasma pre-treatment for improving the anti-corrosion properties of thin  $\text{Al}_2\text{O}_3$  films deposited using atomic layer deposition on steel, *Thin Solid Films*, 534 (2013) 384–393.
213. ASTM G48-11, Standard Test Methods for Pitting and Crevice Corrosion Resistance of Stainless Steels and Related Alloys by Use of Ferric Chloride Solution, ASTM International, West Conshohocken, PA (2015), DOI: 10.1520/G0048-11R15.
214. Y. D. Zhang, J. A. Bertrand, R. G. Yang, S. M. George Y. C. Lee, Electroplating to visualize defects in  $\text{Al}_2\text{O}_3$  thin films grown using atomic layer deposition, *Thin Solid Films*, 517 (2009) 3269–3272.

## **PUBLICATIONS**

# CURRICULUM VITAE

Name: Lauri Aarik  
Date of birth: November 22. 1980  
Citizenship: Estonian  
Contact: Institute of Physics, University of Tartu,  
W.Ostwaldi 1, 50411, Tartu, Estonia  
Telephone: +3727374673  
E-mail: lauri.aarik@ut.ee

## **Education**

2012–2017 University of Tartu, PhD studies  
1999–2004 University of Tartu, BSc.  
1987–1999 Tartu Tamme Gymnasium

## **Main research areas**

Atomic layer deposition of thin films, reactors for atomic layer deposition, thin film characterization, barrier and protective layers

## **Language skills**

Estonian, mother tongue  
English, good  
Russian, basic  
German, basic

## **List of publication:**

1. L. Lind, E. Adoberg, **L. Aarik**, P. Kulu, R. Veinthal, Tribological properties of PVD coatings with lubricating films, *Estonian Journal of Engineering*, 18 (2012) 193–201
2. K. Fröhlich, B. Hudec, M. Čapajna, K. Hušeková, A. Rosová, P. Eliáš, J. Aarik, R. Rammula, A. Kasikov, T. Arroval, **L. Aarik**, K. Murakami, M. Rommel, A.J. Bauer, TiO<sub>2</sub>-based Metal-Insulator-Metal Structures for Future DRAM Storage Capacitors, *ECS Transactions*, 50 (2012) 79–87.
3. V. Sammelselg, **L. Aarik**, M. Merisalu. Patent: Method of preparing corrosion resistant coatings. Patent: WO 2014102758 A1. Priority date: December 31, 2012.
4. **L. Aarik**, T. Arroval, R. Rammula, H. Mändar, V. Sammelselg, J. Aarik, Atomic layer deposition of TiO<sub>2</sub> from TiCl<sub>4</sub> and O<sub>3</sub>, *Thin Solid Films*, 542 (2013) 100–107.
5. V. Sammelselg, I. Netšipailo, A. Aidla, A. Tarre, **L. Aarik**, J. Asari, P. Ritslaid, J. Aarik, Chemical resistance of thin film materials based metal oxides grown by atomic layer deposition, *Thin Solid Films*, 542, (2013) 219–224.

6. A. Tamm, A.-L. Peikolainen, J. Kozlova; H. Mändar, A. Aidla, R. Rammula, **L. Aarik**, K. Roosalu, J. Lu, L. Hultman, M. Koel, K. Kukli, J. Aarik, Atomic layer deposition of high-k dielectrics on carbon nanoparticles, *Thin Solids Films*, 538 (2013) 16–20.
7. J. Aarik, T. Arroval, **L. Aarik**, R. Rammula, A. Kasikov, H. Mändar, B. Hudec, K. Hušeková, K. Fröhlich, Atomic layer deposition of rutile-phase  $TiO_2$  on  $RuO_2$  from  $TiCl_4$  and  $O_3$ : Growth of high-permittivity dielectrics with low leakage current, *J. Cryst. Growth*, 382 (2013) 61–66.
8. R. Rammula, **L. Aarik**, A. Kasikov, J. Kozlova, T. Kahro, L. Matisen, A. Niilisk, H. Alles, J. Aarik, Atomic layer deposition of aluminum oxide films on graphene, *IOP Conf. Series: Materials Science and Engineering* 49 (2013) 012014.
9. A. Tamm, A.-L. Peikolainen, J. Kozlova, **L. Aarik**, K. Roosalu, I. Kärkkänen, H. Mändar, J. Aarik, K. Kukli, Atomic Layer Deposition of Zirconium Oxide on Carbon Nanoparticles, *IOP Conf. Series: Materials Science and Engineering* 49 (2013) 012019.
10. R. Jaaniso, T. Kahro, J. Kozlova, J. Aarik, **L. Aarik**, H. Alles, A. Floren, A. Gerst, A. Kasikov, A. Niilisk, V. Sammelselg, V, Temperature induced inversion of oxygen response in CVD graphene on  $SiO_2$ , *Sensor and Actuators B* 190 (2014) 1006–1013.
11. **L. Aarik**, T. Arroval, R. Rammula, H. Mändar, V. Sammelselg, B. Hudec, K. Hušeková, K. Fröhlich, J. Aarik, Atomic layer deposition of high-quality  $Al_2O_3$  and Al-doped  $TiO_2$  thin films from hydrogen-free precursors, *Thin Solid Films*, 565 (2014) 19–24.
12. V. Sammelselg, J. Kostamo, W. Bayerl, J. Aarik, **L. Aarik**, S. Lindfors, P. Adam, J. Poutiainen, Protecting an interior of a gas container with an ALD coating, Patent: WO 2015/132443 A1. Priority date March 3, 2014.
13. V. Sammelselg, J. Kostamo, T. Malinen, J. Aarik, **L. Aarik**, Protecting an interior of a hollow body with an ALD coating, Patent: WO 2015/132444 A1. Priority date March 3, 2014
14. **L. Aarik**, H. Alles, A. Aidla, T. Kahro, K. Kukli, J. Niinistö, H. Mändar, A. Tamm, R. Rammula, V. Sammelselg, J. Aarik, Influence of process parameters on atomic layer deposition of  $ZrO_2$  thin films from  $CpZr(NMe_2)_3$  and  $H_2O$ , *Thin Solid Films*, 565 (2014) 37–44
15. T. Arroval, **L. Aarik**, R. Rammula, H. Mändar, J. Aarik, B. Hudec, K. Hušeková, and K. Fröhlich, Influence of growth temperature on the structure and electrical properties of high-permittivity  $TiO_2$  films in  $TiCl_4$ - $H_2O$  and  $TiCl_4$ - $O_3$  atomic-layer-deposition processes, *Phys. Status Solidi A* 211 (2014) 425–432.
16. A. Tamm, J. Kozlova, **L. Aarik**, A. Aidla, J. Lu, A.-A. Kiisler, A. Kasikov, P. Ritslaid, H. Mändar, L. Hultman, V. Sammelselg, K. Kukli, J. Aarik, Atomic layer deposition of  $ZrO_2$  for graphene-based multilayer structures: In situ and ex situ characterization of growth process, *Phys. Status Solidi A* 211 (2014) 397–402.

17. J. Mondal, **L. Aarik**, J. Kozlova, A. Niilisk, H. Mändar, U. Mäeorg, A. Simões, V. Sammelselg, Functionalization of Titanium Alloy Surface by Graphene Nanoplatelets and Metal Oxides: Corrosion Inhibition, *J. Nanosci. Nanotechnol.*, 15 (2015) 6533–6540.
18. A. Tamm, J. Kozlova, **L. Aarik**, J. Aarik, K. Kukli, J. Link, R. Stern, Dysprosium oxide and dysprosium-oxide-doped titanium oxide thin films grown by atomic layer deposition, *J. Vac. Sci. Technol. A*, 33 (2015) 01A127.
19. A. Tamm, J. Kozlova, T. Arroval, **L. Aarik**, P. Ritslaid, H. Garcia, H. Castan, S. Duenas, K. Kukli, J. Aarik, Atomic Layer Deposition and Characterization of Dysprosium Doped Zirconium Oxide Thin Films, *Chem. Vap. Deposition*, 21 (2015) 181–187.
20. T. Arroval, **L. Aarik**, R. Rammula, J. Aarik, Growth of  $Ti_xAl_{1-x}O_y$  films by atomic layer deposition using successive supply of metal precursors. *Thin Solid Films*, 591 (2015) 276–284.
21. K. Möldre, **L. Aarik**, H. Mändar, A. Niilisk, R. Rammula, A. Tarre, J. Aarik, Atomic layer deposition of rutile and  $TiO_2$ -II from  $TiCl_4$  and  $O_3$  on sapphire: Influence of substrate orientation on thin film structure, *J. Cryst. Growth*, 428 (2015) 86–92.
22. T. Arroval, **L. Aarik**, R. Rammula, V. Kruusla, J. Aarik, Effect of substrate-enhanced and inhibited growth on atomic layer deposition and properties of aluminum–titanium oxide films, *Thin Solid Films*, 600 (2016) 119–125.
23. J. Mondal, A. Marques, **L. Aarik**, J. Kozlova, A. Simões, V. Sammelselg, Development of thin ceramic-graphene nanolaminated coating for corrosion protection of stainless steel. *Corrosion Science*, 105 (2016) 161–169.

### Conference presentation

1. **L. Aarik**, J. Kozlova, M. Merisalu, R. Rammula, I. Netšipailo, J. Aarik, V. Sammelselg, High-Temperature Corrosion Resistive ALD Coatings for Nickel Alloys. Poster presentation at European Materials Research Society (E-MRS) Spring meeting (2011) Nice, France
2. **L. Aarik**, J. Asari, K. Kukli, H. Mändar, A. Tamm, J. Aarik, V. Sammelselg, Properties of  $ZrO_2$  thin films grown in  $C_5H_5Zr[N(CH_3)_2]_3 \cdot H_2O$  and  $ZrCl_4 \cdot H_2O$  atomic layer deposition processes. Poster presentation at AVS-ALD & Baltic ALD 2012 - 12<sup>th</sup> International Conference on Atomic Layer Deposition (2012), Dresden, Germany
3. **L. Aarik**, T. Arroval, V. Sammelselg, J. Aarik, Atomic layer deposition of high-quality nanostructured  $TiO_2$  and  $Al_2O_3$  thin films in hydroxyl-free chloride-based processes. Poster presentation at the 8th International Conference on Surfaces, Coatings and Nanostructured Materials (NANOSMAT-2013) 2013, Granada, Spain.
4. **L. Aarik**, T. Arroval, R. Rammula, H. Mändar, V. Sammelselg, J. Aarik, Titanium dioxide thin films grown from titanium chloride and ozone by Atomic layer deposition. Poster presentation at 8th International conference Functional Materials and Nanotechnologies, (FM&NT) 2013, Tartu, Estonia.

5. **L. Aarik**, H. Alles, J. Asari, K. Kukli, A. Tamm, J. Aarik, V. Sammelselg, Zirconium dioxide thin films grown from Tris(dimethylamino)cyclopentadienylZirconium and water vapour by atomic layer deposition. Poster presentation at the Functional Materials and Technologies Graduate School onferences (FMTDK) 2013, Tallinn, Estonia.
6. **L. Aarik**, T. Arroval, V. Sammelselg, J. Aarik, Atomic layer deposition of  $\text{Al}_2\text{O}_3$  thin films in hydroxyl-free chloride-based process, Poster presentation at the Functional Materials and Technologies Graduate School onferences (FMTDK) 2014, Tartu, Estonia.
7. **L. Aarik**, H. Mändar, V. Sammelselg, J. Aarik, Chemical resistivity of  $\text{Al}_2\text{O}_3$  and  $\text{TiO}_2$  grown by atomic layer deposition from hydrogen-free precursors. Poster presentation at the 13<sup>th</sup> International Baltic Conference on Atomic Layer Deposition (Baltic ALD) 2015, Tartu, Estonia.
8. **L. Aarik**, H. Mändar, V. Sammelselg, J. Aarik, Properties of the atomic layer deposited  $\text{Al}_2\text{O}_3$  and  $\text{TiO}_2$  films using hydrogen free precursors. Poster presentation at the conference Functional Materials and Nanotechnologies (FM&NT-2015) 2015 Vilnius, Lithuania.
9. **L. Aarik**, V. Sammelselg, J. Aarik, Using the  $\text{TiO}_2$ ,  $\text{Al}_2\text{O}_3$  one layer and multilayer coatings for protecting stainless steel (grade 310). Poster presentation at the 16<sup>th</sup> International Conference on Atomic Layer Deposition (ALD 2016), 2016, Dublin, Ireland.

# ELULOOKIRJELDUS

Nimi: Lauri Aarik  
Sünnaeg: 22. november 1980  
Kodakondsus: Eesti  
Kontakt: Tartu Ülikool, Füüsika Instituut,  
W.Ostwaldi tn 1, 50411, Tartu, Eesti  
Telefon: +372 737 4673  
E-mail: lauri.aarik@ut.ee

## Haridus

2012–2017 Tartu Ülikool, doktoriõpe  
1999–2004 Tartu Ülikool, BSc.  
1987–1999 Tartu Tamme Gümnaasium

## Peamised uurimisvaldkonnad

Tahkiskilede aatomkihtsadestamine, sadestamismetoodika täiustamine, tahkiskilede koostise, struktuuri ja optiliste omaduste uurimine, üliõhukeste tahkiskilede kasutamine kaitsekatetena.

## Keelteoskus

Eesti keel, emakeel  
Inglise keel, hea  
Vene keel, hea  
Saksa keel, rahuldav

## Publikatsioonid:

1. L. Lind, E. Adoberg, **L. Aarik**, P. Kulu, R. Veinthal, Tribological properties of PVD coatings with lubricating films, Estonian Journal of Engineering, 18 (2012) 193–201
2. K. Fröhlich, B. Hudec, M. Čapajna, K. Hušeková, A. Rosová, P. Eliáš, J. Aarik, R. Rammula, A. Kasikov, T. Arroval, **L. Aarik**, K. Murakami, M. Rommel, A.J. Bauer, TiO<sub>2</sub>-based Metal-Insulator-Metal Structures for Future DRAM Storage Capacitors, ECS Transactions, 50 (2012) 79–87.
3. V. Sammelselg, **L. Aarik**, M. Merisalu. Patent: Method of preparing corrosion resistant coatings. Patent: WO 2014102758 A1. Priority date: December 31, 2012.
4. **L. Aarik**, T. Arroval, R. Rammula, H. Mändar, V. Sammelselg, J. Aarik, Atomic layer deposition of TiO<sub>2</sub> from TiCl<sub>4</sub> and O<sub>3</sub>, Thin Solid Films, 542 (2013) 100–107.
5. V. Sammelselg, I. Netšipailo, A. Aidla, A. Tarre, **L. Aarik**, J. Asari, P. Ritslaid, J. Aarik, Chemical resistance of thin film materials based metal oxides grown by atomic layer deposition, Thin Solid Films, 542, (2013) 219–224.

6. A. Tamm, A.-L. Peikolainen, J. Kozlova; H. Mändar, A. Aidla, R. Rammula, **L. Aarik**, K. Roosalu, J. Lu, L. Hultman, M. Koel, K. Kukli, J. Aarik, Atomic layer deposition of high-k dielectrics on carbon nanoparticles, *Thin Solids Films*, 538 (2013) 16–20.
7. J. Aarik, T. Arroval, **L. Aarik**, R. Rammula, A. Kasikov, H. Mändar, B. Hudec, K. Hušeková, K. Fröhlich, Atomic layer deposition of rutile-phase  $TiO_2$  on  $RuO_2$  from  $TiCl_4$  and  $O_3$ : Growth of high-permittivity dielectrics with low leakage current, *J. Cryst. Growth*, 382 (2013) 61–66.
8. R. Rammula, **L. Aarik**, A. Kasikov, J. Kozlova, T. Kahro, L. Matisen, A. Niilisk, H. Alles, J. Aarik, Atomic layer deposition of aluminum oxide films on graphene, IOP Conf. Series: Materials Science and Engineering 49 (2013) 012014.
9. A. Tamm, A.-L. Peikolainen, J. Kozlova, **L. Aarik**, K. Roosalu, I. Kärkkänen, H. Mändar, J. Aarik, K. Kukli, Atomic Layer Deposition of Zirconium Oxide on Carbon Nanoparticles, IOP Conf. Series: Materials Science and Engineering 49 (2013) 012019.
10. R. Jaaniso, T. Kahro, J. Kozlova, J. Aarik, **L. Aarik**, H. Alles, A. Floren, A. Gerst, A. Kasikov, A. Niilisk, V. Sammelselg, V, Temperature induced inversion of oxygen response in CVD graphene on  $SiO_2$ , *Sensor and Actuators B* 190 (2014) 1006–1013.
11. **L. Aarik**, T. Arroval, R. Rammula, H. Mändar, V. Sammelselg, B. Hudec, K. Hušeková, K. Fröhlich, J. Aarik, Atomic layer deposition of high-quality  $Al_2O_3$  and Al-doped  $TiO_2$  thin films from hydrogen-free precursors, *Thin Solid Films*, 565 (2014) 19–24.
12. V. Sammelselg, J. Kostamo, W. Bayerl, J. Aarik, **L. Aarik**, S. Lindfors, P. Adam, J. Poutiainen, Protecting an interior of a gas container with an ALD coating, Patent: WO 2015/132443 A1. Prioriteedi kuupäev 3 Märts 2014.
13. V. Sammelselg, J. Kostamo, T. Malinen, J. Aarik, **L. Aarik**, Protecting an interior of a hollow body with an ALD coating, Patent: WO 2015/132444 A1. Prioriteedi kuupäev 3 Märts 2014
14. **L. Aarik**, H. Alles, A. Aidla, T. Kahro, K. Kukli, J. Niinistö, H. Mändar, A. Tamm, R. Rammula, V. Sammelselg, J. Aarik, Influence of process parameters on atomic layer deposition of  $ZrO_2$  thin films from  $CpZr(NMe_2)_3$  and  $H_2O$ , *Thin Solid Films*, 565 (2014) 37–44
15. T. Arroval, **L. Aarik**, R. Rammula, H. Mändar, J. Aarik, B. Hudec, K. Hušeková, and K. Fröhlich, Influence of growth temperature on the structure and electrical properties of high-permittivity  $TiO_2$  films in  $TiCl_4$ - $H_2O$  and  $TiCl_4$ - $O_3$  atomic-layer-deposition processes, *Phys. Status Solidi A* 211 (2014) 425–432.
16. A. Tamm, J. Kozlova, **L. Aarik**, A. Aidla, J. Lu, A.-A. Kiisler, A. Kasikov, P. Ritslaid, H. Mändar, L. Hultman, V. Sammelselg, K. Kukli, J. Aarik, Atomic layer deposition of  $ZrO_2$  for graphene-based multilayer structures: In situ and ex situ characterization of growth process, *Phys. Status Solidi A* 211 (2014) 397–402.

17. J. Mondal, **L. Aarik**, J. Kozlova, A. Niilisk, H. Mändar, U. Mäeorg, A. Simões, V. Sammelselg, Functionalization of Titanium Alloy Surface by Graphene Nanoplatelets and Metal Oxides: Corrosion Inhibition, *J. Nanosci. Nanotechnol.*, 15 (2015) 6533–6540.
18. A. Tamm, J. Kozlova, **L. Aarik**, J. Aarik, K. Kukli, J. Link, R. Stern, Dysprosium oxide and dysprosium-oxide-doped titanium oxide thin films grown by atomic layer deposition, *J. Vac. Sci. Technol. A*, 33 (2015) 01A127.
19. A. Tamm, J. Kozlova, T. Arroval, **L. Aarik**, P. Ritslaid, H. Garcia, H. Castan, S. Duenas, K. Kukli, J. Aarik, Atomic Layer Deposition and Characterization of Dysprosium Doped Zirconium Oxide Thin Films, *Chem. Vap. Deposition*, 21 (2015) 181–187.
20. T. Arroval, **L. Aarik**, R. Rammula, J. Aarik, Growth of  $Ti_xAl_{1-x}O_y$  films by atomic layer deposition using successive supply of metal precursors. *Thin Solid Films*, 591 (2015) 276–284.
21. K. Möldre, **L. Aarik**, H. Mändar, A. Niilisk, R. Rammula, A. Tarre, J. Aarik, Atomic layer deposition of rutile and  $TiO_2$ -II from  $TiCl_4$  and  $O_3$  on sapphire: Influence of substrate orientation on thin film structure, *J. Cryst. Growth*, 428 (2015) 86–92.
22. T. Arroval, **L. Aarik**, R. Rammula, V. Kruusla, J. Aarik, Effect of substrate-enhanced and inhibited growth on atomic layer deposition and properties of aluminum–titanium oxide films, *Thin Solid Films*, 600 (2016) 119–125.
23. J. Mondal, A. Marques, **L. Aarik**, J. Kozlova, A. Simões, V. Sammelselg, Development of thin ceramic-graphene nanolaminated coating for corrosion protection of stainless steel. *Corrosion Science*, 105 (2016) 161–169.

### Konverentsiettekanded

1. **L. Aarik**, J. Kozlova, M. Merisalu, R. Rammula, I. Netšipailo, J. Aarik, V. Sammelselg, “High-Temperature Corrosion Resistive ALD Coatings for Nickel Alloys”. Stendiettekanne konverentsil “European Materials Research Society (E-MRS) Spring meeting” (2011) Nice, Prantsusmaa
2. **L. Aarik**, J. Asari, K. Kukli, H. Mändar, A. Tamm, J. Aarik, V. Sammelselg, “Properties of  $ZrO_2$  thin films grown in  $C_5H_5Zr[N(CH_3)_2]_3\text{-}H_2O$  and  $ZrCl_4\text{-}H_2O$  atomic layer deposition processes”. Stendiettekanne konverentsil “AVS-ALD & Baltic ALD 2012 – 12<sup>th</sup> International Conference on Atomic Layer Deposition” (2012), Dresden, Saksamaa
3. **L. Aarik**, T. Arroval, V. Sammelselg, J. Aarik, “Atomic layer deposition of high-quality nanostructured  $TiO_2$  and  $Al_2O_3$  thin films in hydroxyl-free chloride-based processes”. Stendiettekanne konverentsil “The 8th International Conference on Surfaces, Coatings and Nanostructured Materials” (NANOSMAT-2013) 2013, Granada, Hispaania.
4. **L. Aarik**, T. Arroval, R. Rammula, H. Mändar, V. Sammelselg, J. Aarik, “Titanium dioxide thin films grown from titanium chloride and ozone by Atomic layer deposition”. Stendiettekanne konverentsil “8<sup>th</sup> International

conference Functional Materials and Nanotechnologies” (FM&NT) 2013, Tartu, Eesti.

5. **L. Aarik**, H. Alles, J. Asari, K. Kukli, A. Tamm, J. Aarik, V. Sammelselg, “Zirconium dioxide thin films grown from Tris(dimethylamino)cyclopentadienylZirconium and water vapour by atomic layer deposition”. Stendiettekanne Funktsionaalsete materjalide ja tehnoloogiate doktorikooli teaduskonverentsil, 2013, Tallinn, Eesti.
6. **L. Aarik**, T. Arroval, V. Sammelselg, J. Aarik, “Atomic layer deposition of  $\text{Al}_2\text{O}_3$  thin films in hydroxyl-free chloride-based process”, Stendiettekanne Funktsionaalsete materjalide ja tehnoloogiate doktorikooli teaduskonverentsil, 2014, Tartu, Eesti.
7. **L. Aarik**, H. Mändar, V. Sammelselg, J. Aarik, “Chemical resistivity of  $\text{Al}_2\text{O}_3$  and  $\text{TiO}_2$  grown by atomic layer deposition from hydrogen-free precursors”. Stendiettekanne “The 13<sup>th</sup> International Baltic Conference on Atomic Layer Deposition” (Baltic ALD) 2015, Tartu, Eesti.
8. **L. Aarik**, H. Mändar, V. Sammelselg, J. Aarik “Properties of the atomic layer deposited  $\text{Al}_2\text{O}_3$  and  $\text{TiO}_2$  films using hydrogen free precursors”. Stendiettekanne konverentsil “Functional Materials and Nanotechnologies” (FM&NT-2015) 2015 Vilnius, Leedu.
9. **L. Aarik**, V. Sammelselg, J. Aarik, “Using the  $\text{TiO}_2$ ,  $\text{Al}_2\text{O}_3$  one layer and multilayer coatings for protecting stainless steel (grade 310)”. Stendiettekanne “The 16<sup>th</sup> International Conference on Atomic Layer Deposition” (ALD 2016), 2016, Dublin, Iirimaa.

## DISSERTATIONES SCIENTIAE MATERIALIS UNIVERSITATIS TARTUENSIS

1. **Martin Järvekülg.** Tubular microstructures by Hf-, Zr- and Ti-butoxide gel sheet rolling. Tartu, 2011, 112 p.
2. **Sergei Vlassov.** Investigation of nanoscale interactions and mechanical properties of nanostructures using quartz tuning fork based real-time measurements. Tartu, 2011, 171 p.
3. **Margus Kodu.** Pulsed Laser Deposition of Magnesium Oxide and Barium Ternary Oxides for Plasma Display Protective Layers. Tartu, 2011, 89 p.
4. **Rainer Pärna.** Surface studies of some oxide films. Tartu, 2011, 129 p.
5. **Jevgeni Sulga.** Self-assembly and interaction of nanostructures. Tartu, 2011, 114 p.
6. **Wojciech Kuznik.** Quantum-chemical computer simulations of the linear and non-linear optical properties of pyrazoloquinoline and dicyanopyrazine derivatives. Tartu, 2012, 89 p.
7. **Leonid Dorogin.** Structural and tribological properties of zero- and one-dimensional nanocrystals. Tartu, 2012, 193 p.
8. **Viljar Palmre.** Fabrication and characterization of microporous carbon-based electroactive polymer actuators. Tartu, 2012, 99 p.
9. **Madis Paalo.** Synthesis of CNT-metal oxide nanocomposites: sol-gel process, rheology, structural and functional properties. Tartu, 2014, 175 p.
10. **Raul Välbe.** Developement of ionic liquid composites by sol-gel method for elaboration of industrial nano- and microstructures. Tartu, 2014, 97 p.
11. **Urmas Joost.** Impurity and preparation dependent properties of titania thin films. Tartu, 2014, 155 p.
12. **Madis Umalas.** Application of sol-gel technology for production of ceramic nanocomposites and functional coatings. Tartu, 2015, 136 p.
13. **Elena Samsonova.** Energy transfer probe as a tool to study morphological and structural origins of fluorescence quenching in rare-earth doped nanoposphors. Tartu, 2015, 114 p.
14. **Jay Mondal.** Novel Corrosion Protective Nanostructured Composite Coatings. Tartu, 2016, 104 p.
15. **Kathriin Utt.** Metal oxide mesostructures for optical applications. Tartu, 2016, 88 p.
16. **Kaido Siimon.** Electrospun gelatin cross-linked by glucose. Tartu, 2016, 84 p.
17. **Marko Part.** Combined three-dimensional sol-gel structures and atomic layer deposited thin films. Tartu, 2017, 162 p.
18. **Pejman Rasti.** Analysis of Remote Sensing Image Super Resolution using Fluid Lenses. Tartu, 2017, 188 p.
19. **Ivo Romet.** Recombination luminescence of doped borates: origin and application prospects in dosimetry. Tartu, 2017, 111 p.

20. **Vladimir I. Kondratiev.** Processing and characterization of transparent electrode materials. Tartu, 2017, 111 p.
21. **Taivo Jõgiaas.** Mechanical properties of atomic layer deposited thin films and nanocomposites. Tartu, 2017, 125 p.